Doctoral Program of Clinical Research
Faculty of Medicine
University of Helsinki
Finland

THE CHALLENGE OF ARTICULAR CARTILAGE REPAIR

STUDIES ON CARTILAGE REPAIR IN ANIMAL MODELS AND IN CELL CULTURE

Eve Salonius

ACADEMIC DISSERTATION

To be presented, with the permission of the Faculty of Medicine of the University of Helsinki, for public examination in lecture room PIII, Porthania, Yliopistonkatu 3, on Friday the 22nd of November, 2019 at 12 o'clock.

Helsinki 2019

Supervisors: Professor Ilkka Kiviranta, M.D., Ph.D.
Department of Orthopaedics and Traumatology
Clinicum
Faculty of Medicine
University of Helsinki
Finland

Virpi Muhonen, Ph.D.
Department of Orthopaedics and Traumatology
Clinicum
Faculty of Medicine
University of Helsinki
Finland

Reviewers: Professor Heimo Ylänen, Ph.D.
Department of Electronics and Communications
Engineering
Tampere University of Technology
Finland

Adjunct Professor Petri Virolainen, M.D., Ph.D.
Department of Orthopaedics and Traumatology
University of Turku
Finland

Opponent: Professor Leif Dahlberg, M.D., Ph.D.
Department of Orthopaedics
Lund University
Sweden

The Faculty of Medicine uses the Urkund system (plagiarism recognition) to examine all doctoral dissertations

ISBN 978-951-51-5613-6 (paperback)
ISBN 978-951-51-5614-3 (PDF)

Unigrafia
Helsinki 2019

ABSTRACT

Articular cartilage is highly specialized connective tissue that covers the ends of bones in joints. Damage to articulating joint surface causes pain and loss of joint function. The prevalence of cartilage defects is expected to increase, and if untreated, they may lead to premature osteoarthritis, the world's leading joint disease. Early intervention may cease this process.

The first-line treatment of non-surgical management of articular cartilage defects is physiotherapy and pain medication to alleviate symptoms. The gold standard of surgical treatment is marrow stimulation, in which cells from bone marrow migrate to the defect site and form a fibrin clot that is later replaced by a fibrocartilaginous scar. More recent techniques include osteochondral grafting and cell-based techniques. Autologous chondrocyte implantation (ACI) is a surgical technique in which the patient's cartilage cells are expanded in laboratory and seeded under a periosteal flap. Biomaterial scaffolds have been studied in replacing the periosteum and creating a supporting structure for regenerating cartilage tissue. Despite promising short term results, a material that is able to support the formation of durable hyaline cartilage is yet to be developed.

This thesis was undertaken to improve current surgical cartilage repair methods by testing the feasibility of novel biomaterial scaffolds in the repair of cartilage and subchondral bone defects, as well as the use of animal models in cartilage repair research.

Type II collagen is the most common fiber structure in articular cartilage. The feasibility of a novel composite material rhCo-PLA that combines recombinant human type II collagen and poly(L/D)lactide felt was tested in a porcine model. The scaffold was used in combination with autologous porcine chondrocytes in the treatment of full-thickness chondral defects in the porcine knee. The novel scaffold resulted in repair tissue with similar histology, biomechanics and subchondral bone structure as a clinically used commercial porcine type I/III collagen membrane. Subchondral bone lesions beneath the repair site developed in all study groups but the novel scaffold resulted in fewer bone defects than the commercial collagen membrane.

In conjunction with deep cartilage defects, the underlying subchondral bone might be damaged as well. These bone defects might require filler material in order to restore the height of the cartilage surface and joint congruence. We aimed at improving the repair of cartilage–bone defects with new bone filler materials. Therefore, a lapine model was used to evaluate the repair of deep osteochondral defects with porous poly-lactic-co-glycolic acid (PLGA) scaffolds and scaffolds combining PLGA with bioactive glass fibers. PLGA resulted in bone volume fraction similar to that of spontaneous healing. Combining PLGA with bioactive glass worsened the repair and histological evaluation revealed that the defects were filled with loose connective tissue

instead of bone. Commercial controls, granular beta-tricalcium phosphate (β-TCP) and bioactive glass (BG), resulted in extensive bone formation with no signs of granular detachment.

Animal models are used in the development of new treatment options. In order to improve the effectiveness and ethical use of the equine model in articular cartilage repair, spontaneous repair capacity of equine carpal cartilage was evaluated to find the critical lesion size beyond which spontaneous repair does not occur. Surgically created circular chondral and osteochondral defects were evaluated after 12 months of spontaneous repair. Superficial chondral defects showed no bone cysts beneath the defect area but in osteochondral defects, bone defects were found in all defect sizes (2 mm, 4 mm and 8 mm). Based on MRI, μCT, polarized light microscopy, immunohistochemistry and standard histology, 2 mm was considered the critical chondral lesion size and 4 mm the critical size of osteochondral defects.

Autologous chondrocytes have been used in cartilage repair for more than 20 years. The main limitations of the traditional chondrocyte implantation technique are the limited amount of cells available and the requirement of two separate surgeries. Bone marrow-derived human mesenchymal stem cells (BM-MSCs) can be used as an alternative cell source. Predifferentiation of these cells in biomaterial scaffolds might improve the repair results. Thus, chondrogenic differentiation of BM-MSCs in three-dimensional biomaterials was evaluated in an *in vitro* study. Passage 3 BM-MSCs were cultured in a chondrogenic culture medium for 14 and 28 days in rhCo-PLA scaffolds manufactured either with recombinant human collagen type II or type III. Commercial collagen membrane served as a control. The chondrogenic differentiation resulted in chondrocyte hypertrophy at an early phase of cell culture. The different collagen types in rhCo-PLA scaffolds did not affect the outcomes.

In conclusion, the novel rhCo-PLA scaffold performed well in a porcine model but the new PLGA-based bone filler materials were unable to produce desired repair tissue in a lapine model. Critical defect diameter in the equine carpus was defined to be 2 mm for chondral and 4 mm for osteochondral defects. The chondrogenic differentiation of BM-MSCs cultured both in the rhCo-PLA scaffold and on commercial type I/III collagen membrane lead to cell hypertrophy. All animal models used in this study, *i.e.*, the porcine, lapine and equine model, demonstrated that subchondral bone defects are associated with cartilage defects and repair procedures. This emphasizes the fact that the synovial joint is a functional unit comprised of several tissues and the challenge of cartilage repair is further complicated by comorbidities in the adjacent tissues.

TIIVISTELMÄ

Nivelrusto on korkeasti erilaistunutta sidekudosta, joka peittää toisiinsa niveltyvien luiden päitä. Rustovauriot aiheuttavat kipua ja nivelen toimintahäiriöitä ja niiden prevalenssin odotetaan kasvavan. Hoitamattomina rustovauriot voivat johtaa ennenaikaiseen nivelrikkoon, joka on maailman yleisin nivelsairaus. Aikaisella puuttumisella voitaneen ehkäistä tätä kehityskulkua.

Rustovaurioiden konservatiivisen ensilinjan hoitoja ovat fysioterapia ja kipulääkitys, joilla voidaan lievittää vaurioihin liittyviä oireita. Kirurgisten toimenpiteiden kultaisena standardina pidetään luuydinstimulaatiota, jossa luuytimen solut muodostavat säierustoisen arven vaurioalueelle. Uudempia tekniikoita ovat osteokondraaliset siirteet ja soluterapiat. Autologinen rustosolusiirre (*autologous chondrocyte implantation*, ACI) on kirurginen tekniikka, jossa potilaan omia rustosoluja viljellään laboratoriossa ja istutetaan luukalvon alle vaurioalueelle. Biomateriaali-istutteita on tutkittu luukalvon korvikkeena. Huolimatta lupaavista lyhyen aikavälin tuloksista vielä ei ole pystytty kehittämään materiaalia, joka pystyisi turvaamaan kestävän lasiruston muodostumista.

Tämän tutkimuksen tarkoituksena on parantaa tämänhetkistä kirurgista rustovauriokorjausta selvittämällä uusien biomateriaali-istutteiden toimivuutta nivelruston ja rustonalaisen luun vaurioissa sekä parantaa eläinmallien käytettävyyttä rustovauriokorjauksen tutkimuksessa.

Tyypin II kollageeni on nivelruston yleisin säierakenne. Rekombinanttitekniikalla valmistettua tyypin II kollageenia ja poly(L/D)-laktidia yhdistävän rhCo-PLA-komposiittibiomateriaalin toimivuutta selvitettiin suureläinmallissa. Istutetta käytettiin yhdessä sian kondrosyyttien kanssa koko rustokerroksen kattavan sian polven rustovaurion korjauksessa. Uuden istutteen avulla muodostunut korjauskudos oli histologialtaan, biomekaniikaltaan ja allaolevan subkondraaliluun rakenteelta samankaltaista kliinisessä käytössä olevan kaupallisen sian tyyppi I/III kollageenista valmistetun kalvon avulla muodostuneen korjauskudoksen kanssa. Rustonalaisen luun vaurioita esiintyi kaikissa tutkimusryhmissä mutta uudella istutteella korjatuissa rustovaurioissa luuvauriot olivat harvinaisempia kuin kaupallisella kollageenikalvolla korjatuissa vaurioissa.

Syvien rustovaurioiden yhteydessä myös rustonalainen luu saattaa vaurioitua. Nämä luuvauriot saattavat vaatia luunkorvikemateriaalia rustopinnan korkeuden ja nivelen kongruenssin palauttamiseksi. Pyrimme parantamaan rusto–luuvaurioiden korjausta kehittämällä uusia luun täyttömateriaaleja. Syvien osteokondraalivaurioiden korjausta tutkittiin kanimallissa huokoisella poly-lactic-co-glycolic acid (PLGA) -istutteella sekä PLGA:ta ja bioaktiivista lasia yhdistävillä istutteilla tutkittiin kaniinimallissa. PLGA:n avulla aikaansaatu luun tilavuusosuus (bone volume fraction) vastasi

spontaania korjautumista. PLGA:n ja bioaktiivisen lasin yhdistelmä heikensi korjaustulosta, ja histologinen tarkastelu paljasti, että tässä ryhmässä vauriot täyttyivät löyhällä sdekudoksella luun sijaan. Kaupalliset kontrollimateriaalit, rakeinen beeta-trikalsiumfosfaatti (β-TCP) ja bioaktiivinen lasi (BG) johtivat laajaan luunmuodostukseen ilman viitteitä rakeiden irtoamisesta.

Eläinmalleja käytetään uusien hoitomuotojen kehitystyössä. Hevosten tehokkaan ja eettisen käytön parantamiseksi hevosen rannenivelen rustovaurioiden spontaania parantumista arvioitiin tavoitteena löytää kriittinen vauriokoko, jota suuremmat vauriot eivät korjaannu spontaanisti. Kirurgisesti tehtyjen pyöreiden rusto- ja rusto-luuvaurioiden spontaania korjaantumista arvioitiin 12 kuukauden seuranta-ajan päätteeksi. Pinnallisissa rustovaurioissa luukystia ei todettu mutta rusto-luuvaurioissa luun puutosta vaurioalueella todettiin halkaisijaltaan niin 2 mm, 4 mm kuin 8 mm kokoisissa vaurioissakin. Magneettikuvantamisen, mikrotietokone-tomografia-kuvantamisen, polarisaatiomikroskopian, immunohistokemian ja perinteisen histologian perusteella kondraalivaurioiden kriittisenä vauriokokona pidettiin 2 mm halkaisijaa ja osteokondraalivaurioiden kriittisenä kokona 4 mm halkaisijaa.

Autologisia kondrosyyttejä on käytetty rustovauriokorjauksessa yli 20 vuoden ajan. Perinteisen rustovauriosiirretekniikan tärkeimpinä rajoitteina on rajallinen saatavilla olevan ruston määrä sekä kahden erillisen leikkauksen tarve. Ihmisen luuydinperäisiä mesenkymaalisia kantasoluja (*bone marrow-derived mesenchymal stem cells*, BM-MSCs) voidaan käyttää vaihtoehtoisena solulähteenä. Näiden kantasolujen esierilaistaminen biomateriaali-istutteessa saattaisi parantaa korjauskudoksen laatua. Näin ollen arvioimme kantasolujen rustoerilaistumista kolmiulotteisissa istutteissa *in vitro*. Joko tyypin II tai tyypin III kollageenillä valmistettuihin rhCo-PLA-istutteisiin siirrostettuja kolmannen solujakautumisen kantasoluja viljeltiin rustoerilaistamisliuoksessa 14 ja 28 päivän ajan. Kontrollina käytettiin kaupallista tyypin I/III kollageenikalvoa. Rustoerilaistaminen johti rustosolujen hypertrofiaan soluviljelyn aikaisessa vaiheessa. RhCo-PLA-istutteiden kaksi erilaista kollageenityyppiä eivät vaikuttaneet lopputulokseen.

Yhteenvetona voidaan todeta, että uusi rhCo-PLA-istute toimi hyvin sikamallissa mutta uudet PLGA-pohjaiset luuntäyttömateriaalit eivät tuottaneet toivottua korjauskudosta kaniinimallissa. Hevosen rannenivelen kriittiseksi vauriokooksi määritettiin 2 mm rustovaurioille ja 4 mm rusto-luuvaurioille. Sekä rhCo-PLA-istutteessa että kaupallisella tyypin I/III kollageenikalvolla viljeltyjen luuydinperäisten kantasolujen rustoerilaistaminen johti solujen hypertrofiaan.

Synoviaalinivel muodostaa toiminnallisen yksikön ja rustovaurion korjauksen haastetta vaikeuttaa entisestään rustoa ympäröivien kudosten vauriot. Tämä tutkimus osoitti, että rustovaurioihin ja niiden korjaukseen liittyvät rustonalaiset luuvauriot ovat yleisiä sioilla, hevosilla ja kaniineilla.

CONTENTS

LIST OF ORIGINAL PUBLICATIONS

This thesis is based on the following publications:

I Muhonen V, **Salonius E**, Haaparanta AM, Järvinen E, Paatela T, Meller A, Hannula M, Björkman M, Pyhältö T, Ellä V, Vasara A, Töyräs J, Kellomäki M, Kiviranta I. Articular cartilage repair with recombinant human type II collagen/polylactide scaffold in a preliminary porcine study. J Orthop Res. 2016 May;34(5):745-53. doi: 10.1002/jor.23099.

II **Salonius E**, Muhonen V, Lehto K, Järvinen E, Pyhältö T, Hannula M, Aula AS, Uppstu P, Haaparanta AM, Rosling A, Kellomäki M, Kiviranta I. Gas-foamed poly(lactide-co-glycolide) and poly(lactide-co-glycolide) with bioactive glass fibers demonstrate insufficient bone repair in lapine osteochondral defects. J Tissue Eng Regen Med. 2019 Mar;13(3):406-415. doi: 10.1002/term.2801.

III **Salonius E**, Rieppo L, Nissi MJ, Pulkkinen HJ, Brommer H, Brünott A, Silvast TS, van Weeren PR, Muhonen V, Brama PAJ, Kiviranta I. Critical-sized cartilage defects in the equine carpus. Connect Tissue Res. 2019 Mar;60(2):95-106. doi: 10.1080/03008207.2018.1455670.

IV **Salonius E**, Kontturi LS, Laitinen A, Haaparanta AM, Korhonen M, Nystedt J, Kiviranta I, Muhonen V. Chondrogenic differentiation of bone marrow-derived mesenchymal stromal cells in a three-dimensional environment. J Cell Physiol. 2019 Sep 25. doi: 10.1002/jcp.29238.

Throughout the dissertation, these papers will be referred to by Roman numerals. This thesis also contains unpublished data.

ABBREVIATIONS

ACAN	*aggrecan*
ACI	autologous chondrocyte implantation procedure
AGE	advanced glycation endproduct
AMIC	autologous matrix-induced chondrogenesis
ANOVA	analysis of variance
ATMP	advanced therapy medicinal product
BG	bioactive glass
BM-MSC	bone marrow-derived mesenchymal stem cell
BV/TV	bone volume fraction
β-TCP	beta-tricalcium phosphate
CAIS	cartilage autograft implantation system
CaP	calcium phosphate
CE	Conformité Européenne
COL2A1	*Collagen, type II, alpha 1*
COL10A1	*Collagen, type X, alpha 1*
CTMP	somatic cell therapy medicinal product
DMEM	Dulbecco's Modified Eagle's Medium
EC	European commerce
ECM	extracellular matrix
EDTA	ethylenediamine tetraacetic acid
E_f	collagen fibril network modulus
E_m	non-fibrillar matrix modulus
EMA	European Medicines Agency
ESC	embryonic stem cell
EU	European Union
GAG	glycosaminoglycan
GAPDH	*glyceraldehyde-3-phosphate dehydrogenase*
GTMP	gene therapy medicinal product
HA	hyaluronic acid
ICRS	International Cartilage Repair Society
iPSC	induced pluripotent stem cell
k_o	permeability
MACI	matrix-applied characterized autologous cultured chondrocytes
MDR	Medical Devices Regulation
MFAP5	*microfibrillar associated protein 5*
MRI	magnetic resonance imaging
MSC	mesenchymal stem cell
μCT	micro-computed tomography imaging
NB	notified body
OA	osteoarthritis
OAT	osteochondral autograft transfer

OCA	osteochondral allograft
PBS	phosphate-buffered saline
pCo	porcine type I/III collagen membrane
PGA	polyglycolic acid
PG	proteoglycan
PI	parallelism index
PJAC	particulated juvenile allograft cartilage
PLA	polylactide
PLGA	poly(lactide-co-glycolide)
PLM	polarized light microscopy
PLGA	poly(lactide-co-glycolide)
PLGA-BGf	poly(lactide-co-glycolide)-bioactive glass fiber scaffold
pRT-PCR	quantitative real-time polymerase chain reaction
rhCo-PLA	recombinant human collagen–poly(L/D)-lactide scaffold
rhCo3-PLA	recombinant human type III collagen–poly(L/D)-lactide scaffold
ROI	region of interest
RT	room temperature
RUNX2	*runt-related transcription factor 2*
SE	standard error
sGAG	sulfated glycosaminoclycan
SOX9	*SRY (sex determining region Y)-box 9*
T_{1Gd}	gadolinium-enhanced T_1 relaxation time
T_1	T_1 relaxation time
T_2	T_2 relaxation time
Tb.N	trabecular number
Tb.Th	trabecular thickness
Tb.Sp	trabecular separation
TE	echo time
TEP	tissue engineered product
TGF-β	transforming growth factor beta
TKA	total knee arthroplasty
TR	repetition time
UK	United Kingdom
VOI	volume of interest
YLD	years lived with disability

1 INTRODUCTION

Articular cartilage is highly specialized connective tissue covering the ends of bones in joints. Cartilage provides joints with low-friction articulating surface and acts as a shock absorber, allowing for painless movement of joints. Injuries to articular cartilage are common and affect people of all ages. They can arise as a consequence of joint torsion injury, fracture, or repetitive loading. Articular cartilage defects of the knee have a prevalence of 11–66% in arthroscopy data (Curl et al. 1997, Hjelle et al. 2002, Aroen et al. 2004, Mor et al. 2015, Everhart et al. 2019). It is estimated that 11% of cartilage injuries documented in arthroscopies are suitable for surgical repair (Aroen et al. 2004). As cartilage is known for its poor repair capacity, the injuries have a tendency to progress to osteoarthritis (OA), which is associated with significant pain and loss of joint function. In Finland, the annual cost of OA accounts for 0.5% of the gross national product (Heliövaara 2008).

Several surgical techniques have been developed in attempt to repair the damaged cartilage and to prevent the progression of OA. In attempt to regenerate healthy articular cartilage, biodegradable materials have been developed, to function as a scaffold and provide the damaged tissue with structural support. Biomaterial scaffolds can be used together with autologous or allogenic cells to improve the healing response. Although cell therapy has improved clinical outcomes of cartilage repair, several limitations associated with these methods remain.

Development of new techniques to tackle the challenge of cartilage repair, as any new therapy, relies on showing their safety and efficacy in animal models before continuing to clinical studies. Each animal model has its strengths and limitations, and it is crucial to understand these properties when designing the study and choosing the animal model.

Despite rigorous research and short-term victories, restoration of the complex structure of fully functional articular cartilage still remains a challenge. Improving biomaterial properties and enhancing neotissue formation with the use of reparative cells could improve the results of cartilage repair, alleviate pain, improve joint functionality and delay, or even hinder, the progress of post-traumatic OA. This study focuses on novel biomaterials and the use of cell therapy both in cell culture and animal models with a translational view from laboratory to clinical setting.

2 REVIEW OF THE LITERATURE

2.1 JOINT STRUCTURE

Synovial joints allow movement of limbs. The general structure of any synovial joint is a synovial fluid-filled cavity where articular cartilage lines the ends of articulating bones (Figure 1). A synovial capsule surrounds the joint. Synovial membrane that lines the inside of the joint capsule is rich in vascular supply. Synovial fluid, produced by the cells of the synovial membrane, lubricates the articulating surfaces and provides nutrition to the cartilage (Buckwalter 2003). Articular cartilage is supported by subchondral bone, which consists of subchondral bone plate and subchondral trabecular bone. The subchondral bone plate includes calcified cartilage and underlying thin layer of cortical bone (Burr 2004).

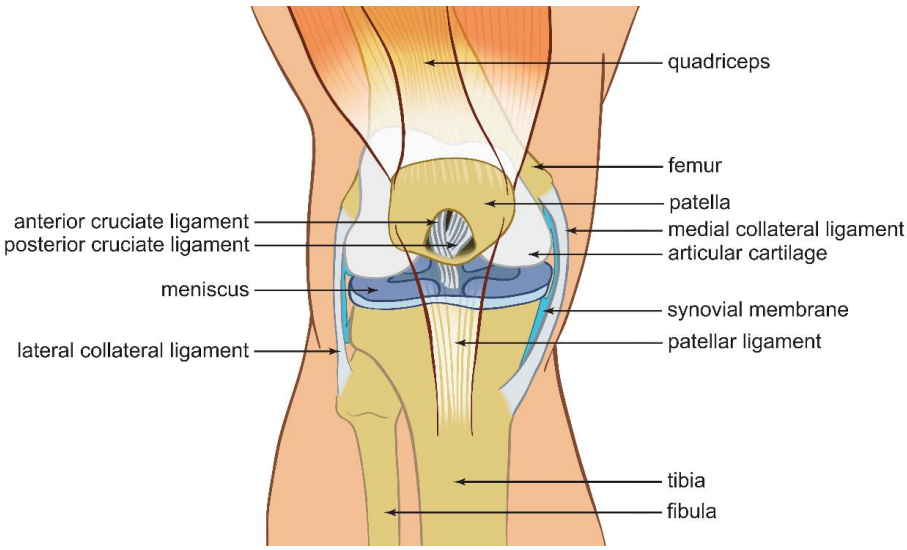

Figure 1 Schematic presentation of the knee joint.

2.1.1 COMPOSITION AND STRUCTURE OF ARTICULAR CARTILAGE

Articular cartilage (hyaline cartilage) covers the abutting ends of bones in joints. It has pearly white macroscopic appearance. Due to its position in the lever system and the vast forces that impact cartilage, its structure needs to be substantially durable. Cartilage provides joints with a smooth, nearly frictionless gliding surface and allows load bearing and shock absorption. These properties are due to the highly specialized structure of the tissue. The main components of the tissue are water, collagens, proteoglycans and

chondrocytes. The specific feature of articular cartilage tissue is that it lacks innervation, blood vessels and lymphatic drainage. This leads to poor intrinsic repair capacity (Buckwalter et al. 2005).

Most of the articular cartilage tissue is composed of extracellular matrix (ECM). During embryonic development, cartilage tissue forms from the mesenchyme as mesenchymal stem cells (MSCs) start to aggregate and express transcription factor SRY (sex determining region Y)-box 9 (SOX9), which activates *procollagen alpha 1 (II)* gene and starts the chondrogenic differentiation (Lefebvre 1997). Cartilage progenitor cells, chondroblasts, produce ECM and while doing so, they are pushed farther away from each other by the matrix. Residing isolated in their lacunae, the cells are called chondrocytes. Being sparse, chondrocytes contribute to only 1–5% of the tissue volume (Buckwalter 2003).

2.1.2 EXTRACELLULAR MATRIX

The dense ECM is composed of water, collagens, glycosaminoglycans (GAGs) and proteoglycans (Figure 2). Water comprises 65–80% of tissue wet weight and accounts for the shock absorbing function of cartilage (Mow et al. 1984). Collagen proteins consist of three polypeptide chains, α chains, that coil into a triple-helical structure to form collagen fibers. The main type of collagen in articular cartilage is type II collagen that constitutes approximately 90—95% of articular cartilage collagen with type IV, V, VI, IX, X, and XI collagens as minor components (Buckwalter 2003, Bhosale 2008).

Hyaluronan, chondroitin sulfate and keratan sulfate are the main GAGs in articular cartilage. GAGs are long polysaccharides that have a negative charge, attracting osmotically active cations. Sulfated GAGs, such as chondroitin sulfate and keratan sufate bind to a protein core, forming proteoglycan monomers, aggrecans (Figure 2c). Hyaluronan is a large non-sulfated GAG. Aggrecan, the main type of articular cartilage proteoglycan, binds with a link protein to a hyaluronan chain to form huge aggregates (Hardingham 1979). One hyaluronan chain typically carries approximately 100 aggrecan monomers, and the molecular weight of the aggregate is 10^8, or more (Mow et al. 1984).

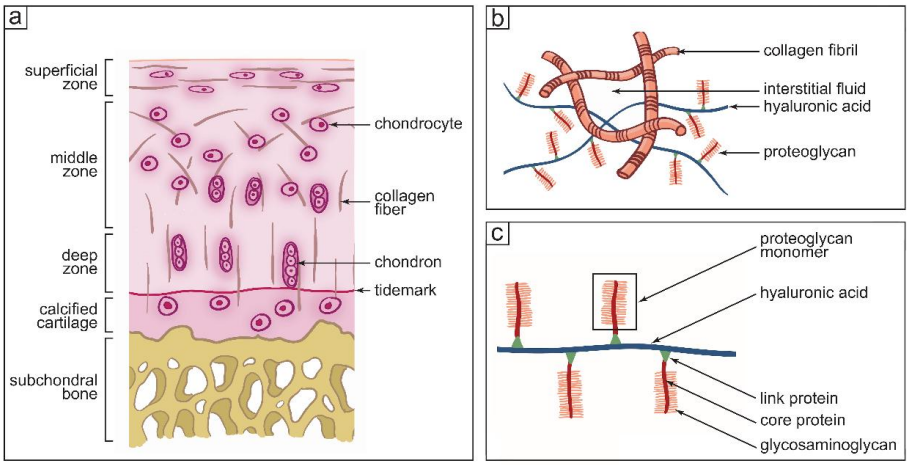

Figure 2 Structure of articular cartilage. a) The zonal organization of articular cartilage and subchondral bone. b) The extracellular matrix is composed of interstitial fluid, collagen fibrils and proteoglycans. c) Glycosaminoglycans, mainly keratan sulfate and chondroitin sulfate, bind to a protein core, which is attached to hyaluronic acid with a link protein.

Cartilage is organized into four distinctive zones by ECM composition and organization (Figure 2a). The superficial zone creates a smooth gliding surface to the articular cartilage. The chondrocytes in this zone are flattened and the collagen fibrils show high anisotropy and organization parallel to the surface, protecting cartilage from shear forces. Unlike in other zones, type I collagen may be present in the superficial zone. The superficial zone accounts for 10–20% of cartilage thickness. (Buckwalter et al. 2005)

The middle or transitional zone makes up approximately 40–60% of articular cartilage thickness. The middle zone contains oval cells, and collagen fibers are organized obliquely (Fox et al. 2012, Buckwalter et al. 2005). The chondrocytes reside at low density in chondrons that are surrounded by ECM.

The deep zone consists of rounded chondrocytes that are organized in a columnar fashion. The highest proteoglycan content and radial orientation of collagen fibers in the deep zone provide protection from compressive forces (Fox et al. 2012). Collagen content and collagen fiber size are the largest in the deep zone and the zone represents approximately 30% of the tissue thickness.

The deep zone is separated from the calcified zone by a tidemark, a mineralization front. Chondrocytes and collagen fibers in the calcified zone are aligned similarly to the deep zone. Hypertrophic chondrocytes of the calcified cartilage express hypertrophy markers such as *type X collagen*, *alkaline phosphatase* and *matrix metalloproteinase-13*. Hypertrophic chondrocytes have the potential to differentiate into osteoblasts to form bone, or become apoptotic, as in growth plates (Anderson 2003). The thick collagen bundles of the deep zone continue to the calcified zone and anchor cartilage tissue to the subchondral bone that lies beneath the calcified zone (Mow et al. 1984).

2.1.3 CARTILAGE FUNCTION AND BIOMECHANICS

The mechanical properties of articular cartilage are closely dependent of its ECM composition (Mow et al. 1984, Lee et al. 2014). As proteoglycans have a strong negative charge, they are responsible of the compressive strength of the articular cartilage via osmotic pressure and swelling of the cartilage tissue. Collagen fibrils limit the swelling and provide the tissue with tensile strength. The mechanical response of articular cartilage is non-linear and dependent on the loading type. Cartilage tissue biomechanics can be modeled as a biphasic medium consisting of a fluid phase and a solid phase (Mow et al. 1984). The extracellular matrix forms the solid phase, and water and inorganic ions form the fluid phase. In biphasic model of cartilage, the solid phase can be further divided to fibrillar modulus representing collagen fibers and non-fibrillar modulus characterizes proteoglycans.

Application of force on cartilage compresses the solid matrix and causes fluid flux out of the ECM. The low permeability of the cartilage, due to compressive stress created by the collagen fibril network and frictional drag of the fluid flow, balances this fluid flow (Maroudas & Bullough 1968, Fox et al. 2012). Constant compressive stress makes cartilage tissue deform until equilibrium strain is reached and fluid flow ceases. As the compressive loading is removed, the hydrophilic, negatively charged proteoglycans of the cartilage ECM have a higher ion concentration than synovial fluid. The Donnan osmotic pressure difference enables the reabsorption of the water and swelling of the cartilage to its original volume (Mow et al. 1984). This controlled water flux leads to the viscoelastic and shock-absorbing properties of cartilage and provides nutrition to the avascular tissue.

The shear stiffness of articular cartilage is due to collagen cross-linking and collagen–proteoglycan interaction (Fox et al. 2012). The parallel orientation of the collagen fibrils in the superficial zone contribute the most to the shear resistance and the perpendicular orientation and high proteoglycan content in the deep zone account for the protection from the compressive stress. Thus, the zonal cartilage structure contributes to the depth-dependent mechanical properties of the tissue with compressive modulus increasing from 0.079 MPa in the superficial zone to 320 MPa in the deep zone (Nooeaid et al. 2012).

Synovial joints are subject to high loads: human knee is subject to loads of 2.5 times body weight during walking and up to 10 times body weight when running (Miller et al. 2015). Physiological loading is required for maintaining normal cartilage function. Dynamic loading increases proteoglycan synthesis through stretch-sensitive ion channels, and immobilization decreases GAG content in cartilage ECM (Kiviranta et al. 1994, Bernhard & Vunjak-Novakovic 2016). Aging and osteoarthritis (OA) increase aggrecan turnover and soften cartilage (DeGroot et al. 2001). Similarly, obesity, unphysiological joint loading and repetitive stresses lead to cartilage damage (Buckwalter et al. 2013).

The half-life of cartilage aggrecan is 3–24 years, allowing cartilage proteoglycans to adapt to changes in joint loading in healthy cartilage

(Maroudas et al. 1998, Verzijl et al. 2001). Collagen, by contrast, has a half-life of more than 100 years, making disruption of collagen molecules irreversible (Maroudas et al. 1998).

Since the mechanical equilibrium is dependent on the solid phase, loss of proteoglycans and disorganization of collagen network lead to impairment of biomechanical properties of the tissue. Cartilage repair procedures aim at restoring the cartilage tissue organization and thus, its functional properties.

2.1.4 SUBCHONDRAL BONE

Subchondral bone is located directly beneath articular cartilage, providing structural support. As an elementary tissue of the musculoskeletal system, bone serves in load-bearing, locomotion and as a mineral reservoir. Bone grows through endochondral ossification from cartilage formed during embryogenesis. Unlike cartilage, bone is vascular tissue. The subchondral bone ECM consists of water, type I collagen and hydroxyapatite. There are three cell types in bone tissue: osteoblasts, osteocytes and osteoclasts. Osteoblasts, the bone forming cells, are responsible for ECM production and mineralization (Han et al. 2018). They are of mesenchymal origin. Osteoblasts that are entrapped by ECM become terminally differentiated osteocytes. They are the most abundant cell type in bone. Osteocytes have a star-shaped phenotype as they develop dendritic-like processes. They produce receptor activator of NFκB ligand (RANKL) and monocyte colony-stimulating factor (M-CSF) that regulate osteoclast differentiation. Osteoclasts are multinucleated cells that are derived from hematopoietic monocyte-macrophage lineage (Suda et al. 1992). Osteoclast is the sole cell type that is capable of resorbing bone. They attach to bone with integrins and through proton pump and chloride channel activity they create an acidic microenvironment that degrades mineralized bone (Teitelbaum 2007). Continuous remodeling by the counteractive action of osteoclasts and osteoblasts maintains the balance between anabolism and catabolism, allowing bone to adapt to changes in loading patterns (Christen et al. 2014).

2.1.5 JOINT HOMEOSTASIS

Joint homeostasis means the physiological equilibrium that maintains normal tissue milieu in the joint (de Grauw 2011). Continuous tissue turnover is needed to adapt to changes in external conditions, such as movement, joint loading, age, and hormonal influences. There is an increasing understanding of joint homeostasis and the interaction of all synovial joint tissues, including meniscus, ligaments, subchondral bone and synovium, in the proper cartilage healing process (Grande et al. 1989, Buckwalter 2003, Gomoll et al. 2010).

Disruption of joint homeostasis is essential in pathogenesis of OA and other joint degenerative diseases. Disturbances in joint homeostasis initiate inflammatory, molecular and cellular changes in the joint, causing increased

matrix catabolism and decreased anabolism. Elevated concentrations of proteoglycan fragments have been documented in both knees after unilateral knee injury, indicating bilateral changes in cartilage metabolism (Dahlberg et al. 1994). Macrophage-like cells in the synovium produce cytokines, such as interleukin-1 and tumor necrosis factor-α, during inflammation and after joint injury (Lee et al. 2009). Matrix metalloproteinases activated by cytokines degrade ECM constitutents (Rose & Kooyman 2016). This degradation is the earliest change seen in OA, and it reduces water retention of the tissue, leading to diminished compression resistance as proteoglycan's level of aggregation is reduced. This appears as softening of the superficial zone and macroscopically as thinning and fibrillation of the cartilage (Moskowitz et al. 2007).

Synovial membrane becomes thickened and increased in vascularity and inflammatory cells in OA. Paracrine and autocrine signals transported via synovial fluid affect tissue turnover and joint homeostasis (de Grauw 2011), and synovial inflammation is typically seen in advanced OA (Loeser et al. 2012). Vascularization of the menisci has also been associated with OA (Loeser et al. 2012).

Articular cartilage is in close proximity to subchondral bone, as discussed above. Diffusion of small molecules and cross-talk between articular cartilage and bone marrow spaces has been shown in mice (Pan et al. 2009, Pan et al. 2012) but whether this cross-talk takes place in human joints is debated (Findlay & Kuliwaba 2016). Activation of endochondral ossification pathway, including chondrocyte hypertrophy, is seen in early stage OA (Glyn-Jones et al. 2015). The increased bone turnover leads to thickening of the subchondral bone. Endochondral ossification leads to osteophytes, joint space narrowing, subchondral cysts and sclerosis, and these features have been used in radiographic classification of OA (Kellgren & Lawrence 1957).

Up to 30% of a joint impact is conveyed through the subchondral bone (Madry et al. 2010). Intralesional osteophytes and subchondral bone cysts have been reported subsequent to cartilage damage and cartilage reparative procedures (Orth et al. 2013). Callus formation and stiffening of the subchondral bone after injury affects the biomechanical properties of the repair cartilage and forces the articular cartilage to absorb a larger part of an impact, which might accelerate its degeneration and predispose the joint for OA (Costa-Paz et al. 2001). Walking on hard surface is demonstrated to cause increased bone volume fraction and cortical stiffness of subchondral bone and decrease the hexosamine content of cartilage, an early indicator of OA (Radin et al. 1982).

Osteochondral defects might have a small degree of spontaneous repair capacity, as bone marrow cells are able to migrate to the defect area through the subchondral plate penetration, although the repair tissue shows inferior properties compared to healthy hyaline cartilage (Bhosale 2008). Subchondral bone and articular cartilage form a functional osteochondral unit, and disruption of either one causes alterations in the other (Pan et al. 2009, Orth et al. 2013).

2.2 CARTILAGE INJURIES

As articular cartilage lacks innervation, some cartilage defects are asymptomatic. The prevalence of cartilage defects is expected to increase, and untreated cartilage defects have a tendency to become symptomatic and to propagate to early-onset OA (Buckwalter 2003). The disabling symptoms associated with cartilage defects include pain, swelling and catching of the joint (McAdams et al. 2010).

2.2.1 PREVALENCE AND ETIOLOGY

Cartilage lesions are common. They vary from small focal defects to deep osteochondral defects. Only a small part of these defects can be repaired with current methods. The prevalence of chondral lesions is reported to be 61–66% in earlier knee arthroscopy studies (Curl et al. 1997, Hjelle et al. 2002, Aroen et al. 2004). A registry study examining knee arthoscopies in Denmark found the prevalence in arthroscopies to be 11% (Mor et al. 2015). The overall prevalence of full-thickness chondral defects in athletes' knees has been shown to be 36% (Flanigan et al. 2010). More recently, the prevalence of full-thickness cartilage defects in knee arthroscopies of athletes under 40 years of age varied between 24–36% (Everhart et al. 2019). Årøen and colleagues suggested that 11% of the cartilage injuries might have been suitable for cartilage reparative procedure (Aroen et al. 2004), whereas in a Danish registry study on arthroscopy-documented cartilage defects, 16.7% of knee cartilage injuries were repaired surgically (Mor et al. 2015). A large part of all cartilage defects occur in elderly people and they often represent the beginning of OA. In the Framingham Osteoarthritis Study based on magnetic resonance imaging (MRI) of the tibiofemoral joint of general population aged 50 years or more, cartilage abnormalities were found in 69% in knees without radiographic signs of OA (Guermazi et al. 2012).

The prevalence of cartilage deterioration is expected to increase rapidly in the following decades as the population ages and the prevalence of obesity increases (Woolf & Pfleger 2003, Heliövaara 2008). The incidence of cartilage lesions is 40/100 000, according to a Danish registry study on knee arthroscopies during the years 1996–2011 (Mor et al. 2015). The incidence was reported to increase by 2.8-fold from 1996 to 2011. Increased popularity of high-demand sports and extreme sports predispose to knee injuries (McAdams et al. 2010, Vannini et al. 2016), and increase in the incidence of sports trauma in the pediatric population predisposes to cartilage trauma at an even younger age (Seto et al. 2010). A retrospective cohort study conducted in Norway showed that the total incidence of cartilage surgery was 56/100 000 during 2008–2011 (Engen et al. 2015). Prosthesis surgery, high tibial osteotomy and patients over 67 years of age were excluded in attempt to omit OA patients from this number.

Factors such as trauma, age, body mass index and unphysiological loading have been associated with cartilage lesions (Buckwalter et al. 2013, Vannini et al. 2016). Årøen and colleagues stated that the most common cause of hyaline cartilage injury is a sports trauma, which accounted for 55% of the injuries (Aroen et al. 2004). Prevention of sports injuries and other traumatic injuries is important in diminishing the prevalence of articular cartilage lesions.

Damage to articular cartilage during normal loading may be due to changes caused by aging and genetic factors. During aging, advanced glycation endproducts (AGEs) accumulate to articular cartilage proteins, decreasing the natural turnover of extracellular matrix proteins and therefore worsening the ability of cartilage to react to environmental changes (DeGroot et al. 2001).

While physiological loading is required for cartilage nutrition and it improves cartilage matrix synthesis, repeated non-physiological joint loading predisposes cartilage to early OA, as shown by Kellgren and Lawrence in the 1950's in a cohort study where miners and cotton workers had more clinical and radiographical OA than people with other occupations (Kellgren & Lawrence 1958). In the same study, overweight was associated with a higher risk of cartilage pathologies.

Joint homeostasis and health of the whole joint also affect cartilage lesions. It has been known for long that meniscectomy and decreased joint congruence such as varus malalignment impair the mechanics of the joints and lead to increased risk of OA (Fairbank 1948, Sharma et al. 2010).

Osteochondral fragmentation and loosening may also be due to osteochondritis dissecans, a joint disease typically affecting children and adolescents (Kessler et al. 2014). Trauma and genetic factors have been proposed as underlying causes of the disease, although the etiology is probably multifactorial (Richie & Sytsma 2013).

2.2.2 DIAGNOSIS

As articular cartilage lacks innervation, cartilage defects may present without pain. Locking and caching of the joint, stiffness and limited function are symptoms associated with cartilage injuries (Buckwalter 2003, McAdams et al. 2010). The diagnosis of cartilage defects requires cartilage imaging or diagnostic arthroscopy.

Conventional radiographs can detect bone abnormalities as well as later signs of cartilage disease such as joint space narrowing, osteophyte formation, subchondral cysts and sclerosis (Kellgren & Lawrence 1957). Radiography can also be used in evaluating the alignment of limbs. However, articular cartilage cannot be seen with radiography and therefore it cannot be used in diagnosing cartilage defects.

Arthroscopy is considered the gold standard of articular cartilage evaluation (Hjelle et al. 2002). It provides direct visualization of the tissue. Although minimally invasive, diagnostic arthroscopy carries the risk of complications and is costly.

Magnetic resonance imaging provides a non-invasive method of evaluating articular cartilage. Conventional MRI sequences, such as T_1-weighted, T_2-weighted, proton density (PD), short tau inversion recovery (STIR), and gradient echo (GE) can be used in evaluating morphological changes of articular cartilage (Liu et al. 2019). The depth of cartilage defect can be evaluated with these techniques but their spatial resolution is limited and they underestimate the size of cartilage defects when compared to arthroscopy (Campbell et al. 2013).

T_1 relaxation time describes the dephasing rate of protons in the longitudinal plane. T_1 has a negative correlation with cartilage water content (Nieminen et al. 2012). The use of this sequence in cartilage imaging is limited with poor contrast between cartilage and fluid (Liu et al. 2019). T_2 relaxation time describes the dephasing rate of protons in the transverse plane after a radio frequency pulse (Guermazi et al. 2015). T_2 relaxation time gives implications on the water content and collagen network of articular cartilage (Nieminen et al. 2012). Similarly, the compositional $T_{1\rho}$ imaging technique can be used to evaluate the collagen network and glycosaminoglycans of cartilage without the use of contrast agents. $T_{1\rho}$ detects slow molecular motion and can therefore be used in evaluating large macromolecules, such as proteoglycans (Nieminen et al. 2012). Delayed gadolinium-enhanced MRI of cartilage (dGEMRIC, T_{1Gd}) is a well validated method of articular cartilage imaging based on T_1 relaxation measurement. It utilizes intravenous administration of gadolinium diethylene triamine pentaacetic acid ($Gd\text{-}DTPA^{2-}$), which distributes inversely to the negatively charged glycosaminoglycans in the joint (Bashir et al. 1996, Guermazi et al. 2015). Thus, it provides information on the glycosaminoglycan content of the tissue (Bashir et al. 1996). Additionally, sodium (Na-23) MR imaging, chemical exchange saturation transfer (CEST), and diffusion-weighted imaging (DWI) are useful imaging techniques for evaluation of the proteoglycan content, although they are not used in the clinical setting (Liu et al. 2019, Guermazi et al. 2015).

2.2.3 CLASSIFICATION

Cartilage lesions may be classified to focal chondral defects and osteochondral defects affecting the subchondral bone. Pure chondral defects can be further divided into partial-thickness and full-thickness defects. Full-thickness defects comprise the entire depth of the cartilage layer, extending to the subchondral bone but not penetrating it.

The Outerbridge classification system, developed in 1961, is the first classification system for cartilage injuries (Outerbridge 1961). Its more recent iteration, the International Cartilage Repair Society Chondral Injury Classification System (ICRS) is the recommended and currently the most commonly used grading systems for cartilage lesions (International Cartilage Repair Society 2000). The ICRS system classifies cartilage defects into four stages according to their severity and depth (Table 1).

Table 1. The ICRS cartilage injury classification.

Grade 0	Normal	
Grade 1	Nearly normal	Superficial lesions or softening, superficial fissures or cracks
Grade 2	Abnormal	Lesions <50% of cartilage depth
Grade 3	Severely abnormal	Lesions >50% of cartilage depth
Grade 4	Severely abnormal	Osteochondral defects penetrating the subchondral bone

2.2.4 OSTEOARTHRITIS AND POST-TRAUMATIC OSTEOARTHRITIS

OA, a degenerative disease of articular cartilage, is the most common joint disease. There are over 237 million OA patients globally, and its worldwide prevalence in over 60-year-olds is 10% for men and 18% for women (Glyn-Jones et al. 2015, Vos et al. 2016). OA is known to develop as a consequence of several biologic, mechanical and structural factors that affect joint homeostasis, but much of the processes responsible for the progression is still unclear (Carbone & Rodeo 2017).

OA is a progressing disease that leads to premature cartilage loss and symptoms that impair the quality of life. However, the plateau stage between the injury and development of OA varies and might be long (Carbone & Rodeo 2017). Non-operative treatment options include physiotherapy and muscle strengthening exercises as well as pain medication. The operative treatment options for end-stage OA are joint replacement and osteotomies for selected patient groups (Coventry 1973, Brouwer et al. 2014). Evidence shows that arthroscopic debridement has no benefit in knee OA (Laupattarakasem et al. 2008).

Post-traumatic osteoarthritis (PTOA) is degeneration of articular cartilage secondary to a joint injury. It has been estimated that PTOA accounts for 12% of overall burden of OA (Brown et al. 2006, Carbone & Rodeo 2017). Treatment of intra-articular fractures and good alignment of the joint surface are also important factors in preventing PTOA. Since PTOA often affects young, active adults, delaying the onset of OA is crucial (Gelber et al. 2000, Flanigan et al. 2010).

2.2.5 SOCIETAL IMPACT AND COST

Cartilage lesions and OA have a tremendous social and economic impact to the society. Cartilage injuries typically affect young and middle-aged, physically active patients (Gelber et al. 2000). Advancing cartilage defects are associated with pain, limitations in activities and reduced quality of life. Although some early stage cartilage defects might be asymptomatic due to the aneural nature

of the tissue, focal articular cartilage defects can affect the quality of life of a patient as much as advanced OA (Heir et al. 2010).

In Germany, the overall cost of a cartilage repair ranges from 13 445€ to 21 204€, depending on the surgical technique. These costs include surgery and hospital stays, imaging, physiotherapy and medication (Koerber et al. 2013).

As untreated cartilage defects have a tendency to propagate to OA, the impact and cost of OA cannot be overlooked when evaluating the outcomes of cartilage injuries. OA is the thirteenth most common cause of years lived with disability (YLD) (Vos et al. 2016). Both the prevalence and YLD of OA are increasing. PTOA has an increasing prevalence with age. YLD of OA has increased with 32.9% in the general population and 3.9% in age-standardized YLDs during the years 2005—2015 (Vos et al. 2016). The suggested treatment option for end-stage OA is total knee arthroplasty (TKA). A total of 12 251 primary knee prosthesis operations were carried out in Finland in 2016 (THL 2018), and the number of the operations is increasing.

The cost of OA in Northern America, United Kingdom, France and Australia accounts for 1% to 2.5% of gross national product. In Finland, OA leads to annual cost of one billion euros in Finland, approximately 0.5% of the Finnish gross national product (Heliövaara 2008). In addition to the direct costs of OA, there is an eight times greater indirect cost that includes loss of productivity, workforce absenteeism, early retirement, leading to reduced taxation revenue (Hunter et al. 2014). Moreover, OA was the cause of 10% of new Finnish disability pensions in 2017 (Eläketurvakeskus ja Kansaneläkelaitos 2018). Thus, the overall cost of OA is often underestimated. Successfull treatment that would reduce disability, preserve the joint and postpone or even obviate the need for joint arthroplasty of even a small proportion of cartilage defects would mean considerable health care cost savings, and improve quality of life and activity level of those affected.

2.3 TREATMENT OF CARTILAGE INJURIES

The difficulty to treat damaged cartilage was noted as early as in 1743 (Hunter 1743). Due to the limited healing capacity and the societal and socioeconomic burden caused by progressed cartilage defects and post-traumatic OA, there is a high attempt to repair articular cartilage defects in an early phase.

Cartilage defects can be managed surgically and non-operatively. Symptom relieving and non-surgical treatment strategies include pain relief with paracetamol or non-steroidal anti-inflammatory drugs (NSAIDs) and physical therapy to improve joint stability, muscle strength and neuromuscular control (Vannini et al. 2016). Rehabilitation and physical therapy are also an important part of the aftercare of surgical procedures. Advanced cartilage defects and osteoarthritis are also being treated with intra-articular injections of corticosteroids, glucosaminoglycans and hyaluronic acid (viscosupplementation). These injections are thought to improve the

mechanical properties of synovial fluid (Peyron & Balasz 1974) and diminish inflammatory cytokines in the joint (Wang et al. 2006). Injections of platelet-rich plasma, blood with supraphysiological concentration of platelets, have also been used as they possess non-inflammatory and anabolic properties, but their clinical efficacy is being debated (Johal et al. 2019). Nutraceuticals, such as glucosamine and chondroitin, lack clinical evidence and should not be used (Runhaar et al. 2017). Although these non-surgical approaches are widely used, they are incapable of producing new cartilage tissue and restoring joint function in the long term. Therefore, surgery is required.

Cartilage repair surgery has evolved from simply removing loose particles and lavaging the joint to current technically demanding procedures. At present, surgical cartilage repair techniques include marrow stimulation, osteochondral transfer, and chondrocyte implantation (Table 2). The choice of the surgical treatment procedure depends on the age and possible previous treatment attempts of the patient as well as the size and location of the defect (de Windt et al. 2009, Nakagawa et al. 2016). Although several different surgical treatment options have been developed, no treatment has demonstrated superiority over another in long-term studies (Filardo et al. 2013).

Review of the literature

Table 2. Comparison of currently used cartilage repair procedures.

Procedure	First described	Type of procedure	Technique	Scaffold	Tissue or cell transplantation	Suitable defect size [f,g]
OCA	Gross 1975 [a]	Osteochondral transfer	Osteochondral grafts taken from a cadaveric donor and transplanted to the defect site.	NO	YES	>4cm^2
OAT	Hangody 1997 [b]	Osteochondral transfer	Multiple osteochondral grafts taken from the patient's knee and transplanted to the defect site.	NO	YES	<2—4 cm^2
MF	Steadman 1997 [c]	Marrow stimulation	Creating holes into subchondral bone to introduce mesenchymal stem cells to the lesion bed to form fibrocartilage.	NO	NO	<2 cm^2
AMIC	Behrens 2003 [d]	Marrow stimulation	MF together with a stabilizing biomaterial.	YES	NO	<4 cm^2
ACI	Peterson 1994 [e]	Cell therapy	Harvest and culture of chondrocytes that are in a second operation implanted into the chondral defect.	YES*	YES	>4 cm^2

Abbreviations: OCA, osteochondral allograft; OAT, osteochondral autograft transfer (mosaicplasty); MF, microfracture; AMIC, autologous matrix-induced chondrogenesis; ACI, autologous chondrocyte implantation.

*Scaffolds are used in the second and third generation ACI.

References [a](Gross et al. 1975), [b](Hangody et al. 1997), [c](Steadman et al. 1997), [d](Behrens 2005), [e](Brittberg et al. 1994), [f](Biant et al. 2015), [g](Richter et al. 2016).

2.3.1 DEBRIDEMENT AND MARROW STIMULATION

Magnuson was the first to describe joint debridement (Magnuson 1941). This simple procedure involves removal of loose particles and leveling the uneven cartilage surface in an open arthrotomy. Debridement and joint lavage aim at brief symptom relief rather than regenerating the articular cartilage tissue. This method does not slow down the process of OA and it might lead to degeneration of the remaining articular cartilage (Kim et al. 1991). Based on the early debridement techniques, Johnson developed abrasion arthroplasty, which is an arthroscopic technique where damaged cartilage and the superficial layer of subchondral bone is removed (Johnson 1986).

Spongialization was proposed by Ficat (Ficat et al. 1979). This is a more radical version of abrasion arthroplasty, as it involves removal of damaged cartilage and the entire subchondral bone and reveiling spongiosa. It is now known that subchondral bone plays an essential role in the mechanical support of the joint, and this technique has been abandoned (Orth et al. 2013).

Marrow stimulation techniques stimulate cells from the bone marrow to migrate to the lesion bed and initially form a blood clot that is later replaced by a fibrocartilaginous scar. In 1959, Pridie (Pridie 1959) was the first to conceive the concept of drilling holes into the subchondral bone to promote spontaneous healing response through marrow-derived cells in osteoarthritic patients. In his original publication, Pridie recommended using a drill bit with the diameter of ¼ of an inch (6.4 mm). The method of Pridie drilling has been modified by Steadman who introduced microfracture technique (Steadman et al. 1997). This treatment is performed with an arthroscopic awl, creating much smaller holes, 2—3 mm in diameter, 3—4 mm apart. Using the awl eliminates heat necrosis associated with drilling (Steadman et al. 1997). Microfracture has been considered the gold standard of cartilage repair, although this status has recently been challenged due to the lack of standardized studies and high scientific evidence (Frehner & Benthien 2018). However, it has remained the most commonly used cartilage repair technique (Gobbi et al. 2014) and it is often used as a control in clinical trials evaluating cartilage treatment methods. A query study found out that 93.7% of all cartilage procedures performed by recently trained orthopaedic surgeons in the United States were marrow stimulation procedures, although the incidence was declining (Frank et al. 2019). Microfracture can be performed arthroscopically, and its other benefits are technical easiness, low costs and fast mobilization of the patient. It is suitable for treatment of small defects (Table 2) (Biant et al. 2015). Microfracture enables 58–66% of athletes to return to sports, and this is achieved 8±1 months post surgery (Mithoefer et al. 2009a). Sports participation continues for 52±6% of the patients (Krych et al. 2017). Microfracture provides improved clinical scores and decreased pain but normal hyaline cartilage cannot be restored. The forming fibrocartilage is less durable than hyaline cartilage and the good initial results deteriorate at 24

months post surgery in most studies (Mithoefer et al. 2009b, Gobbi et al. 2014, Makris et al. 2015). Another complication of microfracture is formation of subchondral cysts in up to 33% of the patients (Mithoefer et al. 2009b).

Chen and colleagues found out that deeper subchondral bone perforations produced superior tissue quality (Chen et al. 2011). Thus, microfracture procedure has recently been further improved with nanofracture technique (Benthien & Behrens 2015), in which a one millimeter thick needle and cannulated pick are used to create standardized subchondral bone perforations that are smaller and deeper than in microfracture, to avoid bone compaction around the awl perforations.

In addition, biomaterial scaffolds have been introduced to microfracture technique to provide the matrix with mechanical stability, as discussed in chapter 2.3.5.

2.3.2 OSTEOCHONDRAL TRANSPLANTATION

Osteochondral transplantation is a reconstructive cartilage procedure with various subtypes. It can be performed with autologous or allogenic grafts from a donor. The axiom of these procedures is that the transferred tissue is immediately functional without maturation time.

Lexer was the first to describe joint allograft transplantation using fresh amputated limbs (Lexer 1908) and cadaveric tissue (Lexer 1925). Gross and colleagues used this technique for PTOA and tumor reconstruction (Gross et al. 1975). Nowadays, fresh osteochondral allografts (OCA) can be used to treat large cartilage defects. A whole joint specimen is collected and restored in nutritive medium. In an athrotomy, a size-matched allograft osteochondral plug is harvested from the donor and press-fitted to the host defect site. The use of allografts obviates the donor site morbidity and does not limit the size of the treatable defect. Ten-year results have shown improved pain and function scores (Cameron et al. 2016). 88% of the patients are able to return to sports, and this is achieved 10±3 months after the surgery (Mithoefer et al. 2009a, Krych et al. 2017). The survivorship of fresh allografts in distal femur has been 91% at 10 years (Cameron et al. 2016, Raz et al. 2014) and 59% at 25 years (Raz 2014). Continued sports participation at preinjury level is 52% (Mithoefer et al. 2009a).

Chondrocyte viability and matrix degeneration limit the use of frozen grafts, whereas refrigerated grafts maintain a 67% chondrocyte viability for 44 days (Pearsall et al. 2004). The risk of disease transmission is decreased by screening the donor for infectious diseases. This screening, however, delays transplantation and decreases cell vitality in the transferred plugs. Osteochondral allografts have also been associated with fissuring and delamination, which lead to poor outcome (Chahal et al. 2013).

Osteochondral autograft transplantation was first reported in 1964 by Wagner (Wagner 1964). In the early 1990's, Matsusue (Matsusue et al. 1993) and Bobic (Bobic 1996) transplanted multiple osteochondral grafts. Bobic

named this method osteochondral autograft transplantation (OAT). Hangody popularized this method by publishing his report on mosaicplasty (Hangody et al. 1997), in which several small osteochondral plugs are harvested from a low-weight-bearing area with a hallow burr and then transferred to the lesion site. The gaps between the plugs are spontaneously filled with fibrocartilage.

Arthroscopic autologous osteochondral grafting has been reported with good results in short term (Barber & Chow 2006) and in a long term study evaluating patient reported outcomes (Hangody & Fules 2003). Return to sports is fast (5±2 to 7±2 months post surgery) and achieved for over 90% of the patients (Mithoefer et al. 2009a, Krych et al. 2017). The results have shown worsening and degeneration progression in longterm studies (Gudas et al. 2012, Filardo et al. 2015), with a failure rate of up to 55% in a 10-year follow-up (Bentley et al. 2012). The autograft survival has been 62.5% at 9–10 years (Tetta et al. 2010). Continued sports participation at preinjury level is 52±21% at 7 years post surgery (Krych et al. 2017). The main limitations of this technique are donor site morbidity and poor integration of the plugs with the host tissue (Hangody & Fules 2003).

2.3.3 MINCED CARTILAGE FRAGMENTS

Single-step chondral repair by transferring cartilage fragments is a relatively new method of cartilage repair. The fragments can be particulated juvenile allograft cartilage (PJAC) or autologous fragments secured to the defect site by a scaffold (CAIS, cartilage autograft implantation system) (Bonasia et al. 2015). More clinical studies are still needed to evaluate their effectiveness.

The use of autologous cartilage fragments in the treatment of cartilage defects was first described by Albrecth in a rabbit model (Albrecht et al. 1983). The clinical operation technique was first described by Cole and colleagues (Cole et al. 2011). Hyaline cartilage is first harvested from a low weight-bearing area of the joint. The harvested cartilage is then particulated into 1 to 2 mm pieces and dispersed onto a biodegradable scaffold by a device (DePuy Mitek). Fibrin glue is used to secure the pieces on place. The CAIS construct is then fixed to the cartilage lesion site with bioabsorbable staple anchors.

Juvenile chondrocytes possess a 100-fold ability to synthesize proteoglycans compared to adult chondrocytes (Yanke & Chubinskaya 2015). The PJAC procedure relies on a commercial product of pieces of juvenile cartilage, harvested from donors younger than 13 years. The cartilage pieces are mixed with fibrin glue and then transplanted onto the cartilage defect. PJAC has provided symptom alleviation in short to medium term (Buckwalter et al. 2014, Bonasia et al. 2015, Wang et al. 2018) but it provides no additional benefit in the appearance of cartilage in postoperative imaging (Wang et al. 2018). Several issues remain. The long-term fate of the juvenile cartilage fragments and the superiority of juvenile tissue over mature cartilage have not been established, and the source of juvenile cartilage is a disadvantage due to ethical considerations (Yanke & Chubinskaya 2015).

2.3.4 CELL-BASED THERAPIES

2.3.4.1 Autologous chondrocyte implantation

Autologous chondrocyte implantation (ACI) is the first cell-based therapy for articular cartilage repair. The concept was introduced in the 1980's in a rabbit model (Grande et al. 1989). In October 1987, the first ACI procedure was performed in a human knee by Lars Peterson and colleagues in Gothenburg, Sweden, and the first pilot results were published in 1994 (Brittberg et al. 1994). In this two-stage surgical procedure, the patient's own chondrocytes are harvested from a less-weight-bearing surface of the femur. The cells are then cultured in a laboratory to increase the cell yield. After 2—3 weeks, in a second surgery, the defect site is debrided and a periosteum graft is sutured onto the defect. The cultured chondrocytes are then injected underneath the graft with a density of 0.5—1 million cells/cm^2, and the graft is then sealed with fibrin glue to minimize cell leakage. Long-term studies have shown clinical improvement (Minas et al. 2014) that is maintained for 20 years (Peterson et al. 2010), as well as a satisfactory 20-year survival rate of 63% (Ogura et al. 2017).

The ACI method is technically challenging, costly, and the requirement of autologous chondrocytes limit the use. Additionally, a long recovery time of 6—12 months after the surgery is required for the maturation of the neotissue (Makris et al. 2015). Return to sports is possible 18±4 months post surgery (Mithoefer et al. 2009a). Given these limitations, ACI accounted only for 2% of all cartilage procedures were carried out with the ACI method in the public sector in Norway in 2008—2009 (Engen et al. 2015) and 1.3% of cartilage procedures carried out by recently trained orthopaedic surgeons in the United States (Frank et al. 2019). Despite the limitations of the method, ACI is the recommended procedure for large chondral defects exceeding 4 cm^2 (Table 2) (Biant et al. 2015, National Institute for Health and Care Excellence (NICE) 2017).

2.3.4.2 Chondrocytes

In 1968, Chesterman and Smith were the first to isolate and transplant lapine articular chondrocytes (Chesterman & Smith 1968). Their findings laid ground to the development of ACI technique and autologous cell transplantation with improved techniques has since been accepted for clinical use. Being the naturally occurring cell of articular cartilage and surviving the anaerobic environment of avascular cartilage, autologous chondrocyte is a widely used cell type for cartilage repair. Chondrocytes are phenotypically right without the need to differentiate them, and they are able to produce the extracellular matrix of cartilage tissue.

Requirement of two separate surgeries is the major shortcoming of this method. The availability of chondrocytes is limited, leading to the need for cell culture to expand the cell yield. This is a concern as chondrocytes have a tendency to dedifferentiate during cell culture expansion (Benya et al. 1978). Previous *in vitro* studies with cadaveric human chondrocytes have confirmed that during multiple passaging up to passage 6, mRNA levels for type II collagen decrease after each passage and type I collagen levels increase already at passage 1 and remain high thoughout the passaging (Diaz-Romero et al. 2008).

2.3.4.3 Mesenchymal stem cells

The tendency of chondrocytes to dedifferentiate during cell culture has sparked the search for novel cell sources. The presence of non-hematopoietic stem cell population in bone marrow was first described by Friedenstien in the late 1960's (Friedenstein et al. 1966). Human mesenchymal stem cells (mesenchymal stromal cells, MSCs), harvested from the posterior ilic crest of volunteer donors, were first isolated and cultured by Haynesworth and Caplan (Haynesworth et al. 1992). As defined by the International Society for Cellular Therapy position statement, MSCs are pluripotent cells that are defined by their adherence to plastic, their capacity to differentiate into several cell lineages including osteoblasts, chondroblasts and adipocytes, and their expression of certain cell surface markers (positive for CD73, CD90 and CD105; negative for CD14, CD11b, CD79a, CD34, CD45 and HLA-DR) (Dominici et al. 2006, Murphy et al. 2013). Alongside bone marrow, which is the most commonly used source in the clinic, MSCs can be obtained from adipose tissue, dermis, periosteum and synovial membrane (Mollon et al. 2013).

Chondrogenic differentiation of MSCs *in vitro* has often been associated with chondrocyte hypertrophy and entering ossification pathway (Chen et al. 2015). Still, MSCs attract great interest for cell-based cartilage repair therapy due to their easy isolation, high proliferative capacity, and ability to differentiate into chondrocytes and osteoblasts (Makris et al. 2015). MSCs also maintain their chondrogenic capacity through multiple passaging (Yoo et al. 1998). Recent research suggests that instead of differentiating into building blocks of repair tissue, the most important function of MSCs in cartilage repair is their release of growth factors, cytokines and other trophic factors that guide tissue regeneration (Murphy et al. 2013, Caplan 2017). Clinical studies utilizing both injected and scaffold-seeded bone marrow-derived MSCs have shown good short-term results (Makris et al. 2015). Given these advantages, MSCs hold great potential for cartilage regeneration.

2.3.4.4 Other stem cells

Embryonic stem cells (ESCs) are cells with the ability to proliferate in an undifferentiated state and later differentiate into any somatic cell (Thomson et al. 1998). Chondrogenesis can be achieved by forming an embryoid body and then selecting mesodermal cells, or by transforming ESCs into MSCs prior to their chondrogenic differentiation (Hwang et al. 2008). The use of ESCs is highly debated due to ethical issues regarding cell harvesting and teratoma formation associated with the use of ESCs (Heng et al. 2004).

Ethical concerns of ESCs can be avoided by using induced pluripotent stem cells (iPSCs). These cells are pluripotent cells derived from somatic cells such as skin (Takahashi & Yamanaka 2006). Their pluripotency is achieved by virally transducing them with transcription factors. They have shown good chondrogenic differentiation potential and less chondrocyte hypertrophy than chondrogenically differentiated MSCs *in vitro* and *in vivo* (Bernhard & Vunjak-Novakovic 2016). Limitations of iPSCs are inadequate cell yield for mass production, genomic instability, and teratoma formation when implanted (Mollon et al. 2013, Bernhard & Vunjak-Novakovic 2016).

2.3.5 SCAFFOLD-BASED THERAPIES

Culturing chondrocytes in a two-dimensional plate causes them to dedifferentiate (Benya et al. 1978). This has initiated the development of three-dimensional scaffolds, which are thought to reverse the dedifferentiation of chondrocytes (Martinez et al. 2008), and to provide mechanical and structural support to the forming repair tissue to restore function at the damaged cartilage area (Dhollander et al. 2011).

Biomaterials have been introduced to ACI to avoid cell suspension leakage, periosteal flap hypertrophy and lengthy operation time of the first generation method described in the 1990's (Brittberg et al. 1994, Harris et al. 2010). In the second generation ACI, a bilayer membrane produced of porcine type I/III collagen is used instead of the periosteum (Filardo et al. 2013). The biomaterial obviates the problems encountered with the graft, and a statistically significant improvement in Lysholm and IKDC scores have been reported in a matched-pair study comparing first and second generation ACI at 10 years postoperatively (Niemeyer et al. 2014). Clinical results of second generation ACI have been good up to 10 years postoperatively (Berruto et al. 2017). For first and second generation ACI, Mithoefer reported an average of 67% return to sports rate (Mithoefer et al. 2009a), whereas in their meta-analysis, Krych and colleagues found the rate to be 82% (Krych et al. 2017).

Third generation ACI (MACI; matrix-applied characterized autologous cultured chondrocytes) utilizes constructs with cells implanted and grown on an animal-originated type I/III collagen membrane before implantation and the construct is secured in place with fibrin glue instead of sutures. This allows for a more even cell spreading and provides the cells with a three-dimensional environment and better structural support. Glue fixation improves the ease of

use of the implant. The use of scaffolds enables repair of large cartilage lesions, shortens procedure time, and improves surgical consistency (Saris et al. 2014). MACI is the most common cartilage repair technique utilizing scaffolds and cells (Makris et al. 2015) and it has shown improved KOOS as well as improved defect filling in MRI at two and five years after the surgery (Saris et al. 2014, Brittberg et al. 2018). The scores were higher for patients receiving MACI treatment than for microfracture. The study, however, showed no statistically significant difference in the defect filling when compared to microfracture treatment.

Microfracture technique, the gold standard treatment for small cartilage defects, has evolved with the introduction of scaffolds. Autologous matrix-induced chondrogenesis (AMIC) technique combines microfracture with a bilayer porcine collagen membrane (Behrens 2005). The procedure was first described by Behrens and colleagues in 2005. This procedure can be performed within a single surgery and it permits treatment of larger defects than the traditional microfracture technique. A study reporting mid-term results demonstrated an improvement of Lysholm, ICRS, Tegner and Cincinnatti scores at 48 months postoperatively (Gille et al. 2010). In a 5-year RCT study comparing AMIC with microfracture, functional ICRS Cartilage Injury Standard Evaluation Form-2000 score improved from 92.3% of abnormal function to 66% in the microfracture treated group and from 100% to 0–7% in the AMIC group five years after the surgery, although histological evaluation showed that the repair tissue in both microfracture- and AMIC-treated groups was fibrocartilage (Volz et al. 2017). Improved IKDC and Lysholm scores were also reported in a study with 7 years of follow-up (Schiavone Panni et al. 2018).

2.3.6 BONE GRAFTING

Bone grafting fills voids, promotes healing and provides mechanical support. It has been estimated that the annual number of bone grafting procedures is 2.2 million in the world (Lewandrowski et al. 2000). Autologous bone, bone graft taken directly from the patient, is considered the gold standard of bone grafting (Pape et al. 2010). Cancellous bone is most often taken from the anterior or posterior iliac crest. Autograft harvesting may cause donor site morbidity including pain, hemorrhage, nerve injury, and wound infection. Allografts from tissue banks are usually taken from a cadaver donor or from prosthesis surgery. Allografts carry the risk of disease transmission and immunological reactions. Due to the limitations of allograft and autograft bone, tissue engineered bone fillers have been developed, as discussed in chapter 2.4.2.

2.3.7 CHOICE OF SURGICAL METHOD

The choice of surgical method depends on several factors, such as the size and depth of the cartilage defect, previous repair attempts, and the age and physical demands of the patient (de Windt et al. 2009, Nakagawa et al. 2016). The consensus of 104 surgeons based in the United Kingdom (UK) states that articular cartilage defects smaller than 2 cm^2 are suitable for treatment with microfracture or osteochondral grafting, whereas defects larger than 4 cm^2 should be repaired with cell-based techniques (Table 2) (Biant et al. 2015). According to the guidelines of National Institute for Health and Care Excellence (NICE) of UK, only ACI is considered effective for treatments larger than 2 cm^2 if non-surgical treatment does not alleviate symptoms (NICE 2017). Treatment of the smallest cartilage defects of <1 cm^2 is not considered beneficial (Biant et al. 2015).

2.4 BIODEGRADABLE BIOMATERIALS IN TISSUE ENGINEERING

Biomaterials are defined as materials that are "*intended to interface with biological systems to evaluate, treat, augment or replace any tissue, organ or function of the body*" (Nair & Laurencin 2007). They can be divided into metals, ceramics and polymers. In medicine, they can be used as temporary prostheses, scaffolds for tissue regeneration, and in drug delivery (Nair & Laurencin 2007). In cartilage repair, they are used to restore the architecture of the cartilage tissue and to support tissue growth. Multiphasic scaffolds that combine biomaterials with different properties to match the architechture of different cartilage layers or cartilage and subchondral bone are used to treat osteochondral defects. Biomaterials used in tissue engineering applications need to degrade over time to give way to newly formed tissue, be biocompatible, give sufficient mechanical support, and not cause inflammatory or toxic reactions (Nair & Laurencin 2007, Bernhard & Vunjak-Novakovic 2016).

Polymeric biodegradable biomaterials for tissue engineering can be in form of gels, porous or fibrous scaffolds, or a combination of these. Hydrogels have been developed to mimic the high water content of cartilage extracellular matrix. They are made of natural or synthetic polymer networks that are rich in water (Bernhard & Vunjak-Novakovic 2016). They should have good biocompatibility, low friction and they are capable of maintaining the spheroid shape of cells (Camarero-Espinosa & Cooper-White 2017). Hydrogels typically have low mechanical strength limiting their use in weight-bearing applications (Bernhard & Vunjak-Novakovic 2016). Porous and fibrous sponges and rigid scaffolds have an improved mechanical strength, making them more suitable in weight-bearing applications (Camarero-Espinosa & Cooper-White 2017).

2.4.1 BIOMATERIAL SCAFFOLDS IN CARTILAGE REPAIR

2.4.1.1 Natural biomaterial scaffolds in cartilage repair

Based on their origin, biomaterials can be classified into natural and synthetic materials. Natural biomaterials were the first biodegradable materials used in a clinical setting. Natural polymers are often extracted from animal tissues, plants or algae. They have good bioactivity and they can be degraded and remodeled by natural pathways. Natural tissue engineered scaffolds mimic tissue environment. However, the major intrinsic limitation of these natural materials is their inadequate mechanical strength, immunogenic responses and batch-to-batch variation. (Nair & Laurencin 2007)

Carbohydrate-based materials, such as hyaluronan, chitosan and polyethylene glycol, are highly hydrophilic cross-linked polymers. As hyaluronan is an important component of extracellular matrix of chondrocytes, hyaluronan hydrogels have good chondrocyte attachment properties (Bernhard & Vunjak-Novakovic 2016) and they promote mesenchymal cell differentiation (Nair & Laurencin 2007). Chitosan, a glucosamine polysaccharide typically derived from crustacean chitin, has improved histological results when used together with microfracture to stabilize the blood clot, as compared to microfracture alone (Methot et al. 2016), and good clinical results at 5 years (Shive et al. 2015).

Protein-based materials, such as collagen, fibrin and gelatin, have good cell attachment properties. Collagen has a vital role in the normal extracellular matrix, and it builds the base for the most commonly used biomaterials in cartilage tissue engineering (Filardo et al. 2013). Collagen-based biomaterials have improved the results of cartilage repair in the ACI and AMIC methods (Niemeyer et al. 2014) with type I collagen being the most commonly used collagen type in the scaffolds (Huang et al. 2016).

Collagen scaffolds are typically produced with bovine- or porcine-based materials. Use of these xenogenic, *i.e.,* animal-derived products, however, carries the risk of disease transmission, the complex purification process of collagen leads to batch-to-batch variation, and immunogenic responses are possible (Horwitz et al. 2002, Heiskanen et al. 2007, Yu et al. 2015). Recombinant technique can produce animal component-free proteins in a scalable, cost-effective manner and with uniform product quality (Baez et al. 2005). Human recombinant type II collagen has been successfully used in cartilage repair in mouse and rabbit models (Pulkkinen et al. 2010, Pulkkinen et al. 2013a). Although recombinant human collagens are not yet used in treating cartilage defects in the clinic, there is clinical evidence on the safety and efficacy of the use of recombinant collagens in ophtalmic applications (Fagerholm et al. 2014).

2.4.1.2 Synthetic biomaterial scaffolds in cartilage repair

Synthetic materials can be manufactured into different shapes and their properties can be readily modified. Fabrication of synthetic polymers can be scaled up to industrial-scale manufacturing. Polyesters, such as polylactic acid (PLA) and polyglycolic acid (PGA) are frequently used synthetic bioabsorbable materials as they degrade by hydrolysis of ester linkage. (Nair & Laurencin 2007)

PLA is a synthetic polymer that is degraded by hydrolysis into lactic acid and metabolized through the citric acid cycle. PLA contains methyl side groups making it hydrophobic and thus reducing its degradation rate. PLA has a high compressive strength. PGA is a synthetic polymer that also degrades by hydrolysis but lacks methyl side groups and thus, it is more hydrophilic and faster degraded than PLA. Copolymer of PLA and PGA can be used in both cartilage and bone repair (Uematsu et al. 2005, Pan et al. 2015).

Several other synthetic biomaterials have been proposed, although not many of them have been used in the clinic. Polyglactin 910/poly-p-dioxanone fleece together with fibrin solution has been used in MACI cartilage repair with good clinical results and complete filling in 73% of patients after 48 months post implantation (Kreuz et al. 2011).

Limitations of synthetic materials include low hydrophilicity and inferior cell attachment properties compared to natural materials (Bernhard & Vunjak-Novakovic 2016). Therefore, hybrid scaffolds combining synthetic and natural components are being developed (Nair & Laurencin 2007).

2.4.2 BIOMATERIALS FOR SUBCHONDRAL BONE REGENERATION

Treatment of osteochondral defects is challenging due to the different demands and dissimilar intrinsic healing capacity of cartilage and bone tissue. The repair material should integrate well to both the surrounding bone and cartilage. The requirements of an optimal bone filler include architectural resemblance of natural bone and highly porous structure with interconnected pores that allow angiogenesis and tissue infiltration (Oryan et al. 2014). Osteochondral scaffolds can be single-phased, or layered biphasic and multiphasic to fulfill the requirements of both tissues (Kon et al. 2014). Only a few clinical studies have investigated biomaterials intended for osteochondral repair (Kon et al. 2018, Di Martino et al. 2015), although bone substitutes and cartilage repair matrices have been extensively studied individually (Lopa & Madry 2014).

2.4.2.1 Natural tissue engineered materials in bone regeneration

Bone grafts have traditionally been decellularized biologic bone grafts that retain the original bone architecture and have excellent biocompatibility (Camarero-Espinosa & Cooper-White 2017). Demineralized bone matrix is

allogenic or xenogenic bone where the mineral component has been removed. It is one of the most popular bone graft substitutes with both osteoconductive and osteoinductive properties (Gruskin et al. 2012). Tissue engineered xenograft, have gained popularity due to their controllable properties as well as superior biocompatibility and regenerative properties compared to synthetic materials (Oryan et al. 2014). Immunological responses and batch-to-batch variation are major disadvantages of using natural materials, as discussed above.

Natural polymers, such as collagen, fibrin and chitosan are used in tissue engineering of bone (Lee et al. 2014). Collagens, especially type I collagen as a natural component of bone ECM, are non-toxic polymers with good biocompatibility and high availability (Oryan et al. 2014). Developed for osteochondral repair, a multilayered scaffold combining equine collagen and hydroxyapatite has shown promising clinical results at a 2-year follow-up (Di Martino et al. 2015, Kon et al. 2018).

2.4.2.2 Synthetic tissue engineered materials in bone regeneration

Inorganic materials, such as ceramics, calcium phosphates and bioactive glasses promote biomineralization (Nooeaid et al. 2012). Calcium phosphate ceramics, such as hydroxyapatite and β-tricalcium phosphate, are osteoconductive as their mineral composition is similar to natural bone mineral (Yu et al. 2015), and β-tricalcium phosphate is resorbed by osteoclastic activity (Eggli et al. 1988). Bioceramics are easy to handle during surgery, and they adapt to the bone cavity (Oryan et al. 2014). There is an over 30-year experience on their use in the clinical practice (Stahl & Froum 1986). Osteoinduction has been reported on several calcium phosphate bioceramics (Yu et al. 2015). However, brittleness and poor mechanical strength might limit their use in weight-bearing applications (Nooeaid et al. 2012).

Bioactive glass was discovered in 1969 and introduced to the class of bioceramics (Hench et al. 1971). Bioactive glasses are typically composed of silicon dioxide, sodium oxide, calcium oxide, and phosphorus. They are capable of forming direct bonds with bone, they promote osteoblast activity (Lee et al. 2014), and even bacteriosidic properties have been reported (Lindfors et al. 2010). Brittleness is a limitation of bioactive glass.

Poly(lactic-co-glycolic adic) (PLGA) can be manufactured with tailored properties by varying the ratios of PLA and PGA. PLGA is a non-active but absorbable material typically used either to mechanically support the tissues when applied as a solid implant or to create a surface for tissue formation when applied as a highly porous scaffold (Muschler et al. 2004). It is suitable for restoring both the bone and the cartilage unit of osteochondral defects (Lopa & Madry 2014, Pan et al. 2015). PLGA is commercially available and exhibits good mechanical strength (Oryan et al. 2014). Inflammatory responses due to bulk hydrolysis of PLGA have been reported (Athanasiou et al. 1996).

2.5 TRANSLATION OF NEW METHODS

Translation of new treatment options from bench to bedside requires the use of animal models, as the safety and efficacy of new treatments need to be validated prior to clinical studies. Animal models are used in closing the gap between *in vitro* laboratory experiments and clinical trials. Evaluation of regenerative potential and possible immune responses of implants require the use of animal models.

When planning animal experiments, the ethical principles of three R's needs to be followed: Refinement, Reduction and Replacement (Russell & Burch 1959). The number of animals used in experiments should be reduced to the minimum. Animal models should be replaced with *in vitro* testing, computer simulation or cadaveric experiments, when possible. Refinement of experiments is essential to minimize the potential suffering of animals (Moran et al. 2016).

In order to effectively use animal models in cartilage repair research, the spontaneous healing capacity for each species needs to be known. Unlike humans, animals typically show some cartilage repair capacity (Ahern et al. 2009). This needs to be taken into consideration when designing translational animal experiments evaluating cartilage repair strategies. The lesion size beyond which spontaneous repair does not occur is called the critical lesion size. The use of critical-sized lesions is justified for the efficacy of the study and the ethical use of the animals.

2.5.1 SMALL ANIMAL MODELS

Animal models can be divided into small and large animal models. Small animals include mice, rats, and rabbits, which are used for proof-of-concept testing of new theories. The advantages of using small animal models include affordability, easiness of handling and housing, and the availability of genetically modified strains (Moran et al. 2016).

Rodents, such as mice and rats, and rabbits are frequently used in cartilage repair experiments. They provide information on degradation times and safety profiles of implants (Moran et al. 2016). The articular cartilage in mice and rats is very thin (Table 3), which does not allow for a realistic translation of the results to humans (Ahern et al. 2009). Additionally, growth plates of rodents remain open throughout their lives, resulting in improved intrinsic repair capacity (Libbin & Rivera 1989).

Chesterman was the first to study chondrocyte transplantation in a rabbit model in the 1960's (Chesterman & Smith 1968). The lapine model possesses the advantages of small animal models and additionally it has a joint size that is suitable for cartilage repair studies. This makes it the most commonly used animal model in musculoskeletal research and a popular testbed for biomaterials in the early stage of translation. However, since rabbits have higher metabolic activity and their joint loading and cartilage thickness differ

from those of humans, the translational value of rabbits is lower than in large animal models (Ahern et al. 2009, Moran et al. 2016).

2.5.2 LARGE ANIMAL MODELS

Large animals include dogs, goats, sheep, pigs, and horses. They have an appropriate joint size and cartilage thickness for cartilage repair research, and they can be used for biocompatibility studies as well as for determining the faith of a biomaterial within a defect (Moran et al. 2016).

Dogs have the advantage of naturally occurring joint diseases that are similar to human, such as osteochondritis dissecans and OA. Arthroscopical cartilage procedures and second look arthroscopies can be performed (Feczko et al. 2003) and temporary immobilization, partial weight-bearing and rehabilitation are possible (Kiviranta et al. 1994). Disadvantages of the canine model are their relatively thin articular cartilage layer (Table 3), anatomical differences in joints and ethical considerations due to their status as companion animals (Moran et al. 2016).

Domestic pigs have cartilage thickness and architecture, joint size and loading similar to humans. This makes them an attractive experimental model in cartilage repair research. However, pigs do not reach skeletal maturity until 2–4 years of age (Swindle 2007), and their husbandry is expensive. Therefore, most research is carried out with skeletally immature pigs (Vasara et al. 2006). Minipigs can be obtained from commercial suppliers and their adult size is significantly smaller than domestic pigs, providing a good option for domestic pigs (Moran et al. 2016).

Sheep and goats are easily obtained and housed and arthroscopy can be performed (Brehm et al. 2006, Ude et al. 2014). Goats have joint anatomy close to human, and appropriate joint size and cartilage thickness that allow for creation of chondral and osteochondral defects (Jackson et al. 2001, Moran et al. 2016). Sheep have a large variation in their cartilage thickness. Both sheep and goats have a high risk of subchondral cyst formation (Jackson et al. 2001, Moran et al. 2016). Equine models are advantageous due to the large joint size, cartilage thickness closest to that of humans that allows for creation of partial-thickness cartilage defects (Table 3) (Moran et al. 2016). Horses suffer from cartilage pathologies similar to those of humans and arthroscopical methods can be applied (Malda et al. 2012). Naturally occurring osteoarthritis in the horse are most common in the metacarpophalangeal and carpal joints (McIlwraith et al. 2012). The equine model is challenging due to its requirement of specialized habitat that leads to increased expenses, and ethical issues due to its status as a companion animal.

Table 3. Comparison of the most commonly used animal models in cartilage repair research.

Species	Skeletal maturity [a,b]	Adult weight [a,d]	Mean cartilage thickness [a,c]	Joints used [c]	Critical lesion diameter [a,c]
Human	18–22 years	60–90 kg	2.4–2.6 mm		10 mm
Horse	24–48 months	500–600 kg	2.0–3.0 mm	Knee, carpus, ankle	9 mm (knee)
Pig	24 months	250 kg	1.5–2.0 mm	Knee	6 mm
Goat	48–36 months	40–70 kg	0.8–2 mm	Knee	6–7 mm
Dog	12–24 months	15–30 kg	0.95–1.3 mm	Knee, shoulder, elbow, hip, ankle	4 mm
Rabbit	4–10 months	3–4 kg	0.16–0.75 mm	Knee, shoulder	3 mm
Rat	Life-long	0.25–0.55 kg	0.1 mm	Knee	Unknown

* Critical lesion diameter is the size of a defect beyond which spontaneous repair does not occur.

References [a] (Moran et al. 2016), [b] (Ahern et al. 2009), [c] (Cook et al. 2014), [d] (Sengupta 2013)

2.6 REGULATION AND PATIENT SAFETY

Cartilage repair therapies may be classified as medical devices or advanced therapy medicinal products (ATMPs), based on their origin, intended purpose and principal mechanism of action. A medical device typically functions by physical means, whereas a medicinal product acts through pharmacological or metabolical means. Marketing authorization is required for all medical devices and medicinal products regulated by the European Union (EU).

The European Union defines medical devices and medicinal products as follows:

> *Medical device*
>
> *"any instrument, apparatus, appliance, software, implant, reagent, material or other article intended by the manufacturer to be used, alone or in combination, for human beings for one or more of the following specific medical purposes:*
>
> *—diagnosis, prevention, monitoring, prediction, prognosis, treatment or alleviation of disease,*
>
> *—diagnosis, monitoring, treatment, alleviation of, or compensation for, an injury or disability,*
>
> *—investigation, replacement or modification of the anatomy or of a physiological or pathological process or state,*

—providing information by means of in vitro examination of specimens derived from the human body, including organ, blood and tissue donations,

and which does not achieve its principal intended action by pharmacological, immunological or metabolic means, in or on the human body, but which may be assisted in its function by such means.

The following products shall also be deemed to be medical devices:

—devices for the control or support of conception;

—products specifically intended for the cleaning, disinfection or sterilisation of devices as referred to in Article 1(4) and of those referred to in the first paragraph of this poin."

(Regulation (EU) 2017/745)

Medicinal product:

—"Any substance or combination of substances presented for treating or preventing disease in human beings."

—"Any substance or combination of substances which may be administered to human beings with a view to making a medical diagnosis or to restoring, correcting or modifying physiological functions in human beings is likewise considered a medicinal product."

(Directive 2001/83/EC)

In order for a medical device to receive a marketing approval in the EU, the product needs to carry a Conformité Européenne (CE) mark, which indicates that the product complies with EU directives. The regulatory framework that govern market access to the EU will soon be changed as the the current European Union Medical Devices Directive 93/42/EEC will be replaced by the Medical Devices Regulation 2017/745 (MDR) that came into force on May 25th 2017. Medical devices must meet the MDR requirements from May 26th 2020 in order to be placed on the market. Manufacturers whose devices have been certified according to the Medical Devices Directive 93/42/EEC can continue to place products on the market until May 26th 2024 on the condition that no essential changes are made to them and they are subject to continued surveillance. (Regulation (EU) 2017/745)

The purpose of the regulation is to protect patients from possible risks of medical devices. Competent Authority, such as National Supervisory Authority for Welfare and Health (Valvira) in Finland and Medicines and Healthcare Products Regulatory Agency in the United Kingdom, is a

governmental body that oversees device approval. Competent Authorities designate NBs, typically private companies.

Based on the risks and intended use, medical devices are categorized into four classes (class I, IIa, IIb, III) (Kramer et al. 2012). High-risk devices, such as implantable materials, require assessment and European commerce (EC) certification by a Notified Body (NB). Depending on selected conformity route, the NB either audits the manufacturer's quality system and reviews the technical file of the device or performs type testing and product verification to ensure the device meets its claims (Kramer et al. 2012, Van Norman 2016). A class I low-risk device, however, may receive market approval by self-certification and declaration of compliance coupled with product registration without the review by an NB. All manufacturers are required to maintain a product technical documentation, quality management system and risk management that is regularly updated. (Regulation (EU) 2017/745)

The European Medicines Agency (EMA) supervises and monitors the safety of medicines in the European Union. ATMPs are medicines that are based on gene therapy medicinal products (GTMPs), somatic cell therapy medicinal products (CTMPs), tissue engineered products (TEPs), or medical devices containing medicine (combined ATMPs). The European Commission Regulation (EC) No 1394/2007 on Advanced Therapy Medicinal Products (ATMP Regulation) together with Directive 2004/23/EC regulate cell and tissue products in the EU. The EMA defines tissue engineered products (TEPs) as products that contain or consist of "engineered cells or tissues" and have properties for or are "used in or administered to human beings with a view to regenerating, repairing or replacing a human tissue." (Directive 2001/83/EC)

Cells and tissues are considered engineered in the regulation, if they have been substantially manipulated by, *e.g.,* cutting, shaping, centrifugation, cell separation, sterilization, freezing, or if they are not intended to be used in the same function in the recipient as in the donor. Thus, mesenchymal stem cells and other cell therapy products are considered ATMPs in the EMA regulations (Murphy & Barry 2015). The ATMP regulations allow the use of ATMPs in treatment of patients with hospital exemption, which can be granted by the Member State if the use is non-routine-based and the ATMP is prepared according to the quality standards (Regulation (EC) No 1394/2007). In Finland, hospital exemption can be obtained from the Finnish Medicines Agency Fimea. The Finnish Act of the Medical Use of Human Organs and Tissues (101/2001) lays down provisions on the use of human cells and tissues.

3 AIMS OF THE STUDY

The purpose of this study is to expand the body of knowledge associated with cartilage lesions and their repair with novel methods. Therefore, the specific questions to answer in this thesis are:

1 Is the new biomaterial scaffold rhCo-PLA able to support cartilage repair in a porcine model? (*I*)

2 Can the novel PLGA-based biomaterials support bone growth in the repair of deep osteochondral lesions in a rabbit model? (*II*)

3 What is the critical chondral and osteochondral lesion size in the equine carpus? (*III*)

4 Can mesenchymal stem cells be chondrogenically differentiated in a three-dimensional rhCo-PLA scaffold? (*IV*)

4 MATERIALS AND METHODS

In this study, three individual animal experiments were conducted to investigate the spontaneous cartilage repair and the ability of novel biomaterials to enhance repair of articular surface defects. Additionally, one *in vitro* experiment was conducted to find out whether chondrogenically predifferentiation of mesenchymal stem cells in biomaterials improves matrix deposition by the cells and thus prepares the construct for implantation.

All of the animals, biomaterials, cells, and analysis methods used in each individual study are listed in Table 4.

Table 4. Summary of the methods used in *studies I–IV*.

	Animal	Biomaterials	Cells	Imaging	Histology	Other methods
Study I	Domestic pig	rhCo-PLA, pCo	Autologous chondrocytes	µCT	Saf-O, Col1, Col2	Biomechanical testing
Study II	Rabbit	PLGA, PLGA-BGf, β-TCP, BG	–	µCT	Masson-Goldner trichrome	Histomorphometry
Study III	Horse	–	–	µCT, MRI	Saf-O, Col1, Col2	PLM
Study IV	–	rhCo-PLA, rhCo3-PLA, pCo	BM-MSCs, Chondrocytes	Confocal microscopy	Saf-O, Col1, Col2	qPCR, sGAG/DNA,

rhCo-PLA, recombinant human type II collagen–poly(D/L)lactide scaffold; pCo, porcine type I/III collagen membrane; PLGA, poly(lactide-co-glycolide) scaffold; PLGA-BGf, PLGA–bioactive glass fiber scaffold; β-TCP, β-tricalcium phosphate granules; BG, bioactive glass; rhCo3-PLA, recombinant human type III collagen–poly(D/L)lactide scaffold; BM-MSC, bone marrow-derived mesenchymal stromal cell; µCT, micro-computed tomography imaging; Saf-O, Safranin-O staining; Col1, type I collagen; Col2, type II collagen; PLM, polarized light microscopy; qPCR, quantitative PCR; sGAG/DNA, sulfated gycosaminoglycan/DNA.

4.1 BIOMATERIALS (*I, II, IV*)

4.1.1 COMPOSITE SCAFFOLD RHCO-PLA (*I, IV*)

Composite scaffold rhCo-PLA was used in *studies I* and *IV*. Recombinant human type II collagen fibrils (rhCo) were manufactured from human type II collagen produced with recombinant technique (Fibrogen Europe Ltd., Helsinki, Finland). Thin fibers of medical grade poly(L/D)lactide 96/4 (PLA) (Corbion Purac, Gorinchem, The Netherlands) was needle punched into a 1 mm thick felt in Tampere University of Technology (Tampere, Finland). The felt was gamma sterilized at 25 kGy. The felt was cut into cylindrical discs with a diameter of 8 mm. The PLA96/4 felt cylinders were immersed with collagen solution and frozen in sample molds ad -30°C for 24h prior to freeze-drying for 24h. The scaffolds were cross-linked with 95% ethanol solution with 14 mM EDC (N-(3-dimethylaminopropyl)-N'-ethylcarbodiimide hydrochloride, Sigma-Aldrich, Helsinki, Finland) and 6 mM NHS (N-Hydroxysuccinimide, Sigma-Aldrich). The rhCo-PLA composite scaffolds were then washed, freeze-dried and packaged. Manufacturing and packaging of the rhCo-PLA scaffolds was done in a laminar flow chamber to prevent contamination.

For *study IV*, the rhCo3-PLA scaffolds were produced similarly but using recombinant human type III collagen (Fibrogen Europe Ltd.) as the natural component instead of type II collagen.

4.1.2 POROUS PLGA AND COMPOSITE SCAFFOLD PLGA-BGF (*II*)

PLGA (poly(lactide-co-glycolide)) was polymerized from medical grade D-lactide and glycolide (Corbion Purac, Gorinchem, the Netherlands) and L-lactide (Futerro, Escanaffles, Spain) by ring-opening polymerization in Åbo Akademi University (Turku, Finland). The PLGA polymer had a lactide to glycolide ratio of 7:3 with equal amounts of D- and L-lactide. The polymer was purified by dissolution in dichloromethane and precipitation in ethanol. PLGA was then extruded into approximately 2.8 mm thick rods that were cut to 16 mm long pieces. The pieces were placed in custom-made Teflon molds with an inner diameter of 4.0 mm. The PLGA scaffolds were gas foamed in the molds in a chamber with a carbon dioxide pressure of 55 bar for 10 h. Scaffolds with the length of 8 mm and a mass of 24–27 mg were then cut from the foamed rods and sterilized with gamma irradiation at 25 kGy.

PLGA-BGf composite scaffolds were produced from the above described PLGA polymer and bioresorbable melt-derived glass fibers (Vivoxid Ltd., Turku, Finland). The bioactive glass fibers (BGf) had a composition of 68.6 SiO_2, 12.5 Na_2O, 9.3 CaO, 7.2 MgO, 1.8 B_2O_3 and 0.6 P_2O_5 (in mol-%) and an average fiber diameter of 13 μm. The BGf was cut into staple fibers of approximately 10 cm in length and carded into mesh. The PLGA polymer was dissolved in 1,4-dioxane as 3 wt-% solution. The PLGA solution was immersed into BGf carded mesh and the samples were frozen to -30°C for 24 h prior to

24 h freeze-drying. The PLGA-BGf composite scaffolds were then cut into pieces and five parallel pieces were glued together with PLGA solution and freeze-dried again. The height of the final rod was 8 mm and diameter 4 mm. The rods were gamma sterilized at 25 kGy.

4.1.3 COMMERCIAL PORCINE COLLAGEN MEMBRANE (*I, IV*)

Commercial collagen membrane (pCo) manufactured from porcine type I and III collagens (Chondro-Gide®, Geistlich Pharma AG, Wolhusen, Switzerland) was used as a control scaffold in *studies I* and *IV*. It is one of the most frequently used biomaterial products in cartilage repair surgery (Brittberg 2010) and as such, it was considered to represent the gold standard.

4.1.4 COMMERCIAL BONE SUBSTITUTE MATERIALS (*II*)

Commercial bioactive glass granules, denoted as BG (BonAlive®, BonAlive Biomaterials Ltd, Turku, Finland) and commercial β-TCP granules (Synthes® chronOS, Synthes GmbH, Oberdorf, Switzerland) were used as controls in *study II*. The BG granules consisted of 53 SiO_2, 23 Na_2O, 20 CaO, and 4 P_2O_5 (in wt-%) and had a diameter of 0.5–0.8 mm. The size of the β-TCP granules was 0.5–0.7 mm and the porosity of the material was 60%.

4.2 ANIMAL MODELS (*I–III*)

For *study I*, a total of 20 female domestic pigs (*Sus scrofa domestica*) were used. The pigs were 4 months old and obtained from a local farmer. All pigs underwent a clinical health examination and were acclimatized to the new environment for two weeks prior to the operations. The animals were randomized into three groups: the rhCo-PLA treatment group received an rhCo-PLA scaffold (n=7); the pCo treatment group received a pCo membrane (n=7), and the spontaneous healing group was left untreated (n=6).

A total of 40 female New Zealand white rabbits (*Oryctolagus cuniculus*) were obtained from a commercial supplier (Harlan laboratories B.V., Venray, the Netherlands) for *study II*. The animals were 18 weeks old. They were acclimatized for one week before the operations. The rabbits were randomized into five groups (n=8 in each group). Four of the groups received a bone substitute material (PLGA, PLGA-BGf, BG, or β-TCP) and one group was left untreated for spontaneous healing.

Five 24-month-old horses (*Equus caballus*) were included in *study III*. Circular full-thickness cartilage defects or osteochondral defects with a diameter of 2, 4, 6, and 8 mm were created in the middle carpal joint. The 6 mm defects were used for other studies and they were not included in this study (Kulmala et al. 2012, Viren et al. 2012, Rautiainen et al. 2013). All defects were left untreated for evaluation of spontaneous healing response.

4.3 SURGERIES (*I–III*)

4.3.1 CHONDRAL INJURY AND REPAIR WITH ACI TECHNIQUE (*I*)

Two operations were carried out in pigs. The first operation was performed in order to create the surgical cartilage defect and to acquire a cartilage biopsy for the repair operation. The pigs were sedated with 0.2 mg/kg (*s.c.*) medetomidine and 10 mg/kg (*s.c.*) ketamine. Preoperative analgesia of 0.05 mg/kg (*s.c.*) buprenorfin and 3 mg/kg (*s.c.*) carprofen as well as antibiotic prophylaxis of 3.0 g (*i.v.*) cefuroxime was administered. Anesthesia was induced with propofol (*i.v.*) and maintained with 1.5–2.5% isoflurane. The animals were set in a supine position on the operating table. Through a medial parapatellar arthrotomy, a single circular chondral lesion of 8 mm in diameter was created on the central area of the medial condyle of the femur with a biopsy punch (Stiefel Laboratories Ltd, Wächtersback, Germany). Cartilage was removed to the level of the subchondral bone. The incision was closed in layers. The animals were allowed free weight-bearing and unrestricted movement after the operation. The operated pigs were housed separately for three postoperative days and grouped thereafter. The harvested cartilage was stored before chondrocyte isolation in sterile phosphate-buffered saline solution (PBS) at 4°C for no more than 12 hours.

Three weeks after the cartilage biopsy, a second operation was performed. The pigs were medicated and anesthetized as previously described. The knee joint was approached through the previously used incision site and the initial lesion was debrided from scar tissue. In the two treatment groups, the entire cell amount yielded from cell expansion was used (Table 5).

In the rhCo-PLA group, approximately 40 µl of chondrocyte suspension was pipetted into a sterile rhCo-PLA scaffold that was then implanted and sutured to the adjacent healthy cartilage rim. The rest of the cell suspension (approximately 160 µl) was pipetted onto the scaffold for maximum cell count.

In the pCo group, protocol described by Brittberg and colleagues (Brittberg et al. 1994) was followed, but the periosteal graft was replaced with the pCo membrane. Cell suspension was injected under the pCo membrane and the sutured seam was secured with fibrin glue.

The cartilage defects in the spontaneous group were debrided as described above, but the lesions were left without treatment for spontaneous repair. The follow-up time for each group was four months.

Table 5. *Number of autologous chondrocytes implanted in each animal.*

Group	Pig n:o	Cells/defect
rhCo-PLA	18	15.0
	21	10.5
	25	5.6
	26	4.6
	29	14.4
	31	12.6
	mean	**10.5**
pCo	19	13.9
	23	14.4
	27	11.9
	28	9.9
	30	9.8
	32	8.5
	mean	**11.4**
spontaneous	5	0
	11	0
	15	0
	16	0
	17	0
	mean	**0**

4.3.2 OSTEOCHONDRAL INJURY AND REPAIR WITH BONE FILLERS (*II*)

All rabbits were operated under general anesthesia induced with 0.5 mg/kg (*s.c.*) medetomidine and 25 mg/kg (*s.c.*) ketamine. Preoperative analgesia of 0.05 mg/kg (*s.c.*) of buprenorphine and 4 mg/kg (*s.c.*) of carprofen was administered. All the animals received 40 mg/kg (*i.m.*) of cefuroxime preoperatively.

The animals were set on a supine position on the operating table. A medial parapatellar arthrotomy was made to the right hind limb. The patella was dislocated laterally, and the femoral condyles were exposed. A single lesion through the articular cartilage of the medial condyle was made with a hand-operated drill. The lesion covered almost the width of the femoral condyle and the bony defect comprised a notable volume of the entire condyle with a diameter of 4 mm, and a depth of 8 mm. The lesions were filled with the studied biomaterial or left empty for spontaneous repair. The granular materials BG and β-TCP were mixed with sterile water to create a paste-like composition prior to implantation. The PLGA and PLGA-BGf samples were semi-rigid plugs which were press-fitted into the lesion. The incisions were closed in layers. After the operation, 1 mg/kg (*s.c.*) of antipamexole was administered for reversal of the sedative effects of medetomidine.

The animals were allowed free weight-bearing and unrestricted movement after the operation. Antibiotic prophylaxis of 40 mg/kg (*s.c.*) of cefuroxime was continued three times a day for three days and postoperative analgesia of 0.01 mg/kg (*s.c.*) of buprenorphine and 4 mg/kg (*s.c.*) of carprofen for four days. The follow-up time was 12 weeks.

4.3.3 CHONDRAL AND OSTEOCHONDRAL INJURIES (*III*)

All the horses were assessed clinically and radiologically prior to inclusion in the study and were found to present no abnormalities. The horses received meloxicam pre-operatively (0.6 mg/kg, *i.v.*, Metacam®, Boehringer Ingelheim, Ingelheim am Rhein, Germany). Surgery was performed under general anesthesia. The middle carpal joints were approached through a latero-dorsal and medio-dorsal 1.5–2 cm length arthrotomy to create defects on the 2nd, 3rd and 4th carpal bones. The defects were pre-punched with a 2 mm, 4 mm, 6 mm, or 8 mm skin biopsy punch. For chondral defects, cartilage was carefully removed with ring curettes onto the level of calcified cartilage (approximately 1 mm in depth) in the left carpus. For osteochondral lesions created in the right carpus, drilling was performed under continuous lavage with Ringer's solution using a hand drill. A 2, 4, 6, or 8 mm pointed drill bit was initially used, followed by a custom-made flattened drill bit of the same size and a custom-made drill sleeve to provide a uniform defect with a flattened bottom and controlled depth of 3.5 mm. Healthy cartilage adjacent to the lesions served as control for all defects.

Postoperatively, the animals were confined to individual box-stalls (3.5×3.5m) for two weeks, after which a gradual six-week rehabilitation program consisting of incremental controlled walking started. Thereafter, depending on the season and weather conditions, the animals were turned out to pasture or kept in box stalls with daily exercise in a mechanical horse walker. The total follow-up period was 12 months during which the lesions were allowed to heal spontaneously.

4.4 CELL CULTURES (*I, IV*)

4.4.1 PORCINE CHONDROCYTE ISOLATION AND MONOLAYER CELL CULTURE (*I*)

A circular chondral biopsy with a diameter of 8 mm was taken with a biopsy punch from the medial femoral condyle of a domestic pig as described above. The cartilage biopsy was minced with a surgical blade and digested overnight in type II collagenase (Worthington Biochemical Corp., Lakewood, NJ, USA) in a cell culture medium comprised of Dulbecco's Modified Eagle's Medium (DMEM-F12, Gibco, Invitrogen, Paisley, UK) supplemented with 10% Fetal Bovine Serum, 1% GlutaMAX™ (Gibco, Invitrogen), 1% Penicillin-

Streptomycin (Gibco, Invitrogen), 1% amphotericin B and 50 µg/ml sodium L-ascorbate (Sigma Aldrich, St. Louis, MO, USA). The obtained chondrocytes were cultured in the above described medium until passage 2 and then stored at -140°C.

4.4.2 HUMAN CHONDROCYTE AND MSC ISOLATION AND THREE-DIMENSIONAL CELL CULTURES (*IV*)

Cartilage was harvested from a male cadaver donor. Both knees were opened through a medial parapatellar incision and the patella was lateralized to expose femoral condyles. Articular cartilage was harvested with a surgical blade from both condyles and the cartilage pieces were placed in sterile PBS. The cartilage pieces were minced and digested as described above. The obtained chondrocytes were cultured until passage 3 in the above described chondrocyte culture medium, where after day 0 samples were collected.

Human bone marrow-derived mesenchymal stem cells were obtained from the Finnish Red Cross Blood Service. Bone marrow samples were drawn from three healthy male volunteers and MSCs were isolated, characterized and cultured in MSC proliferation medium until passage 1 before storing them in liquid nitrogen in aliquots. The cells were then thawed and cultured until passage 2 before collecting day 0 control samples. The proliferation medium consisted of DMEM-F12 supplemented with GlutaMAX (21885-025, Gibco, Invitrogen), 10% platelet rich plasma (Finnish Red Cross Blood Service, Helsinki, Finland), 1% PenStrep (Gibco, Invitrogen), and 40 IU/ml heparin (LEO Pharma, Ballerup, Denmark).

Three types of biomaterial scaffolds (rhCo2-PLA, rhCo3-PLA, pCo) were placed on a 24-well plate and a suspension of 0.5×10^6 chondrocytes or MSCs was pipetted onto each scaffold. The cells were then cultured in chondrocyte proliferation medium, MSC proliferation medium, or xeno-free differentiation medium. The xeno-free chondrogenic differentiation medium for MSCs comprised of Dulbecco's Modified Eagle Medium (41966-029, Invitrogen) supplemented with 1% PenStrep, 1.5 mg/ml human serum albumin (Sigma Aldrich), 40 µg/ml L-proline (Sigma Aldrich), 25 µg/ml ascorbic acid (Sigma Aldrich), 10 µg/ml insulin (Insuman Rapid, Sanofi), 8 µg/ml human transferrin (Sigma Aldrich), 5.5 µg/ml linoleic acid (Sigma Aldrich), 40 ng/ml dexamethasone (Oradexon, Shering-Plough), 10 ng/ml sodium selenite (Sigma Aldrich), and 10 ng/ml TGF-β1 (R&D Systems, Minneapolis, MN, USA) (Skog et al. 2015).

4.5 MACROSCOPIC EVALUATION (*I–III*)

After sacrifice, the operated and contralateral non-operated knees of the pigs (*study I*) and rabbits (*study II*), and left and right carpal joints of the horses (*study III*) were dissected free and the cartilage surfaces were photographed.

In *studies I* and *III*, cylindrical osteochondral samples containing the defect site in the middle were cut and the cylinders were stored at -20°C until further processing. In *study II*, the detached lapine femurs were stored in 10% buffered formalin at +4°C until further processing.

The porcine photographs were blinded and evaluated by four independent observers following the ICRS Cartilage Repair Assessment System (Brittberg & Winalski 2003).

4.6 IMAGING (*I–III*)

4.6.1 µCT (*I–III*)

Quantitative analyses of the subchondral bone in *studies I–III* were carried out with µCT imaging. The volume of interest (VOI) in each study was a cylinder that was chosen to cover the operated area and underlying subchondral bone. Osteochondral plugs in *studies I–II* were scanned with MicroXCT-400 (Zeiss Xradia, Pleasanton, CA, USA) with unfiltered X-ray beam, 100 kV source. The cross-sectional images were reconstructed with XMReconstructor software (version 8.1, Zeiss Xradia). The images were post-processed and analyzed with Avizo Fire 8.1 (FEI Visualization Sciences Group, Hillsboro, OR, USA) software and Fiji with BoneJ plugin (Doube et al. 2010, Schindelin et al. 2012). In *study III*, SkyScan-1172 scanner (SkyScan, Aartselaar, Belgium) with X-ray tube voltage of 100 kV was used to analyze the subchondral bone. Image analysis was conducted with the CT Analyser (version 1.10.1.0; SkyScan). The analyzed parameters in each study were bone volume fraction (*BV/TV*), trabecular thickness (*Tb.Th*), trabecular separation (*Tb.Sp*), and trabecular number (*Tb.N*).

4.6.2 MRI (*III*)

In *study III*, samples were thawed, placed in a test tube and immersed in saline. Magnetic resonance imaging was carried out with a 9.4 T device (Oxford 400 NMR vertical magnet; Oxford Instruments, Witney, England), equipped with a Varian DirectDrive console (VnmrJ 2.3, Varian, Palo Alto, CA, USA) and a 19 mm quadrature volume coil (RAPID Biomedical, Rimpar, Germany). T_2 relaxation time was measured in a single slice of 1 mm thickness using a single echo spin echo sequence with echo times (TEs) of 12, 24, 50, 80 and 110 ms, a repetition time (TR) of 2.5 s and in-plane resolution of 70×140 µm. Native T_1 relaxation time was measured in the same slice with the same

resolution, using a progressive saturation recovery sequence with TRs of 0.3, 0.6, 1.2, 2.4, and 4.8 s and TE of 11.7 ms. Gadolinium-enhanced T_1 values (T_{1Gd}) were retrieved by imaging the samples after 20 hour immersion in a 1.0 mM Gd-DTPA^{2-} solution using TRs of 0.1, 0.2, 0.4, 0.8, and 1.6 s.

The tissue was analyzed at two regions of interest (ROIs). ROI1 covered any repair tissue at the lesion sites. ROI2 was aligned with the adjacent healthy cartilage and split into superficial and deep halves. A control ROI at the site of healthy tissue was also split into superficial and deep halves.

4.7 MECHANICAL TESTING (*I*)

Osteochondral samples of the porcine knees were thawed and their cartilage thickness at the defect site was measured with ultrasound imaging (Clear View Ultra, Boston Scientific). Indentation technique was used for biomechanical testing. The testing was carried out in a chamber filled with PBS containing metalloprotease inhibitors 5 mM EDTA (ethylenediamide tetraacetic acid disodium salt, VWR International LCC, Fontenay, France) and 5 mM benzamidine hydrochloride (Sigma-Aldrich) (PBSI). A cylindrical plane-ended indenter (diameter 610 μm) was brought into contact with the cartilage surface at the site of the cartilage thickness measurement. Stepwise stress-relaxation tests (four steps, compression of 5% of cartilage thickness each, 0.1 mm/s ramp rate, 30 minutes relaxation between each step) were performed. A fibril reinforced poroelastic finite element cartilage model was constructed with Abaqus (V6.12-3, Dassault Systèmes Simulia Corp, Providence, RI, USA) to characterize the mechanical parameters of the repair tissue. In this model, collagen fibrils are modeled as nonlinear springs and biphasic porohyperelastic non-fibrillar matrices represent porous proteoglycan structure filled with fluid. Material parameters (non-fibrillar matrix modulus E_m, collagen fibril network modulus E_f, and permeability k_o) of the articular cartilage samples were optimized by minimizing the mean absolute error of the second stress-relaxation step between the simulations and experimental stress-relaxation data with Matlab software (V7.14.0, Mathworks Inc, USA). Other parameters in the model were kept constant.

4.8 MICROSCOPIC METHODS (*I–IV*)

4.8.1 TISSUE SECTIONS (*I–IV*)

*4.8.1.1 Paraffinized sections (*I, III, IV*)*

Osteochondral sample cylinders (*studies I* and *III*) and cell pellets (*study IV)* were fixed in 0.1M phosphate-buffered 10% formalin at room temperature (RT). The samples were decalcified in 10% EDTA and 4% formaldehyde in 0.1 M phosphate buffer at RT, then cut in half, dehydrated in ascending alcohol series and cleared with xylene before embedding in paraffin.

*4.8.1.2 Hard tissue sections (*II*)*

The formalin-fixed rabbit femurs were carefully split into two using a jig saw. The samples were dehydrated in ethanol, cleared with xylene immersions and subsequently embedded in methyl methacrylate.

4.8.2 STAININGS (*I–IV*)

For *studies I, III* and *IV*, the 5 μm thick tissue sections were deparaffinized with xylene and rehydrated in descending alcohol series. The sections were incubated in 0.5% Safranin-O (in 0.1M acetate buffer, pH 4.6) and subsequently washed in running water for 10 minutes.

In *study II*, the hardened tissue blocks were cut into 5–10 μm thick sections with a Leica SM 2500 hard tissue slide microtome and stained with Masson's Goldner trichrome.

4.8.3 HISTOLOGICAL SCORING OF REPAIR TISSUE (*I, III*)

In *study I*, the Safranin-O stained tissue sections were evaluated by two blinded, independent observers according to ICRS Histological Visual Assessment Scale (Mainil-Varlet et al. 2003). The score evaluates the repair tissue surface, matrix, cell distribution, cell viability, subchondral bone, and cartilage mineralization. Normal hyaline cartilage receives an overall score of 18.

The Safranin-O stained tissue sections in *study III* were evaluated using the OARSI equine histopathology score (McIlwraith et al. 2010). The sections were scored by three independent, blinded observers. The defects that lacked any repair tissue were given the worst total score of 20.

4.8.4 HISTOMORPHOMETRY (*II*)

The stained sections were imaged with Olympus BX-60 microscope with an integrated Scion color digital camera. The qualitative assessment of the amount of osteoid and lymphocytes was carried out with the naked eye. The specimens were classified according to the number of lymphocytes and macrophages into having 0—50 cells, 50—100 cells, 100—500 cells, or over 500 cells per tissue slide. Due to the low quantity of osteoid in the samples, quantitative assessment of the amount of osteoid could not be made.

4.8.5 IMMUNOHISTOCHEMISTRY (*I, III, IV*)

The 5 μm thick tissue sections were digested in hyaluronidase (2 mg/ml, Sigma-Aldrich) and pronase (2 mg/ml, Calbiochem, Merck KGaA). The sections were treated with 0.03% hydrogen peroxide (EnVision®+ System-HRP (AEC), Dako North America Inc.) to block endogenous peroxidase activity and with 10% normal goat serum (Dako Denmark A/S, Glostrup, Denmark) to block non-specific staining. The sections were then incubated overnight at 4°C with primary antibodies against collagen type II (ab34712, Abcam) and collagen type I (ab34710), and diluted to 4 μg/ml with PBS supplemented with 1% bovine serum albumin (Sigma-Aldrich) and 0.1% Triton X-100 (Sigma-Aldrich). Negative controls were incubated with rabbit immunoglobulin. Horseradish peroxidase (HRP)-conjugated goat anti-rabbit secondary antibody (Dako) was subsequently applied on the slides. Antibody binding was visualized with AEC (3-amino-9-ethylcarbazole) substrate chromogen (Dako).

4.8.6 POLARIZED LIGHT MICROSCOPY (*III*)

Polarized light microscopy (PLM) describes cartilage structure and collagen fibril network. Unstained 5 μm thick tissue sections were imaged using polarized light microscopy (Leitz Ortholux II POL, Leitz Wezlar, Wezlar, Germany) as described by Rieppo (Rieppo et al. 2008). The repair tissue was evaluated using a 300-μm-wide ROI, which was divided into ten layers of equal thicknesses for the analysis. The orientation of collagen fibrils in relation to the cartilage surface (0–90 degrees), and parallelism index (PI), which describes the randomness of fibril orientations within the pixel (0—1, where 0 indicates completely random organization and 1 indicates completely parallel organization), were determined from the most superficial, middle and the deepest layer.

4.8.7 CONFOCAL MICROSCOPY (*IV*)

The cells in the scaffolds were fixed with 10% buffered formalin and stained with Hoechst (Invitrogen). The cell nuclei were then imaged with a fluorescent

confocal microscope Leica TC SP8 CARS (Leica Microsystems) with 25× HCX IR APO L water objective and Leica Application Suite Advanced Fluorescence software (version 3.3.0.10134). For each sample, three fields of view from the most representative areas were imaged and a maximum projection image was created with a mean stack size of 320 μm.

4.9 BIOCHEMICAL METHODS (*IV*)

4.9.1 RNA EXTRACTION

To obtain the nucleic acids from each sample, the cell–scaffold constructs were mechanically disrupted using Tissue Lyser II (Qiagen, Hilden, Germany) with carbide beads. The samples were homogenized with QIAzol® Lysis Reagent (Qiagen Sciences, Maryland, USA, cat. no. 79306) and the RNA was separated from the organic phase with chloroform (Sigma-Aldrich). RNeasy Mini Kit (Qiagen) was used to further purify the samples. Total RNA yield and RNA purity were measured with NanoDrop 1000 spectrophotometer (Thermo Scientific, Wilmington, DE, USA). The RNA samples with 260/280 values <1.6 and 260/230 values <0.1 were omitted from the final analyses.

4.9.2 CDNA SYNTHESIS

Reverse transcription of RNA to single-stranded cDNA was carried out in PCR tubes (Nippon Genetics Europe GmbH, Dueren, Germany) using a commercial kit (High Capacity cDNA Reverse Transcription Kit with RNase Inhibitor; Applied Biosystems, Foster City, CA, USA) according to the manufacturer's instructions. The RNA amount used in the reactions was 100 ng for each sample. The reverse transcription program was as follows: 25°C for 10 min, 37°C for 120 min, 85°C for 5 minutes. The resulted cDNA was stored in -20°C.

4.9.3 QPCR

The expression levels were measured for chondrogenic genes *SOX9*, *COL2A1, ACAN;* for osteogenic markers *RUNX2* and *COL10A1*; and for synovial fibroblast marker *MFAP5* using a commercial gene expression assay (TaqMan® Gene Expression Assay, Applied Biosystems; Table 6). The real-time qPCR analysis was performed with iQTM5 Multicolor Real-Time PCR Detection System (Bio-Rad Laboratories, Hercules, CA, USA). The amplification reaction conditions were as follows: Hold in 50°C for 2 minutes, hold in 95°C for 10 minutes, cycle 95°C for 15 seconds and 60°C for 1 minute repeated 40 times. The gene expression levels were normalized to *GAPDH* and day 0 samples in the ΔΔCT method (Livak & Schmittgen 2001).

Table 6. Gene expression assays used in *study IV*.

Gene	Full name	TaqMan code
GAPDH	*Glyceraldehyde-3-phosphate dehydrogenase*	Hs99999905_m1
ACAN	*Aggrecan*	Hs00153936_m1
COL2A1	*Collagen, type II, alpha 1*	Hs00264051_m1
COL10A1	*Collagen, type X, alpha 1*	Hs00166657_m1
MFAP5	*Microfibrillar Associated Protein 5*	Hs00185803_m1
RUNX2	*Runt-related transcription factor 2*	Hs00231692_m1
SOX9	*SRY (sex determining region Y)-box 9*	Hs00165814_m1

4.9.4 SGAG/DNA

The amount of sulfated glycosaminoglycans in each cell-scaffold-construct was analyzed using the dimetyhylmethylene blue-based (DMMB) assay. The scaffold—cell contstructs were washed twice with PBS, placed dry in Eppendorf tubes and stored immediately at -80°C. The samples were digested in 1 mg/ml Proteinase K (Sigma-Aldrich) in PBS at +60°C overnight. Subsequently, the samples were centrifuged at 10 000 g for 10 min and the supernatant was collected for the measurements. The sGAG amount was quantified using Blyscan assay (Biocolor, UK) according to the manufacurer's protocol. Briefly, 100 µl of sample supernatant was mixed with 1 ml of Blyscan reagent and incubated in gentle shaking for 30 min. The samples were centrifuged at 8 000 g for 10 min and supernatant was discarded. Precipitated sGAG pellets were dissolved with 0.5 ml of dissociation reagent and vortexing. Samples were transferred t a 96-well plate in duplicates, and the absorbance was measured with a microplate reader at 656 nm. To normalize the sGAG amount to DNA content, PicoGreen assay (Molecular Probes, Invitrogen) was used according to the manufacturer's instructions. The samples were diluted 1:10 and 50 µl of the dilutions was transferred to a 96-well plate in duplicates. Subsequently, 50 µl of PicoGreen working solution was added to each sample and incubated for 2—5 min at RT. The fluorescence of DNA was measured with a microplate reader at 480/520 nm.

4.10 STATISTICAL ANALYSES (*I–IV*)

The data in *studies I–IV* are presented as mean±standard error (SE), unless otherwise specified. A p value under 0.05 was used as the threshold to indicate a statistically significant difference in each study.

4.10.1 *STUDY I*

Relative differences between the operated and the non-operated contralateral knees were calculated and the differences in the relative values were revealed by one-way analysis of variance (ANOVA) testing and Kruskall-Wallis testing with exact p values. Differences between the operated knees of each group were calculated with permutation ANOVA. Correlation analysis for cell count and histological score was carried out with Spearman's correlation test.

4.10.2 *STUDY II*

Each parameter for operated knees was compared with the corresponding non-operated control to calculate relative μCT values. The relative values were used to compare the groups with each other. Statistical analyses were carried out using the permutation type ANOVA test with Holm adjustment.

4.10.3 *STUDY III*

Osteochondral and chondral lesions of the same diameter were compared to each other. The significances of differences in the μCT, MRI and polarized light microscopy parameters were evaluated with a pairwise t-test, and Sidak adjustment was made for multiple testing. Significances of difference in lesion filling was calculated with repeated ANOVA testing and Sidak adjustment.

4.10.4 *STUDY IV*

Differences between scaffolds were determined with permutation type ANOVA. In cases of $p<0.05$, it was followed by pairwise multiple comparisons with the Bonferroni procedure.

4.11 ETHICAL CONSIDERATIONS

Studies I–III involved the use of experimental animals. Although Russel's principal of 3R's encourage to replace animal models with methods of other kinds, articular cartilage repair in weight-bearing conditions cannot be investigated without the use of animal models. *Studies I–II* were conducted according to the ethical guidelines and regulations of the Finnish Act on Animal Experimentation (62/2006). *Studies I–II* were authorized by the Finnish National Animal Experiment Board (ESAVI-3146/04.10.03/2011 and ESAVI-3785/04.10.03/2011) prior to the commencement of the studies. *Study III* was authorized by the Utrecht University Animal Experiments Committee (0412.0601) in compliance with the Dutch Act on Animal Experimentation and the animal care was in accordance with Utrecht University guidelines.

The use of cadaveric chondrocytes and human mesenchymal stem cells in *Study IV* were approved by Ethics Committee, Department of Surgery of the Helsinki University Hospital (7/13/03/02/2014), and an informed consent was received in written form from all volunteer bone marrow donors.

5 RESULTS

5.1 SURGICAL PROCEDURES AND ANIMAL WELLBEING (*I–III*)

In *study I*, one animal from the spontaneous group and one from the pCo group developed a severe wound infection after the repair operation and were prematurely euthanized. In *study II*, three animals (one from groups PLGA, β-TCP and spontaneous, each) died during the induction of anesthesia, probably due to respiratory arrest caused by the combination of ketamine and medetomidine (Calasans-Maia et al. 2009). Otherwise, surgeries in *studies I—III* were carried out without complications and the animals recovered well and no clinical abnormalities were detected.

5.2 MACROSCOPIC EVALUATION OF REPAIR TISSUE (*I–III*)

Modest synovial fluid excess and inflammation of synovial tissue was observed in two pigs (one from group rhCo-PLA and one from group pCo) at the time of the sacrifice. Otherwise, no synovitis or degenerative changes were observed in any of the operated knees. According to the ICRS consensus score, ≥75% filling of the defects was observed in 2/5 specimens in spontaneous group, 3/6 in rhCo-PLA group and 3/6 in pCo group, respectively. The mean macroscopic ICRS score was highest in spontaneous group (7.0±1.5) compared to rhCo-PLA treatment (5.3±2.0) and pCo treatment group (6.8±1.6) but the differences were not statistically significant (p=0.75).

In *study II*, all groups showed good macroscopic lesion filling up to the cartilage surface. The surface of the repair tissue in the defect areas in each group was uneven and differed by color from healthy cartilage but no deep tissue deficiencies or degenerative changes around the defect areas or in the articulating surfaces were detected.

In *study III*, the 2 mm chondral lesions showed good macroscopic filling (Figure 3). The 4 mm and 8 mm chondral lesions were clearly distinguishable from the surrounding healthy cartilage and were incompletely filled (Figure 3). Lesion filling was better in the osteochondral lesions in which the repair tissue reached the level of the surrounding cartilage surface in all of the 2 mm lesions (Figure 3). The overall filling of osteochondral samples did not differ from healthy control cartilage (p=0.085), whereas the filling of the 4 mm and 8 mm chondral samples was decreased in comparison to controls (p<0.001).

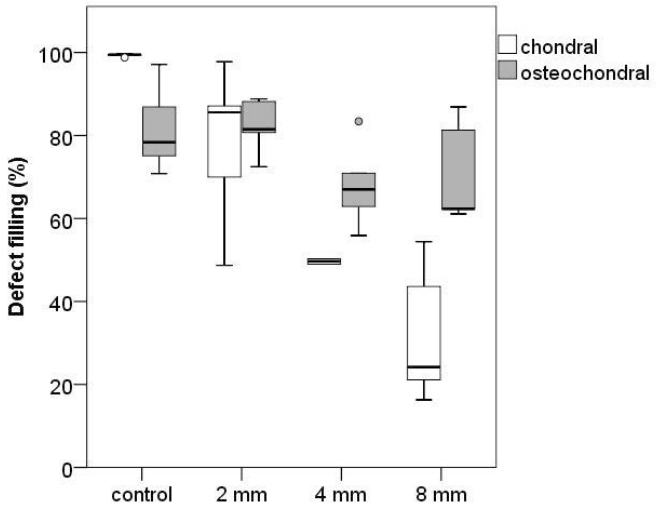

Figure 3 Filling of the chondral and osteochondral defects in *study III*. The top and bottom of each box represent the first and third quartiles, the horizontal line inside the box is the median, and the whiskers are the 10th and 90th percentiles. The circles are outliers.

5.3 VISUAL APPEARANCE OF BONE STRUCTURE IN µCT IMAGING (*I–III*)

In *study I*, subchondral bone voids in the pigs were greater in the treatment groups than in the spontaneously healed group (Figure 4), although no statistically significant differences were found between the study groups (p=0.24). Mean void volumes for rhCo-pPLA, pCo and spontaneous groups were 53.1±18.6 mm^3, 50.0±10.2 mm^3 and 21.1±7.6 mm^3, respectively. Subchondral bone voids were more common in the pCo-treated group (6/6) than in the rhCo-PLA-treated group (3/6) or the untreated control group (2/5).

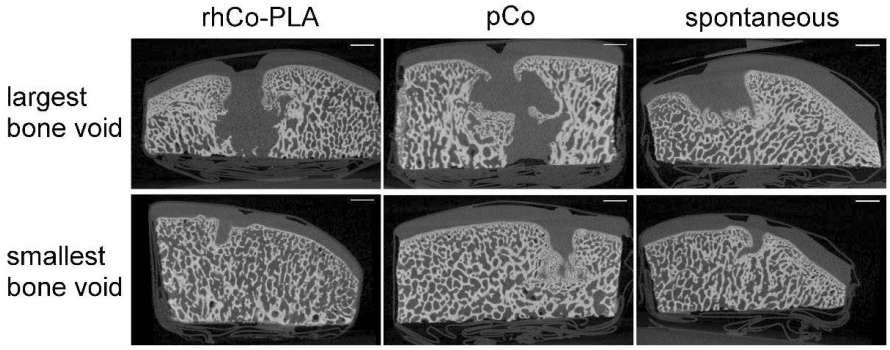

Figure 4 µCT image of the largest and smallest bone void in each study group in *study I*. Scale bars 2 mm.

In the lapine study, no signs of granular biomaterial detachment from the defect areas or bone cysts were observed. PLGA rods resulted in variable defect filling with partial bony repair which migrated from the defect periphery towards the middle of the defect. The bone–cartilage interface showed an uneven mineral surface. One defect in the PLGA group and all defects filled with PLGA-BGf appeared empty in visual evaluation of μCT images.

The granular commercial controls β-TCP and BG resulted in repair tissue that was visually slightly depressed on the surface, under which the mineral structure appeared very dense (Figure 5). One BG-filled specimen showed an empty void in the middle of the original burr canal in an otherwise well filled defect (Figure 5b). Unresolved β-TCP and BG were clearly distinguishable in the μCT images.

For spontaneously healed control defects, it was typical that there was a slight depression of the joint interface (Figure 5c). The defects in the group were variably healed, either with good filling, a layer of dense bone with an empty defect underneath or repair tissue with a non-healed shaft in the middle. Canal-like voids extending from the joint surface towards the marrow spaces were seen in 3/7 specimens.

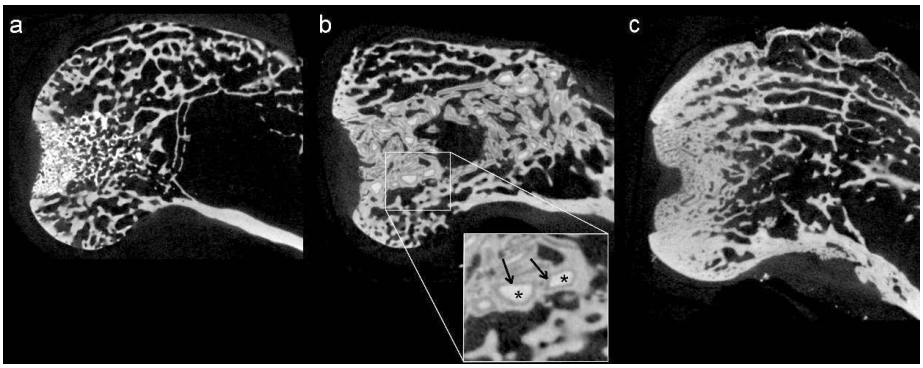

Figure 5 a) Unresolved granular biomaterials were clearly visible in defect areas. β-TCP was visually distinguishable from the bone by its clearer white color. b) The asterisks mark the unreacted BG granules and arrows show the darker gray area of silica gel layer onto which hydroxyapatite crystallizes. c) Spontaneously healed defects showed a depression near the surface.

In the equine study, bone structure was normal under the 2 mm and 4 mm chondral lesions in visual observation of the μCT images. Subchondral bone showed signs of decreased compactness in 4/5 large 8 mm chondral lesions and one of these samples showed a small bone cyst underneath the chondral defect. By contrast, subchondral bone changes were observed in 14/15 osteochondral defects. Only two osteochondral samples with a diameter of 2 mm presented without bone cysts. All osteochondral lesions of 4 mm and 8 mm in diameter had unhealed bone or a cystic bone lesion.

5.4 BONE STRUCTURAL PARAMETERS (*I–III*)

BV/TV and *Tb.Th* in the operated porcine femurs were slightly increased in comparison to non-operated contralateral control knees (Table 7) but the different study groups did not differ from one another with respect to any of the studied parameters.

In the lapine study, trabeculae were thin and densely located in both the β-TCP and BG groups, whereas trabeculae in the spontaneously healed and PLGA groups were thick and sparse. The β-TCP-treated knees showed the highest relative bone volume fraction when compared with all other groups ($p<0.001$).

In the equine study, variation between individual horses and individual samples was large, leading to no statistically significant changes in the subchondral bone trabecular parameters.

Table 7. The structural bone parameters in each study group and controls. All values are presented as mean±SE. BV/TV, bone volume fraction; Tb.Th, trabecular thickness; Tb.Sp, trabecular separation; Tb.N, trabecular number.

	***BV/TV* (%)**	***Tb.Th* (µm)**	***Tb.Sp* (µm)**	***Tb.*N (µm^{-1})**
Porcine femur, chondral defects				
rhCo-PLA	54.5±2.9	211.3±9.8	273.0±30.6	2.1±0.1
pCo	54.1±2.8	205.2±10.0	253.2±15.5	2.2±0.1
spontaneous	54.8±3.1	217.4±9.0	284.0±12.5	2.0±0.0
healthy[a]	49.1±1.2	183.4±4.6	287.3±5.0	2.1±0.0
Lapine femur, osteochondral defects				
PLGA	33.6±1.4	354.3±19.0	1050.1±121.5	0.7±0.1
PLGA-BGf	25.1±3.6	295.5±17.7	1983.7±178.0	0.5±0.0
β-TCP	46.0±1.3	225.5±9.5	528.6±26.1	1.3±0.0
BG	30.5±1.7	161.1±8.6	631.8±48.5	1.3±0.1
spontaneous	37.1±1.6	364.1±29.5	1143.8±95.9	0.7±0.1
healthy[a]	33.6±0.6	250.0±6.3	611.5±14.6	1.2±0.0
Equine carpus, chondral defects				
2 mm	44.2±13.4	84.8±12.5	149.7±23.2	4.6±1.0
4 mm	47.3±8.3	89.9±8.5	131.3±8.5	5.1±0.7
8 mm	46.6±10.3	89.9±8.1	141.6±12.8	5.0±0.8
healthy[b]	31.7±9.1	85.3±10.1	227.5±36.2	3.4±0.8
Equine carpus, osteochondral defects				
2 mm	45.7±8.3	93.1±3.2	120.8±11.8	4.8±0.7
4 mm	33.5±4.9	87.5±3.1	158.2±11.3	3.8±0.5
8 mm	48.9±4.4	94.6±1.4	141.9±10.3	5.2±0.4
healthy[b]	43.5±3.2	103.5±2.2	180.7±11.4	4.2±0.2

[a] contralateral non-operated knees. [b] tissue adjacent to the defect sites in carpus

5.5 MR IMAGING OF EQUINE REPAIR TISSUE (*III*)

Repair tissue in the defects showed a trend of shorter T_{1Gd} relaxation times and longer T_1 relaxation times than control tissue (Figure 6). Osteochondral defects had longer T_{1Gd} relaxation times than the chondral defects, although the differences were not statistically significant. The T_2 relaxation time was shorter in the 8 mm osteochondral lesions than in chondral lesions with the same diameter in ROI1 (repair tissue only) (33.8±0.8 ms and 41.0±1.3 ms, respectively; p=0.017) and deep part of ROI2 (lesion area aligned to adjacent healthy cartilage) (48.9±8.4 ms and 103.9±12.2 ms, respectively; p=0.020). There were no statistically significant differences in T_1 relaxation times between the groups. In ROI2, there was a trend of increasing T_1 relaxation time with lesion diameter and towards the cartilage surface in the chondral samples, an implication of increasing water content and structural disorganization (Figure 6).

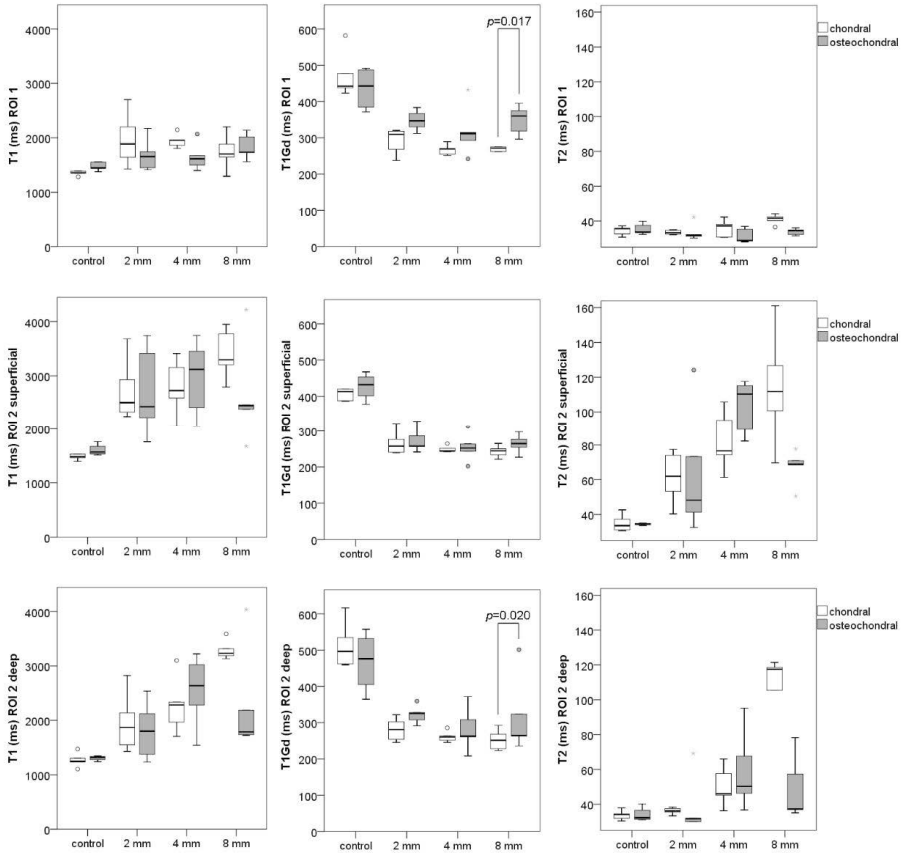

Figure 6 Boxplot graphs showing the results of the MRI analyses. The top and bottom of each box represent the first and third quartiles, the horizontal line inside the box is the median, and the whiskers are the 10th and 90th percentiles. The circles are outliers. All statistically significant *p* values are marked in the figure.

5.6 HISTOLOGICAL EVALUATION OF REPAIR TISSUE (*I–III*)

Visualization of proteoglycans with Safranin-O staining demonstrated that the repair tissue had abundant proteoglycan content in all porcine study groups (Figure 7). In one of the two collapsed rhCo-PLA samples, the scaffold was detached since no polylactide fibers could be detected in the histological sections. In the other one, the scaffold was sunken into the subchondral bone. When the rhCo-PLA scaffold was well aligned with the native cartilage, the integration was good with no borderline between native and repair tissue (Figure 7). The pCo treatment group and the spontaneously healed group showed lesion perimeter collapse and grainy lesion borders in the majority of the samples.

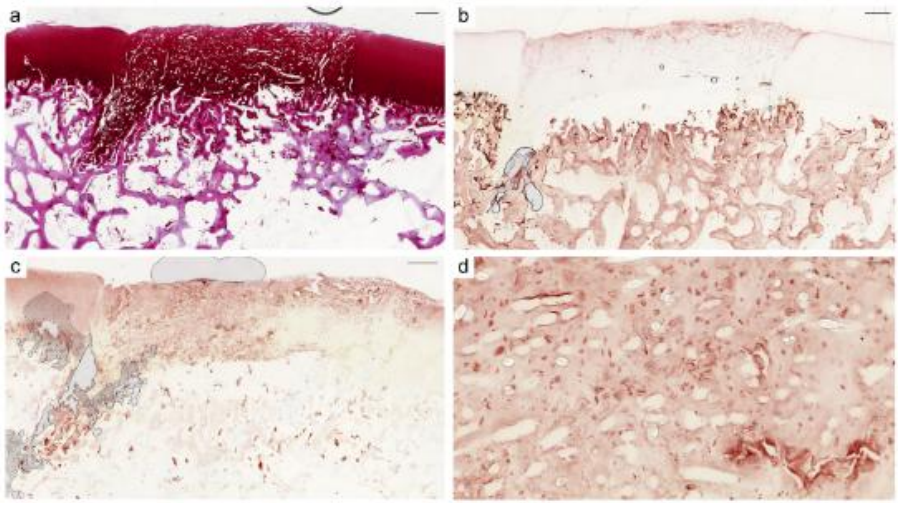

Figure 7 Representative image showing the repair tissue in an rhCo-PLA-treated defect. a) Safranin-O staining showed abundant proteoglycans throughout the repair tissue area. Polylactide fibers appeared as white dots and rods within the cartilage tissue. b) Immunohistochemical staining for type I collagen showed that the stain was mostly on the surface of the cartilage tissue. c) Immunohistochemical staining for type II collagen showed abundant type II collagen throughout the repair tissue. Air bubble artefact appears as gray areas on the slide. d) Magnification of the type II collagen stain showed the pericellular distribution of the stain. Scale bars: a-c: 500 µm, d: 50 µm.

The total ICRS Visual Histological Assessment Scale score (mean±SE) for rhCo-PLA group was 11.8±1.9, for pCo group 8.5±2.7 and for spontaneous group 9.6±1.5 (p=0.43). Variation between individual animals was large (Figure 8a).

The OARSI histological score showed worse score in all of the equine lesions compared to the control tissue (Salonius et al. unpublished data). Dispersion of the results was large especially in the 4 mm and 8 mm chondral lesions, as depicted in Figure 8b.

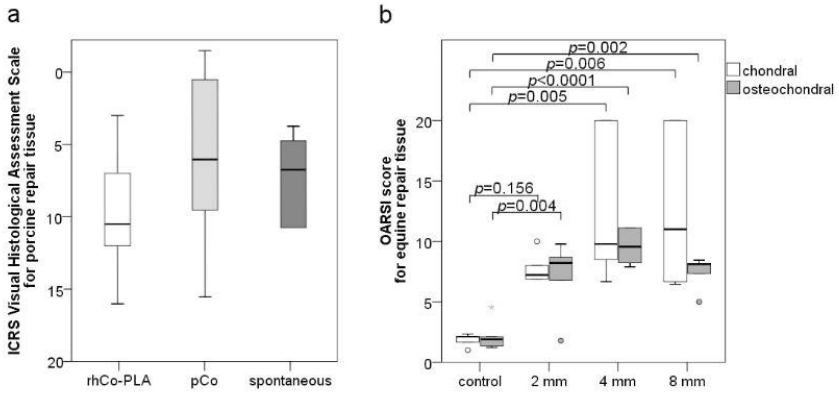

Figure 8 a) The total histological ICRS score (0–20, where 0 represents healthy cartilage) in *study I*. No statistically significant differences were found between the study groups. b) The OARSI score (0–20 where 20 represents healthy cartilage) in *study III*. All *p* values for comparison of each study group with adjacent healthy control tissue are marked in the figure. Only chondral defects with a diameter of 2 mm did not differ from healthy control tissue. The dark line in the middle of the boxes represents the median value. The bottom of the box indicates the first quartile and the top of the box indicatesthe third quartile. The whiskers represent the 10th and 90th percentiles.

In *study III*, only 1/15 chondral lesions showed Safranin-O positivity in the histological sections, whereas 11/15 of osteochondral defects stained positively for Safranin-O. Typically, the osteochondral samples showed mixture of hyaline-like and fibrous cartilage in the deep or middle part of the repair tissue and fibrous tissue on the surface (Figure 9).

In the histological evaluation of the bone defects in the lapine model (*study II*), PLGA and spontaneous group were filled with a mixture of fibrous tissue and mineralized bone. In the PLGA-BGf group, the bone defects were filled with fibrous tissue only. The areas that appear empty in μCT images consisted of connective tissue and bone marrow (Figure 10). Osteoid was most abundant in the β-TCP group where it encircled numerous small islands of mineralized bone. Both commercial controls showed comprehensive lesion filling with tissue where mineralized bone and osteoid alternated with cell-rich fibrous tissue. Although the bone defect filling was good, there was a connective tissue-filled depression of the joint interface in the β-TCP and BG groups.

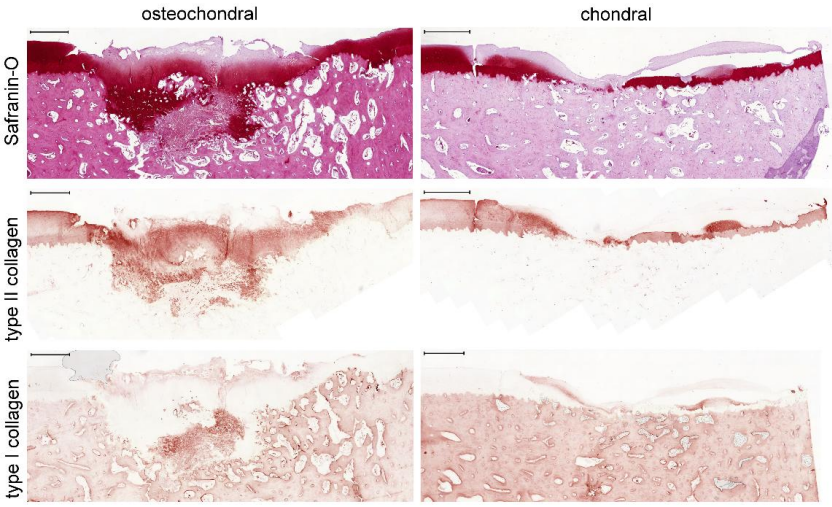

Figure 9 Examples of Safranin-O and type I and II collagen stainings of 8 mm defects in the equine model. The left panel shows a representative osteochondral defect and the right panel shows a representative chondral defect. Scale bars: 1 mm.

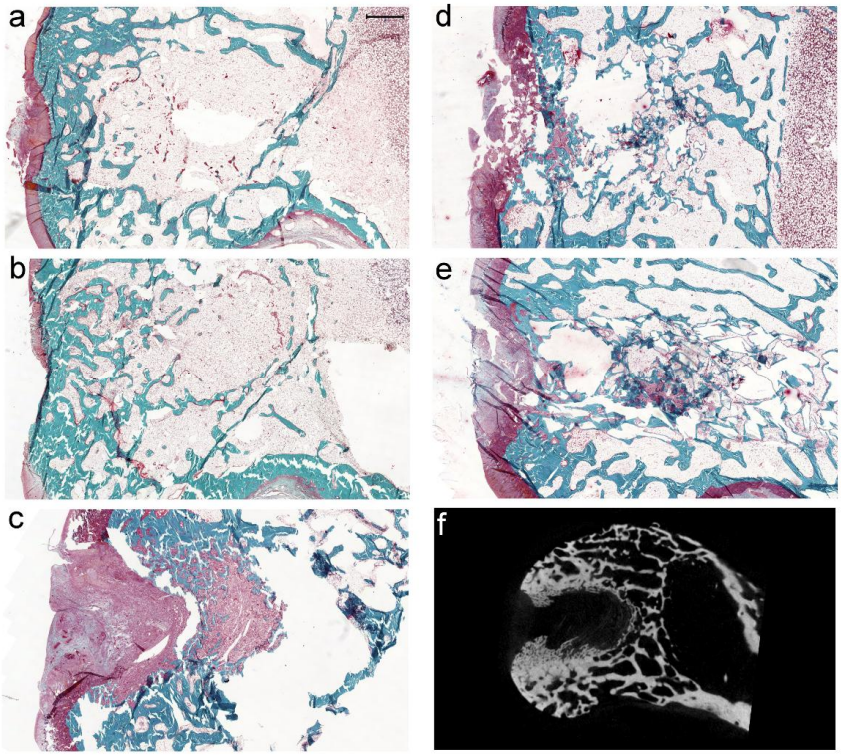

Figure 10 Masson-Goldner trichrome stained sections showing the tissue structure of the defect area in each group. Scale bar a-e: 1 mm. a) PLGA; b) PLGA; c) PLGA-BGf; d) β-TCP; e) BG, f) Micro-CT image showing the unhealed defect area in a representative PLGA-BGf specimen.

The overall number of lymphocytes and macrophages in the histological sections was low. The semi-quantitative evaluation of the inflammatory cells showed that 3/7 specimens in PLGA group and 2/7 in PLGA-BGf group showed 50—100 inflammatory cells on the slide. No other group presented with an increase in the number of lymphocytes or macrophages.

Histological evaluation of chondral repair in *study I* and *study III* showed that the repair tissue seemed to originate from the bone marrow spaces (Figure 9). Lack of bone marrow connection resulted in fibrous repair tissue both in the spontaneously healed porcine and equine samples and in the ACI-repaired porcine samples.

5.7 IMMUNOHISTOCHEMICAL EVALUATION OF REPAIR TISSUE (*I, III*)

Type II collagen was evenly and pericellularily distributed throughout the rhCo-PLA-treated specimens, whereas the pCo-treated specimens showed type II collagen in the peripheral rim of the repair cartilage (Figure 7). Type I collagen was only present in the superficial part of the cartilage in all study groups (Figure 7). All groups showed repair tissue which was predominantly positive for type II collagen and negative for type I collagen staining (Table 8). One specimen from the spontaneously healed group showed detachment of repair tissue.

Almost all of the spontaneously healed equine osteochondral samples with the diameter of 2 mm showed positive type II collagen staining and only one of these samples showed positive type I collagen staining (Table 8). In the 2 mm chondral samples, positive staining for type II and type I collagen was shown in 1/5 and 4/5 samples, respectively. Fibrocartilage formation was evident in the larger chondral and osteochondral lesions where a mixture of type I and type II collagen positive tissue was present (Figure 9). Poor quality of the repair tissue affected the evaluation of the specimens. Two of the 4 mm and four of the 8 mm chondral specimens were lacking any repair tissue and were thus perceived negative for staining.

Table 8. Number of samples in each study group with positive staining for type I or II collagen. Detached tissue was perceived negative for staining.

	type I collagen	type II collagen
porcine 8 mm		
rhCo-PLA	2/6	5/6
pCo	1/6	5/6
spontaneous	1/5[a]	4/5[a]
equine 2 mm		
chondral	4/5	1/5
osteochondral	1/5	4/5
equine 4 mm		
chondral	2/5[b]	0/5[b]
osteochondral	2/5	2/5
equine 8 mm		
chondral	1/5[c]	0/5[c]
osteochondral	2/5	3/5

[a] repair tissue detached from one spontaneously healed specimen; [b] repair tissue detached from two of the 4 mm chondral specimens; [c] repair tissue detached from four of the 8 mm chondral specimens

5.8 BIOMECHANICAL EVALUATION OF REPAIR TISSUE (*I*)

The non-fibrillar matrix modulus (E_m), indicative of proteoglycan content, was the highest in the rhCo-PLA-treated group and the lowest in the untreated group (Figure 11). No statistically significant differences were found between the groups (p=0.20).

Collagen fibril network modulus (E_f) and permeability (k_o) showed no statistically significant differences between the study groups (p=0.18 and p=0.14, respectively). The permeability of the contralateral non-operated knees in the untreated group was greatly increased compared to the treatment groups, indicating worsened tissue quality (Figure 11).

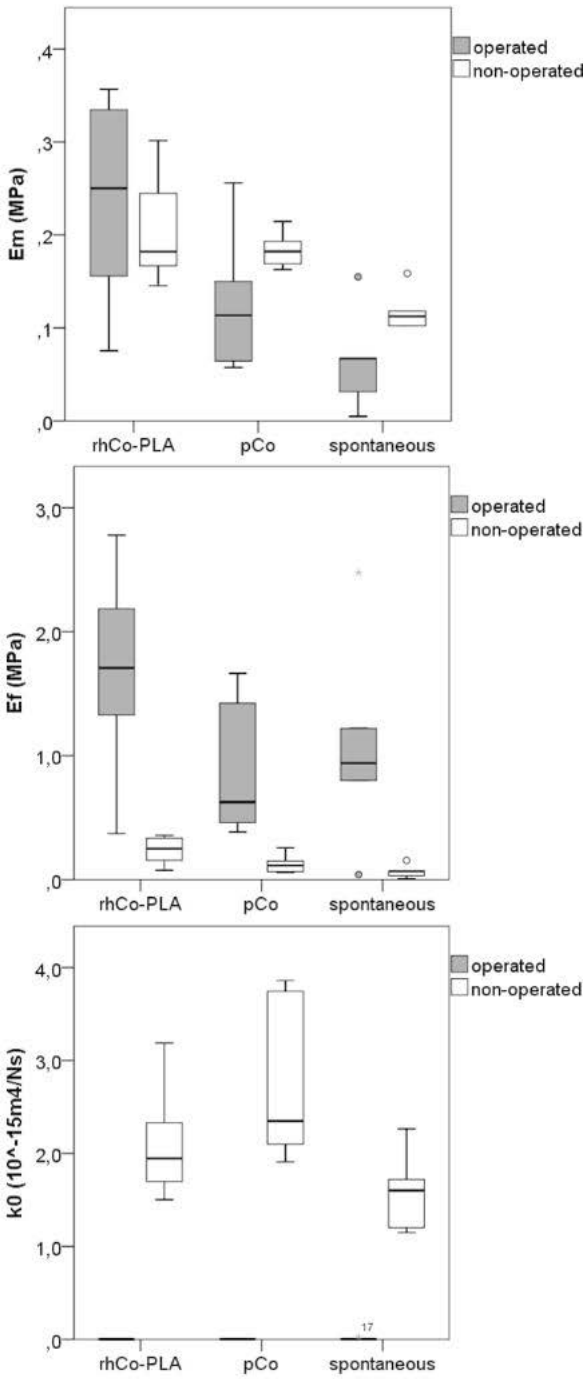

Figure 11 Biomechanical testing of the operated and contralateral non-operated articular cartilage showed no statistically significant differences between the study groups.

5.9 COLLAGEN FIBRIL NETWORK ORGANIZATION OF EQUINE REPAIR TISSUE (*III*)

PI was high in all samples. PI was higher in chondral lesions than in osteochondral lesions, although this difference was statistically significant only in 2 mm lesions in the deep part of the repair tissue in which the PI was 0.89±0.02 for chondral and 0.79±0.03 for osteochondral defects (p=0.042).

Collagen fibril orientation showed large variation between the groups and between individual samples. Collagen orientation changed toward the typical tangential orientation in the superficial part of the 2 mm lesions. Osteochondral lesions showed a higher level of collagen fibril organization compared to the chondral lesions in the deep part of the tissue: In 4 mm defects, the orientation was 61.6±4.3° for osteochondral and 35.4±7.0° for chondral defects (p=0.047) and in 8 mm defects, 69.5±2.7° for osteochondral and 33.6±2.2° for chondral defects, respectively (p=0.004).

5.10 GENE EXPRESSION ANALYSES OF *IN VITRO* STUDY (*IV*)

Only chondrogenically differentiated MSCs showed upregulation of studied genes; chondrocytes and proliferated MSCs showed no upregulation of any of the studied genes at any time point. The chondrogenic gene *SOX9* was not upregulated in any of the studied samples.

The chondrogenic gene *ACAN* was slightly upregulated in the MSC-C samples cultured in the pCo on day 14 and with a slight increase on day 28 (1.29±0.15 and 3.88±0.81 fold, respectively). In other samples, the expression of *ACAN* was decreased from day 0 or even absent. The cartilage gene *COL2A1* was transiently upregulated in the chondrogenically differentiated stem cells on pCo membrane on day 14 (Figure 12); otherwise, no expression of *COL2A1* was detected.

The chondrocyte hypertrophy and osteogenesis marker genes, *RUNX2* and *COL10A1*, were only upregulated in the MSC-C samples (Figure 12). The expression of *RUNX2* was noted in rhCo3-PLA and pCo scaffolds on day 14 (3.49±0.52 and 3.53±0.29 fold, respectively), whereas in the rhCo-PLA scaffold it was absent. On day 28, the expression level of *RUNX2* was highest in pCo (6.55±0.84 fold; p<0.001) but in rhCo3-PLA it had returned close to the level of day 0 controls (1.63±0.15). MSC-Cs seeded on the pCo membrane showed upregulation of *COL10A1* on day 14 (29.64±4.81 fold) and the expression level remained high on day 28 (20.32±5.15 fold).

Only MSC-Cs showed upregulation of the fibroblast/synovial marker *MFAP5* on day 14. The expression level was highest in the rhCo-PLA scaffold, which showed a statistically significant difference to pCo scaffold (p=0.011). Other cell types or time points showed no upregulation of *MFAP5*.

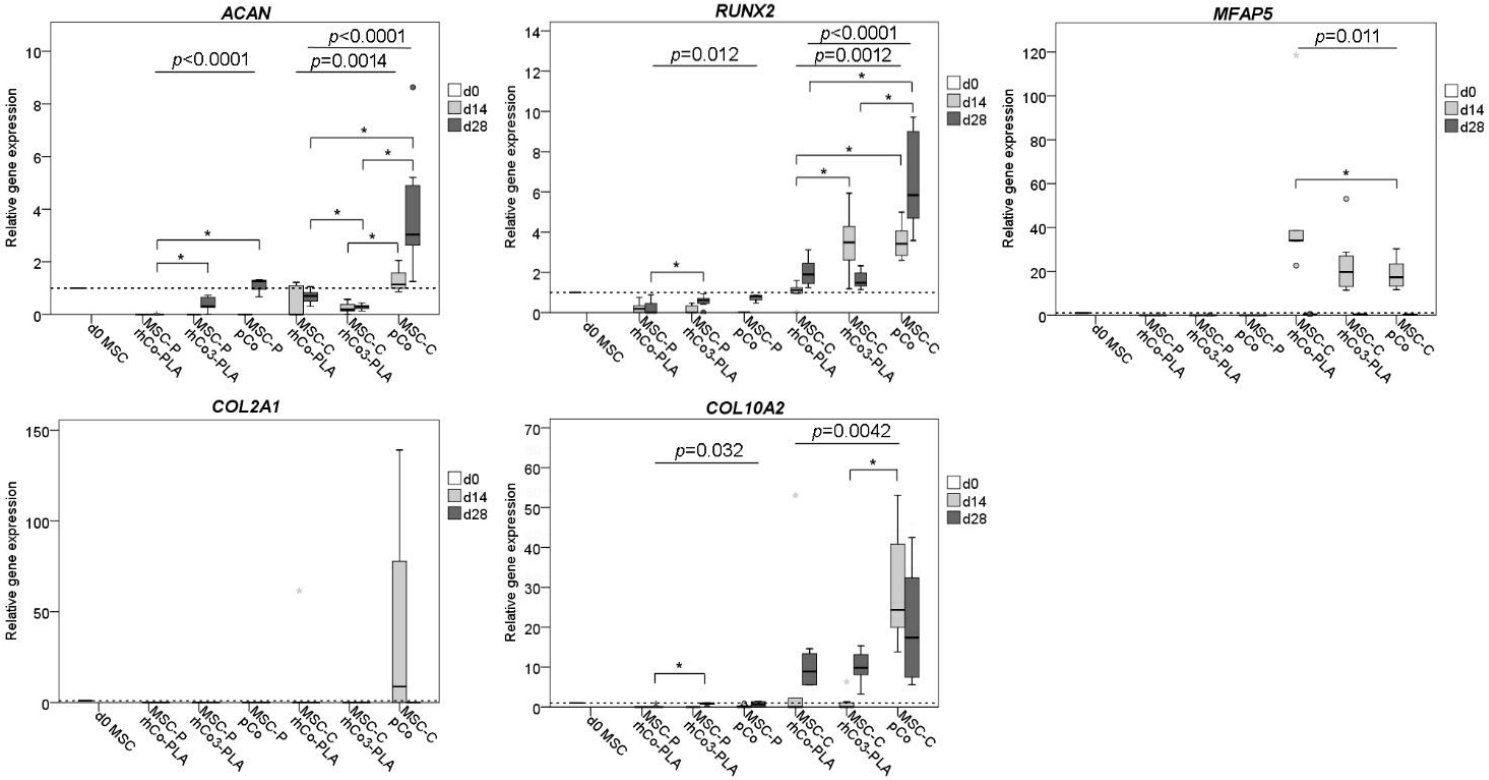

Figure 12 Relative gene expressions in differentiated and proliferated MSCs in *study IV*. Dashed line shows the gene expression level for day 0 samples. MSC-P, proliferated mesenchymal stem cell; MSC-C, chondrogenically differentiated mesenchymal stem cell.

5.11 SULFATED GLYCOSAMINOGLYCANS (*IV*)

The highest sGAG content was found in the MSC-Ps and the lowest in the ACs. When comparing the different scaffold types, pCo membrane showed the highest glycosaminoglycan content in undifferentiated MSCs ($p<0.001$) and lowest in the chondrogenically differentiated stem cells (MSC-C) ($p<0.005$) at both time points. No statistically significant differences were found between the different types of rhCo-PLA scaffolds.

5.12 CELL DISTRIBUTION ON THE SCAFFOLDS (*IV*)

Confocal imaging of the specimens demonstrated the polarity of the pCo membrane: the cells resided in a sheet-like manner on one side of the membrane. The cells residing in the rhCo-PLA scaffolds were distributed more evenly at the entire depth of the scaffold. The imaging showed that there was a good amount of cells in all scaffolds and all cell types.

6 DISCUSSION

Cartilage defects have posed a vast challenge for surgeons for centuries (Hunter 1743). Despite rigorous development of new treatment strategies, healthy articular cartilage with its zonal architecture still cannot be produced. The studies presented in this thesis improved current translational approaches by defining the critical defect size in the equine carpus and by introducing new biomaterials to cartilage repair. These studies evaluated surgical cartilage repair with a broad perspective. The feasibility of several novel biomaterials, both for chondral and osteochondral defects, was studied. Both *in vitro* evaluation of biomaterials in cell culture and *in vivo* studies assessing spontaneous and augmented repair in different animal models were covered. The novel composite scaffold rhCo-PLA was evaluated both *in vitro* and *in vivo*, following the roadmap of translation from bench to bedside.

6.1 TRANSLATION OF NEW TECHNIQUES: *IN VITRO* STUDY

Translation of new techniques usually starts with choosing the best possible *in vitro* model to investigate clinically meaningful aspects of the new approach in controlled surroundings. For example, cellular responses to biomaterials can be evaluated *in vitro*. *Study IV* formed a large entity, in which the fate of different cell types in three different biomaterials were studied at several time points *in vitro*. Although bovine chondrocytes are used in many laboratory studies, future clinical use of the studied materials takes advantage of human cells. Human mesenchymal stem cells and human cadaveric chondrocytes were used in the *in vitro* study of the scaffold material rhCo-PLA. All cells used in the study were derived from young donors for the best possible regeneration potential. The xeno-free chondrogenic differentiation medium used in the study would allow for a cell-scaffold combination completely free of animal-derived products.

When assessing the differences of rhCo-PLA and pCo, the latter showed a sheet-like cell distribution on one side of the membrane whereas rhCo-PLA scaffold showed a more even cell distribution. There were slightly more hypertropic cells growing on pCo membrane than in rhCo-PLA. This might be due to the monolayer-like structure of the pCo in comparison to the three-dimensional structure of the rhCo-PLA scaffold (Caron et al. 2012). However, cell type and cell culture medium showed a larger impact on the cell fate than the scaffold type.

Differentiating human BM-MSCs in chondrogenic differentiation medium and in scaffolds intended for cartilage repair resulted in increased expression of osteogenic pathway markers. The cells also showed a transiet upregulation

of fibroblast marker MFAP5, showing the multilineage differentiation potential of these cells. BM-MSCs as a cell source might have a predefined fate of endochondral ossification (Vinardell et al. 2012, Somoza et al. 2014) although chondrogenic differentiation in pellet culture has been successful in this study and previously (Skog et al. 2015).

Poor yield of cadaveric chondrocytes in *study IV* required multiple passaging of the cells. The passage 3 cadaveric chondrocytes did not express any of the studied chondrogenic genes, nor did they produce extracellular matrix with sulfated glycosaminoglycans in scaffolds. This finding indicates that these cells have undergone dedifferentiation at an early phase of cell culturing, and that the three-dimensional environment of rhCo-PLA scaffolds and collagen membrane was not sufficient for reversing this change. It has been known for decades that long monolayer culturing of chondrocytes causes their dedifferentiation (Benya et al. 1978). The dedifferentiation process starts already on day 2 of the culture as the cells start to synthetize type I collagen but the transition extends through several weeks (von et al. 1977).

Nevertheless, passage 3 chondrocytes have been reported to produce good quality cartilage repair tissue in a clinical setting in MACI® (Vericel Corporation, USA), which has an FDA approval (Corbett et al. 2017, US Food and Drug Adminstration 2016). This emphasizes the fact that the ability of *in vitro* testing to predict clinical repair responses is limited. The entire joint environment with its mechanical stresses, synovial fluid and underlying bone affect cartilage restoration. Animal models are used in closing the gap between *in vitro* testing and clinical studies.

6.2 SPONTANEOUS ARTICULAR CARTILAGE REPAIR IN ANIMAL MODELS

When designing a preclinical *in vivo* study, the choice of animal model is critical. Small animal models can be used for proof-of-principle testing, but testing of implantable medical devices and gaining of regulatory approval for clinical trials requires cartilage thickness and joint size in which the device can be implanted. In addition to the biological properties and translational value of the animal model, the housing requirements and costs must be taken into consideration. Many animal species used in *in vivo* models, such as rats and rabbits, have capacity of spontaneous cartilage repair, unlike humans. This creates a limitation that needs to be borne in mind in translational research.

Previous study by Vasara and colleagues (Vasara et al. 2006) on porcine osteochondral defects showed that the spontaneous healing of skeletally immature pigs is good with repair tissue rich in type II collagen, even though the defects were 6 mm in diameter, which is considered the critical lesion size in porcine cartilage (Moran et al. 2016). Our *study I* confirmed that spontaneous healing of full-thickness chondral defects with the diameter of 8 mm was inferior to ACI-treated defects. The small study groups in our

feasibility study, however, resulted that the differences between the groups were small and not statistically significant.

Critical osteochondral defect size in rabbit femur is 3×5 mm (Levingstone et al. 2016, Moran et al. 2016). Although we created a large defect of 4 mm in diameter and 8 mm in depth covering most of the medial femoral condyle of rabbits, no large, empty voids were observed in the spontaneously repaired defects. All untreated deep intra-articular bone defects in rabbits showed an attempt of repair, although the trabeculae were sparse and canals from the bone surface into the bone marrow spaces were not uncommon.

Similarly, osteochondral defects in the horse showed subchondral bone changes still at 12 months post surgery. However, the overall filling of equine osteochondral defects 2 mm in diameter did not differ from control tissue. This repair tissue also showed good proteoglycan and type II collagen content in all defect sizes. We concluded that the diameter of 4 mm should be considered the critical osteochondral defect size in the equine carpus.

Previous studies evaluating critical cartilage defect size have focused on evaluating the filling of the defects (Convery et al. 1972, Hurtig et al. 1988). Although equine model has been used in cartilage repair research, long term fate of the spontaneously formed repair tissue in the equine carpus has remained unknown. State-of-the-art methods, including MRI, μCT, polarized light microscopy, standard histology and immunohistochemistry, were used in evaluating equine cartilage repair in *study III*. The repair tissue of the chondral defects of all sizes demonstrated structural disorganization and loss of proteoglycans and type II collagen staining. Defects with the diameter of 4 mm and 8 mm showed inadequate defect filling in the equine carpus. Smaller defects of 2 mm demonstrated lesion filling with fibrocartilage. As fibrocartilage is prone to wearing out due to its inferior mechanical strength to hyaline cartilage (Vachon et al. 1986), tissue quality needs to be analyzed for objective evaluation of success. Based on the results of this study, 2 mm is to be considered the critical chondral defect size in the equine carpus. These new recommendations for the critical defect size allow for a more ethical use of horse as a model in cartilage repair, as the defects are considerably smaller than the previously recommended 9 mm, validated for the stifle joint (Russell & Burch 1959, McIlwraith et al. 2011).

6.3 CONTRALATERAL LIMB IS AFFECTED BY CARTILAGE DEFECTS

In animal models, only one limb is often used and the contralateral limb is used as a control, representing a healthy joint (Vasara et al. 2006, Pulkkinen et al. 2013b). The use of an age-adjusted healthy control group with no interventions increases the number of animals used and therefore increases costs and might be considered to contradict the Reduction principle of the three R's (Russell & Burch 1959). However, the biomechanical testing in the

porcine study (*study I*) showed that untreated cartilage defects resulted in considerably higher cartilage permeability to water in the contralateral non-operated limb than the non-operated limbs of the treatment groups. This indicates a worsened tissue quality with loss of proteoglycans (Korhonen et al. 2003). It is possible that an altered loading pattern, due to pain or lack of mechanical support, might have promoted this change (Kiviranta et al. 1994, Vanwanseele et al. 2003), even though deviant limping of the animals in the untreated group was not detected during the study period.

Studies I and *II* were limited by the lack of a healthy control group. However, in both studies, the comparison of different study groups is possible as all groups used the non-operated limb as an animal-specific control. The use of a healthy control group with no interventions is recommended in order to see the real effect of the treatment.

6.4 SUBCHONDRAL BONE CYSTS ASSOCIATED WITH CARTILAGE DEFECTS IN ANIMAL MODELS

Subchondral bone cysts are common after cartilage procedures. They have been reported both in patients (Vasiliadis et al. 2010, Orth et al. 2013) and in animal models (Vasara et al. 2004, Orth et al. 2013). Porcine subchondral bone is soft and immature porcine cartilage lacks calcified layer (Vasara et al. 2006, Li et al. 2009). Therefore, it might easily lead to sinking of the scaffold material into the bone, as seen in one animal in *study I*. In this porcine experiment, in which all articular cartilage was removed and the subchondral bone was exposed, bone cysts were seen both in the treatment groups and the spontaneously healed control group. In a previous study, the softness of porcine subchondral bone plate as a risk factor for bone cysts was discussed in more detail (Vasara et al. 2006). However, the spontaneously healed group in *study I* showed less and smaller bone cysts than the two augmented repair groups.

In the equine study (*study III*), the surgically created osteochondral defects extended approximately 2—3 mm into the subchondral bone. Although the defects 2 mm in diameter showed good filling with repair tissue, 4/5 specimens showed bone pathologies 12 months post-surgery. This demonstrates poblems in subchondral bone repair even in the small defects. Shallow chondral lesions in the equine carpus presented with no subchondral bone cysts. This is in line with previous studies that conclude that bone cysts commonly arise after disruption of the subchondral plate in the equine and caprine model (Hurtig et al. 2011)(Jackson et al. 2001). As the porcine cartilage lacks the calcified layer, full-thickness chondral porcine defects can be seen as osteochondral in nature. Our study shows that both augmented and spontaneous repair of osteochondral defects lead to cysts and other bone voids in different large animal models.

Trabecular bone structure varied between the different animals. The equine model showed thinner and denser trabecular structure compared to the two other animal species. Both the porcine and equine trabecular parameters in this study (Table 7) are in line with previously published values (Furst et al. 2008, Holzer et al. 2012). Trabecular thickness and spacing in the rabbit was larger in this study than in previous reports (Voor et al. 2008), probably due to the large voids in the analyzed area.

Thickened trabeculae have been associated both with early OA and increased joint loading (Ding et al. 2003). In *study I*, pigs with iatrogenic cartilage lesions showed thickened trabeculae underneath the cartilage defect, compared to non-operated contralateral limbs but their separation and number was close to non-operated knees. Similarly, in deep intra-articular bone defects in the rabbits of *study II*, the bone trabeculae of the spontaneously healed defects were thick and sparse and thus differed from the contralateral healthy knees.

It seems that disruption of the cartilage layer, whether iatrogenic or natural, leads to these trabecular structural changes. However, in the equine model (*study III*) where tissue adjacent to the defects was used as control, the trabecular thickness of the bone underneath the cartilage defects and adjacent tissue did not differ from one another. This may suggest that the changes in the subchondral bone trabecular architecture are due to altered loading conditions, rather than a local or a direct effect of the defect on the underlying bone.

6.5 FEASIBILITY OF THE NOVEL RHCO-PLA SCAFFOLD

The repaired cartilage tissue in both the novel rhCo-PLA scaffold and the well-established commercial pCo membrane showed similar structure histologically and biochemically in the porcine study (*study I*). However, in the *in vitro* study (*study IV*), in which human chondrocytes and BM-MSCs were cultured in the scaffolds, porcine type I/III collagen membrane induced cartilage hypertrophy and osteogenic commitment at a higher level than the three-dimensional rhCo-PLA scaffolds, shown by upregulation of osteogenic genes *COL10A2* and *RUNX2*. The type of recombinant human collagen used in the manufacturing of the rhCo-PLA scaffolds did not affect the results. This implicates that the three-dimensional structure might be more important for the cell fate than the type of protein component used in the scaffold.

The results of *study I* showed promising *in vivo* results with the novel rhCo-PLA scaffold. Treatment of porcine cartilage defects with the rhCo-PLA implant resulted in fewer bone cysts than treatment with porcine type I/III collagen membrane. This is probably due to the porous structure of rhCo-PLA which allows for a natural multidirectional fluid flow during cyclic loading, unlike the collagen membrane in which one side is hydrophilic, intended to keep the cells in place. This membrane might function as a valve, filling the

defect site with synovial fluid but restricting its backword flow. As fluids are incompressible, each loading cycle during the joint movement presses the fluid into the slit, thus expanding it into the subchondral bone (Kold et al. 1986).

6.6 BONE FILLERS IN REPAIR OF DEEP OSTEOCHONDRAL DEFECTS

Creating biodegradable cylindrical plugs to fill the bony part of a deep osteochondral defect was hypothesized to result in joint reconstruction, to ultimately be used in biological joint repair instead of conventional joint replacement surgery. Filling of deep osteochondral defects in rabbits with the gas-foamed PLGA scaffold in *study II* resulted in repair worse or similar to spontaneous healing. PLGA induced a mild inflammatory response in the treated defects as seen by the presence of inflammatory cells, which is probably due to the acidic surrounding caused by its degradation (Gentile et al. 2014, Haaparanta et al. 2015).

In *study II*, granular bone fillers did not erode from the defect site during the 3-month follow-up. Extensive bone defect filling with mineralized tissue was observed in both the β-TCP and BG-treated groups. A small depression was detected on the surface, indicating sagging of the granules. Bone architecture in the granule-treated groups was similar to non-operated controls. Thus, the granular bone substitutes might have the potential to be used in the repair of the bony part of deep osteochondral defects.

Bioactive glass has provided good results in terms of osteoconduction (Lindfors et al. 2009). In our study, bioactive glass alone showed bone trabecular parameters that were closest to those of the non-operated contralateral limbs, indicating good overall repair tissue quality. Brittleness of bioactive glass has limited its use in weight-bearing applications but combining it with polymers has been reported to improve the mechanical properties of the construct (El-Rashidy et al. 2017). Surprisingly, PLGA combined with bioactive glass fibers in *study II* worsened the repair result as the defects were filled with loose connective tissue rather than osteoid or mineralized bone. A possible explanation might be that the porosity of both PLGA-based scaffolds might have been compromised by collapse of the pores and the small size of the pores (Haaparanta et al. 2015, Uppstu et al. 2015). Although this study focused on the bony part of the defect, it needs to be stated that none of the studied materials was capable of restoring the cartilage surface in the lapine model. Therefore, a separate cartilage restorative procedure should be considered on top of the bone repair to restore the joint surface.

6.7 SYNOVIAL JOINT AS A FUNCTIONAL UNIT

A synovial joint comprises a functional unit in which all its parts play a crucial role. Malalignment and damage to stabilizing ligaments and menisci have been shown to lead to cartilage defects (Gomoll et al. 2010, Sharma et al. 2010). Similarly, the importance of crosstalk between articular cartilage and subchondral bone has been acknowledged (Pan et al. 2009, Orth et al. 2013, Findlay & Kuliwaba 2016).

Lack of support from the subchondral bone underneath cartilage defects lead to increased loading on the surrounding articular cartilage (Jackson et al. 2001). This might lead to early degeneration of the cartilage adjacent to the defect site. Shallow chondral defects created in the equine carpus in *study III* did not present with subchondral bone cysts, but deeper osteochondral defects, in which the subchondral bone plate was disrupted, did. Correspondingly, deep osteochondral defects in the lapine model showed very little cartilage formation on the joint surface even in the defects repaired with granular commercial bone substitutes that resulted in satisfactory bone repair. Although rabbits typically possess good intrinsic healing capacity (Ahern et al. 2009, Moran et al. 2016), absence of a separate cartilage regenerative procedure hampered the repair of articular cartilage. Similar results were noted in minipigs where osteochondral defects repaired with PLGA-hydroxyapatite-β-TCP scaffolds (Matsuo et al. 2015).

Although the mechanical support of subchondral bone is needed for proper cartilage repair, the connection between the disrupted cartilage and bone marrow spaces seem important for the repair of chondral defects. This was noted in *study I*, in which one chondral defect did not reach the subchondral bone plate (animal 25, rhCo-PLA group). In spite of 5.6×10^6 autologous chondrocytes being implanted with the rhCo-PLA scaffold on the defect site with a diameter of 8 mm, no hyaline cartilage was formed. This cell amount is 11.2×10^6 cells/cm^2, more than double the amount of cells used in the original ACI procedure by Brittberg and colleagues in which $2.6–5.0\times10^6$ cells were used in cartilage defects with a mean size of 3.1 cm^2 (Brittberg et al. 1994). The amount of autologous chondrocytes implanted to defect site in clinical studies varies between $0.5–12\times10^6$ (Foldager et al. 2012). Therefore, the mesenchymal stem cells and trophic factors originating from marrow spaces and repair of the entire osteochondral unit seem important for cartilage regeneration as previously proposed (Murphy et al. 2013, Caplan 2017, de Vries-van Melle et al. 2014).

6.8 FUTURE PROSPECTS

Articular cartilage repair constitutes an immense challenge. Although the Holy Grail of cartilage repair still remains to be discovered, progress has been made in terms of better understanding the tissue structure and behavior. Articular cartilage and subchondral bone have an effect on one another. The exact mechanism of the cross-talk between the bone and cartilage in humans is, however, still unknown. Finding out the mechanism would probably be highly valuable in developing articular cartilage repair.

Biomaterial scaffolds have been extensively studied but no material has proven superiority over another. The novel rhCo-PLA scaffold showed promising results in the feasibility study in the porcine model but further studies, including a healthy control group, are required in order to confirm the safety and the efficacy of the scaffold.

The pilot cell pellet study of *study IV* and previous studies both with human (Georgi et al. 2015, Skog et al. 2015) and animal MSCs (Zayed et al. 2017) showed that the chondrogenic potential of human mesenchymal stem cells varies between individual donors. A study investigating the chondrogenic potential of BM-MSCs in patients with and without PTOA after knee trauma might be able to provide insight about the regenerative potential of articular cartilage.

7 CONCLUSIONS

In this study, cartilage repair with novel biomaterial scaffolds and cell therapies was investigated using both *in vitro* and animal models. Based on the results, the specific conclusions are the following:

1 The new composite biomaterial rhCo-PLA showed fewer bone cysts but similar cartilage repair tissue to that obtained with commercial pCo membrane. Thus, the new biomaterial rhCo-PLA seems to be suitable for the repair of chondral defects with the ACI method.

2 The new PLGA-based biomaterials are insufficient in the repair of deep osteochondral lesions. Repair tissue produced with these materials was similar to or worse than spontaneous repair.

3 Spontaneous defect healing in the equine carpus is more restricted than previously thought. The new proposed critical lesion size for chondral lesions is 2 mm in diameter and for osteochondral lesions 4 mm in diameter in the equine carpus.

4 Chondrogenic differentiation of BM-MSCs was not successful in the rhCo-PLA or the pCo scaffolds *in vitro*. The chondrogenic differentiation lead to cell hypertrophy.

This study demonstrated the capacity of the novel rhCo-PLA scaffold to produce hyaline cartilage in a porcine model. However, subchondral bone defects in association with cartilage repair procedures and surgically created osteochondral defects were common in pigs (*study I*), rabbits (*study II*), and in horses (*study III*).

As seen in *study I*, non-operated contralateral limb is also affected by the defect and repair procedure. Untreated cartilage defect leads to an increased cartilage permeability to water in the contralateral limb.

Synovial joints comprise a functional unit in which each component is to be taken into consideration. Successful chondral repair is jeopardized if the integrity of the subchondral bone is compromised. Similarly, repair of the bony part of an osteochondral defect requires an additional repair of articular cartilage in order to restore joint health.

ACKNOWLEDGEMENTS

This study was carried out in the Orthopadic Research Group, Department of Orthopeadics and Traumatology and Doctoral Program of Clinical Research, Faculty of Medicine, University of Helsinki, during the years 2013–2019.

This thesis was financially supported by The University of Helsinki Research Foundation, Suomen Lääketieteen Säätiö, The Maud Kuistila Memorial Foundation, Finska Läkaresällskapet, and the Finnish Research Foundation for Orthopaedics and Traumatology. I am grateful for this support.

During the thesis project I have had the privilege of working with many talented people whom I would like to acknowledge.

I owe my deepest gratitude to my principal supervisor Professor Ilkka Kiviranta for the opportunity to work with such inspiring topics and for the support and freedom you have given me through the project. You have the amazing capability of turning every impossible situation into success. I am forever in debt to your priceless advice. I also thank PhD Virpi Muhonen for being my mentor and supervisor and teaching me laboratory methods. Thank you for the great and fun discussions throughout the years. I am extremely grateful that both of you agreed to supervise this work and for always being available to solve problems with me. Thank you for expressing confidence in my research project.

The pre examiners Professor Emeritus Heimo Ylänen and Docent Petri Virolainen are appreciated for their critical review of this thesis and for the insightful comments and suggestions that helped me improve the thesis. I thank Professor Leif Dahlberg for kindly agreeing to be my opponent.

I thank all the collaborators and co-authors for making this thesis possible. Anne-Marie Haaparanta (Tampere University of Technology), Peter Uppstu (Åbo Akademi University), Ville Ellä (Tampere University of Technology), Professor Minna Kellomäki (Tampere University of Technology) and Professor Ari Rosling (Åbo Akademi University) are thanked for providing the materials for the studies and for sharing their knowledge on biomaterials. I thank Elina Järvinen for teaching me cell culture. Teemu Paatela, Anna Vasara and Tuomo Pyhältö from Helsinki University Hospital are thanked for surgeries of the swine and rabbits, and for teaching me the basics of cartilage surgery. Anna Meller (University of Helsinki), without you the swine studies would not have succeeded. Professor Pieter Brama (University College Dublin) and Professor René van Weeren (Utrecht University) are warmly thanked for all the help and insights regarding equine cartilage repair. Mikko Nissi (University of Oulu) is thanked for MRI analyses of the equine cartilage and great discussions on the topic. Anita Laitinen, Matti Korhonen and Johanna Nystedt from the Finnish Red Cross Blood Service for enabling *study IV* by providing the valuable BM-MSC lines. I would also like to extend my thanks

to Markus Hannula, Antti Aula, Kalle Lehto, Tuomo Silvast, Lassi Rieppo, Virpi Tiitu, Leena Kontturi, Mimmi Björkman, Juha Töyräs, Hertta Pulkkinen, Harold Brommer, and Anne Brünott.

I would like to extend my thanks to Hannu Kautiainen for his work on the statistical analyses of the studies. Late Professor Yrjö Konttinen (University of Helsinki) is thanked for enabling access to some relevant equipment. Thank you Kevin Salonius for turning my drawings into great illustrations.

I wish to thank my friends for taking my mind off work and research every once and awhile – and for peer support when needed.

Special thanks goes to my mother Raija and my father Seppo for all their support. You filled my childhood home with love and books, and you always encouraged me to pursue my dreams.

I am also indebted to Kenneth, my beloved husband, for all his love and support in life and during this research project. Any day spent with you is my favorite day.

Our son William – this work is dedicated to you.

Kirkkonummi, October 2019

Eve Salonius

REFERENCES

Ahern BJ, Parvizi J, Boston R, Schaer TP. Preclinical animal models in single site cartilage defect testing: a systematic review. Osteoarthritis Cartilage 2009, 17: 705-713.

Albrecht F, Roessner A, Zimmermann E. Closure of osteochondral lesions using chondral fragments and fibrin adhesive. Arch Orthop Trauma Surg 1983, 101: 213-217.

Anderson HC. Matrix vesicles and calcification. Curr Rheumatol Rep 2003, 5: 222-226.

Aroen A, Loken S, Heir S, Alvik E, Ekeland A, Granlund OG, Engebretsen L. Articular cartilage lesions in 993 consecutive knee arthroscopies. Am J Sports Med 2004, 32: 211-215.

Athanasiou KA, Niederauer GG, Agrawal CM. Sterilization, toxicity, biocompatibility and clinical applications of polylactic acid/ polyglycolic acid copolymers. Biomaterials 1996, 17: 93-102.

Baez J, Olsen D, Polarek JW. Recombinant microbial systems for the production of human collagen and gelatin. Appl Microbiol Biotechnol 2005, 69: 245-252.

Barber FA, Chow JC. Arthroscopic chondral osseous autograft transplantation (COR procedure) for femoral defects. Arthroscopy 2006, 22: 10-16.

Bashir A, Gray ML, Burstein D. Gd-DTPA^{2-} as a measure of cartilage degradation. Magn Reson Med 1996, 36: 665–673.

Behrens P. Matrixgekoppelte Mikrofrakturierung. Arthroskopie 2005, 18: 193-197.

Benthien JP, Behrens P. Nanofractured autologous matrix induced chondrogenesis (NAMIC(c)) – Further development of collagen membrane aided chondrogenesis combined with subchondral needling: A technical note. Knee 2015, 22: 411-415.

Bentley G, Biant LC, Vijayan S, Macmull S, Skinner JA, Carrington RW. Minimum ten-year results of a prospective randomised study of autologous chondrocyte implantation versus mosaicplasty for symptomatic articular cartilage lesions of the knee. J Bone Joint Surg Br 2012, 94: 504-509.

Benya PD, Padilla SR, Nimni ME. Independent regulation of collagen types by chondrocytes during the loss of differentiated function in culture. Cell 1978, 15: 1313-1321.

Bernhard JC, Vunjak-Novakovic G. Should we use cells, biomaterials, or tissue engineering for cartilage regeneration? Stem Cell Res Ther 2016, 7: 3.

Berruto M, Ferrua P, Pasqualotto S, Uboldi F, Maione A, Tradati D, Usellini E. Long-term follow-up evaluation of autologous chondrocyte implantation for symptomatic cartilage lesions of the knee: A single-centre prospective study. Injury 2017, 48: 2230-2234.

Bhosale AM. Articular cartilage: structure, injuries and review of management. Br Med Bull 2008, 87: 77-95.

Biant LC, McNicholas MJ, Sprowson AP, Spalding T. The surgical management of symptomatic articular cartilage defects of the knee: Consensus statements from United Kingdom knee surgeons. Knee 2015, 22: 446-449.

Bobic V. Arthroscopic osteochondral autograft transplantation in anterior cruciate ligament reconstruction: a preliminary clinical study. Knee Surg Sports Traumatol Arthrosc 1996, 3: 262-264.

Bonasia DE, Marmotti A, Rosso F, Collo G, Rossi R. Use of chondral fragments for one stage cartilage repair: A systematic review. World J Orthop 2015, 6: 1006-1011.

Brehm W, Aklin B, Yamashita T, Rieser F, Trub T, Jakob RP, Mainil-Varlet P. Repair of superficial osteochondral defects with an autologous scaffold-free cartilage construct in a caprine model: implantation method and short-term results. Osteoarthritis Cartilage 2006, 14: 1214-1226.

Brittberg M. Cell carriers as the next generation of cell therapy for cartilage repair: a review of the matrix-induced autologous chondrocyte implantation procedure. Am J Sports Med 2010, 38: 1259-1271.

Brittberg M, Lindahl A, Nilsson A, Ohlsson C, Isaksson O, Peterson L. Treatment of deep cartilage defects in the knee with autologous chondrocyte transplantation. N Engl J Med 1994, 331: 889-895.

Brittberg M, Recker D, Ilgenfritz J, Saris DBF, SUMMIT Extension SG. Matrix-Applied Characterized Autologous Cultured Chondrocytes Versus Microfracture: Five-Year Follow-up of a Prospective Randomized Trial. Am J Sports Med 2018, 46: 1343-1351.

Brittberg M, Winalski CS. Evaluation of cartilage injuries and repair. J Bone Joint Surg Am 2003, 85-A Suppl 2: 58-69.

Brouwer RW, Huizinga MR, Duivenvoorden T, van Raaij TM, Verhagen AP, Bierma-Zeinstra S, Verhaar JA. Osteotomy for treating knee osteoarthritis. Cochrane Database Syst Rev 2014, (12):CD004019. doi: CD004019.

Brown TD, Johnston RC, Saltzman CL, Marsh JL, Buckwalter JA. Posttraumatic osteoarthritis: a first estimate of incidence, prevalence, and burden of disease. J Orthop Trauma 2006, 20: 739-744.

Buckwalter JA. Sports, joint injury, and posttraumatic osteoarthritis. J Orthop Sports Phys Ther 2003, 33: 578-588.

Buckwalter JA, Anderson DD, Brown TD, Tochigi Y, Martin JA. The Roles of Mechanical Stresses in the Pathogenesis of Osteoarthritis: Implications for Treatment of Joint Injuries. Cartilage 2013, 4: 286-294.

Buckwalter JA, Bowman GN, Albright JP, Wolf BR, Bollier M. Clinical outcomes of patellar chondral lesions treated with juvenile particulated cartilage allografts. Iowa Orthop J 2014, 34: 44-49.

Buckwalter JA, Mankin HJ, Grodzinsky AJ. Articular cartilage and osteoarthritis. Instr Course Lect 2005, 54: 465-480.

Burr DB. Anatomy and physiology of the mineralized tissues: role in the pathogenesis of osteoarthrosis. Osteoarthritis Cartilage 2004, 12 Suppl A: S20-30.

Calasans-Maia M, Monteiro ML, Ascoli FO, Granjeiro JM. The rabbit as an animal model for experimental surgery. Acta Cir Bras 2009, 24: 325-328.

Camarero-Espinosa S, Cooper-White J. Tailoring biomaterial scaffolds for osteochondral repair. Int J Pharm 2017, 523: 476-489.

Cameron JI, Pulido PA, McCauley JC, Bugbee WD. Osteochondral Allograft Transplantation of the Femoral Trochlea. Am J Sports Med 2016, 44: 633-638.

Campbell AB, Knopp MV, Kolovich GP, Wei W, Jia G, Siston RA, Flanigan DC. Preoperative MRI Underestimates Articular Cartilage Defect Size Compared With Findings at Arthroscopic Knee Surgery. Am J Sports Med 2013, 41: 590-595.

Caplan AI. Mesenchymal Stem Cells: Time to Change the Name! Stem Cells Transl Med 2017, 6: 1445-1451.

Carbone A, Rodeo S. Review of current understanding of post-traumatic osteoarthritis resulting from sports injuries. J Orthop Res 2017, 35: 397-405.

Caron MM, Emans PJ, Coolsen MM, Voss L, Surtel DA, Cremers A, van Rhijn LW, Welting TJ. Redifferentiation of dedifferentiated human articular chondrocytes: comparison of 2D and 3D cultures. Osteoarthritis Cartilage 2012, 20: 1170-1178.

Chahal J, Gross AE, Gross C, Mall N, Dwyer T, Chahal A, Whelan DB, Cole BJ. Outcomes of osteochondral allograft transplantation in the knee. Arthroscopy 2013, 29: 575-588.

Chen H, Hoemann CD, Sun J, Chevrier A, McKee MD, Shive MS, Hurtig M, Buschmann MD. Depth of subchondral perforation influences the outcome of bone marrow stimulation cartilage repair. J Orthop Res 2011, 29: 1178-1184.

Chen S, Fu P, Cong R, Wu H, Pei M. Strategies to minimize hypertrophy in cartilage engineering and regeneration. Genes Dis 2015, 2: 76-95.

Chesterman PJ, Smith AU. Homotransplantation of articular cartilage and isolated chondrocytes. An experimental study in rabbits. J Bone Joint Surg Br 1968, 50: 184-197.

Christen P, Ito K, Ellouz R, Boutroy S, Sornay-Rendu E, Chapurlat RD, van Rietbergen B. Bone remodelling in humans is load-driven but not lazy. Nat Commun 2014, 5: 4855.

Cole BJ, Farr J, Winalski CS, Hosea T, Richmond J, Mandelbaum B, De Deyne PG. Outcomes after a single-stage procedure for cell-based cartilage repair: a prospective clinical safety trial with 2-year follow-up. Am J Sports Med 2011, 39: 1170-1179.

Convery FR, Akeson WH, Keown GH. The repair of large osteochondral defects. An experimental study in horses. Clin Orthop Relat Res 1972, 82: 253-262.

Cook JL, Hung CT, Kuroki K, Stoker AM, Cook CR, Pfeiffer FM, Sherman SL, Stannard JP. Animal models of cartilage repair. . Bone Joint Res 2014, 3: 89-94.

Corbett MS, Webster A, Hawkins R, Woolacott N. Innovative regenerative medicines in the EU: a better future in evidence? BMC Med 2017, 15: 4.

Costa-Paz M, Muscolo DL, Ayerza M, Makino A, Aponte-Tinao L. Magnetic resonance imaging follow-up study of bone bruises associated with anterior cruciate ligament ruptures. Arthroscopy 2001, 17: 445-449.

Coventry MB. Osteotomy about the knee for degenerative and rheumatoid arthritis. J Bone Joint Surg Am 1973, 55: 23-48.

Curl WW, Krome J, Gordon ES, Rushing J, Smith BP, Poehling GG. Cartilage injuries: a review of 31,516 knee arthroscopies. Arthroscopy 1997, 13: 456-460.

Dahlberg L, Roos H, Saxne T, Heinegård D, Lark MW, Hoerrner LA, Lohmander LS. Cartilage metabolism in the injured and uninjured knee of the same patient. Ann Rheum Dis. 1994, 53: 823-7.

de Grauw JC. Molecular monitoring of equine joint homeostasis. Vet Q 2011, 31: 77-86.

de Vries-van Melle ,M.L., Narcisi R, Kops N, Koevoet WJ, Bos PK, Murphy JM, Verhaar JA, van der Kraan ,P.M., van Osch GJ. Chondrogenesis of mesenchymal stem cells in an osteochondral environment is mediated by the subchondral bone. Tissue Eng Part A 2014, 20: 23-33.

de Windt TS, Bekkers JE, Creemers LB, Dhert WJ, Saris DB. Patient profiling in cartilage regeneration: prognostic factors determining success of treatment for cartilage defects. Am J Sports Med 2009, 37 Suppl 1: 62S.

DeGroot J, Verzijl N, Jacobs KM, Budde M, Bank RA, Bijlsma JW, TeKoppele JM, Lafeber FP. Accumulation of advanced glycation endproducts reduces chondrocyte-mediated extracellular matrix turnover in human articular cartilage. Osteoarthritis Cartilage 2001, 9: 720-726.

Dhollander AA, De Neve F, Almqvist KF, Verdonk R, Lambrecht S, Elewaut D, Verbruggen G, Verdonk PC. Autologous matrix-induced chondrogenesis combined with platelet-rich plasma gel: technical description and a five pilot patients report. Knee Surg Sports Traumatol Arthrosc 2011, 19: 536-542.

Di Martino A, Kon E, Perdisa F, Sessa A, Filardo G, Neri MP, Bragonzoni L, Marcacci M. Surgical treatment of early knee osteoarthritis with a cell-free osteochondral scaffold: results at 24 months of follow-up. Injury 2015, 46 Suppl 8: 33.

Diaz-Romero J, Nesic D, Grogan SP, Heini P, Mainil-Varlet P. Immunophenotypic changes of human articular chondrocytes during monolayer culture reflect bona fide dedifferentiation rather than amplification of progenitor cells. J Cell Physiol 2008, 214: 75-83.

Ding M, Odgaard A, Hvid I. Changes in the three-dimensional microstructure of human tibial cancellous bone in early osteoarthritis. J Bone Joint Surg Br 2003, 85: 906-912.

Directive 2001/83/EC of the European Parliament and of the Council of 6 November 2001 on the Community code relating to medicinal products for human use. Official Journal of the European Communities (L 311).

Dominici M, Le Blanc K, Mueller I, Slaper-Cortenbach I, Marini F, Krause D, Deans R, Keating A, Prockop D, Horwitz E. Minimal criteria for defining multipotent mesenchymal stromal cells. The International Society for Cellular Therapy position statement. Cytotherapy 2006, 8: 315-317.

Doube M, Klosowski MM, Arganda-Carreras I, Cordelieres FP, Dougherty RP, Jackson JS, Schmid B, Hutchinson JR, Shefelbine SJ. BoneJ: Free and extensible bone image analysis in ImageJ. Bone 2010, 47: 1076-1079.

Eggli PS, Muller W, Schenk RK. Porous hydroxyapatite and tricalcium phosphate cylinders with two different pore size ranges implanted in the cancellous bone of rabbits. A comparative histomorphometric and histologic study of bony ingrowth and implant substitution. Clin Orthop Relat Res 1988, (232): 127-138.

Eläketurvakeskus ja Kansaneläkelaitos 2018. Tilasto Suomen eläkkeensaajista 2017.

El-Rashidy A, Roether JA, Harhaus L, Kneser U, Boccaccini AR. Regenerating bone with bioactive glass scaffolds: A review of in vivo studies in bone defect models. Acta Biomater 2017, 62: 1-28.

Engen CN, Aroen A, Engebretsen L. Incidence of knee cartilage surgery in Norway, 2008-2011. BMJ Open 2015, 5: 008423.

Everhart JS, Boggs Z, DiBartola AC, Wright B, Flanigan DC. Knee Cartilage Defect Characteristics Vary among Symptomatic Recreational and Competitive Scholastic Athletes Eligible for Cartilage Restoration Surgery. Cartilage 2019, 1947603519833144.

Fagerholm P, Lagali NS, Ong JA, Merrett K, Jackson WB, Polarek JW, Suuronen EJ, Liu Y, Brunette I, Griffith M. Stable corneal regeneration four years after implantation of a cell-free recombinant human collagen scaffold. Biomaterials 2014, 35: 2420-2427.

Fairbank TJ. Knee joint changes after meniscectomy. J Bone Joint Surg Br 1948, 30B: 664-670.

Feczko P, Hangody L, Varga J, Bartha L, Dioszegi Z, Bodo G, Kendik Z, Modis L. Experimental results of donor site filling for autologous osteochondral mosaicplasty. Arthroscopy 2003, 19: 755-761.

Ficat RP, Ficat C, Gedeon P, Toussaint JB. Spongialization: a new treatment for diseased patellae. Clin Orthop Relat Res 1979, (144): 74-83.

Filardo G, Kon E, Perdisa F, Tetta C, Di Martino A, Marcacci M. Arthroscopic mosaicplasty: long-term outcome and joint degeneration progression. Knee 2015, 22: 36-40.

Filardo G, Kon E, Roffi A, Di Martino A, Marcacci M. Scaffold-based repair for cartilage healing: a systematic review and technical note. Arthroscopy 2013, 29: 174-186.

Findlay DM, Kuliwaba JS. Bone-cartilage crosstalk: a conversation for understanding osteoarthritis. Bone Res 2016, 4: 16028.

Flanigan DC, Harris JD, Trinh TQ, Siston RA, Brophy RH. Prevalence of chondral defects in athletes' knees: a systematic review. Med Sci Sports Exerc 2010, 42: 1795-1801.

Foldager CB, Gomoll AH, Lind M, Spector M. Cell Seeding Densities in Autologous Chondrocyte Implantation Techniques for Cartilage Repair. Cartilage 2012, 3: 108-117.

Fox AJ, Bedi A, Rodeo SA. The basic science of human knee menisci: structure, composition, and function. Sports Health 2012, 4: 340-351.

Frank RM, Cotter EJ, Hannon CP, Harrast JJ, Cole BJ. Cartilage Restoration Surgery: Incidence Rates, Complications, and Trends as Reported by the American Board of Orthopaedic Surgery Part II Candidates. Arthroscopy 2019, 35: 171-178.

Frehner F, Benthien JP. Microfracture: State of the Art in Cartilage Surgery? Cartilage 2018, 9: 339-345.

Friedenstein AJ, Piatetzky-Shapiro I, Petrakova KV. Osteogenesis in transplants of bone marrow cells. J Embryol Exp Morphol 1966, 16: 381-390.

Furst A, Meier D, Michel S, Schmidlin A, Held L, Laib A. Effect of age on bone mineral density and micro architecture in the radius and tibia of horses: an Xtreme computed tomographic study. BMC Vet Res 2008, 4: 3.

Gelber AC, Hochberg MC, Mead LA, Wang NY, Wigley FM, Klag MJ. Joint injury in young adults and risk for subsequent knee and hip osteoarthritis. Ann Intern Med 2000, 133: 321-328.

Gentile P, Chiono V, Carmagnola I, Hatton PV. An overview of poly(lactic-co-glycolic) acid (PLGA)-based biomaterials for bone tissue engineering. Int J Mol Sci 2014, 15: 3640-3659.

Georgi N, Taipaleenmaki H, Raiss CC, Groen N, Portalska KJ, van Blitterswijk C, de Boer J, Post JN, van Wijnen AJ, Karperien M. MicroRNA Levels as Prognostic Markers for the Differentiation Potential of Human Mesenchymal Stromal Cell Donors. Stem Cells Dev 2015, 24: 1946-1955.

Gille J, Schuseil E, Wimmer J, Gellissen J, Schulz AP, Behrens P. Mid-term results of Autologous Matrix-Induced Chondrogenesis for treatment of focal cartilage defects in the knee. Knee Surg Sports Traumatol Arthrosc 2010, 18: 1456-1464.

Glyn-Jones S, Palmer AJ, Agricola R, Price AJ, Vincent TL, Weinans H, Carr AJ. Osteoarthritis. Lancet 2015, 386: 376-387.

Gobbi A, Karnatzikos G, Kumar A. Long-term results after microfracture treatment for full-thickness knee chondral lesions in athletes. Knee Surg Sports Traumatol Arthrosc 2014, 22: 1986-1996.

Gomoll AH, Madry H, Knutsen G, van Dijk N, Seil R, Brittberg M, Kon E. The subchondral bone in articular cartilage repair: current problems in the surgical management. Knee Surg Sports Traumatol Arthrosc 2010, 18: 434-447.

Grande DA, Pitman MI, Peterson L, Menche D, Klein M. The repair of experimentally produced defects in rabbit articular cartilage by autologous chondrocyte transplantation. J Orthop Res 1989, 7: 208-218.

Gross AE, Silverstein EA, Falk J, Falk R, Langer F. The allotransplantation of partial joints in the treatment of osteoarthritis of the knee. Clin Orthop Relat Res 1975, (108):7-14. doi: 7-14.

Gruskin E, Doll BA, Futrell FW, Schmitz JP, Hollinger JO. Demineralized bone matrix in bone repair: History and use. Advanced Drug Delivery Reviews 2012, 64(12): 1063-77.

Gudas R, Gudaite A, Pocius A, Gudiene A, Cekanauskas E, Monastyreckiene E, Basevicius A. Ten-year follow-up of a prospective, randomized clinical study of mosaic osteochondral autologous transplantation versus microfracture for the treatment of osteochondral defects in the knee joint of athletes. Am J Sports Med 2012, 40: 2499-2508.

Guermazi A, Niu J, Hayashi D, Roemer FW, Englund M, Neogi T, Aliabadi P, McLennan CE, Felson DT. Prevalence of abnormalities in knees detected by MRI in adults without knee osteoarthritis: population based observational study (Framingham Osteoarthritis Study). BMJ 2012, 345: e5339.

Guermazi A, Alizai H, Crema MD, Trattnig S, Regatte RR, Roemer FW. Compositional MRI techniques for evaluation of cartilage degeneration in osteoarthritis. Osteoarthritis Cartilage 2015, 23: 1639-53.

Haaparanta AM, Uppstu P, Hannula M, Ella V, Rosling A, Kellomaki M. Improved dimensional stability with bioactive glass fibre skeleton in poly(lactide-co-glycolide) porous scaffolds for tissue engineering. Mater Sci Eng C Mater Biol Appl 2015, 56: 457-466.

Han Y, You X, Xing W, Zhang Z, Zou W. Paracrine and endocrine actions of bone-the functions of secretory proteins from osteoblasts, osteocytes, and osteoclasts. Bone Res 2018, 6: 6. eCollection 2018.

Hangody L, Fules P. Autologous osteochondral mosaicplasty for the treatment of full-thickness defects of weight-bearing joints: ten years of experimental and clinical experience. J Bone Joint Surg Am 2003, 85-A Suppl 2: 25-32.

Hangody L, Kish G, Karpati Z, Szerb I, Udvarhelyi I. Arthroscopic autogenous osteochondral mosaicplasty for the treatment of femoral condylar articular defects. A preliminary report. Knee Surg Sports Traumatol Arthrosc 1997. 5(4): 262-7.

Hardingham TE. The role of link-protein in the structure of cartilage proteoglycan aggregates. Biochem J 1979. 177: 237-247.

Harris JD, Siston RA, Pan X, Flanigan DC. Autologous chondrocyte implantation: a systematic review. J Bone Joint Surg Am 2010, 92: 2220-2233.

Haynesworth SE, Goshima J, Goldberg VM, Caplan AI. Characterization of cells with osteogenic potential from human marrow. Bone 1992, 13: 81-88.

Heir S, Nerhus TK, Rotterud JH, Loken S, Ekeland A, Engebretsen L, Aroen A. Focal cartilage defects in the knee impair quality of life as much as severe osteoarthritis: a comparison of knee injury and osteoarthritis outcome score in 4 patient categories scheduled for knee surgery. Am J Sports Med 2010, 38: 231-237.

Heiskanen A, Satomaa T, Tiitinen S, Laitinen A, Mannelin S, Impola U, Mikkola M, Olsson C, Miller-Podraza H, Blomqvist M, Olonen A, Salo H, Lehenkari P, Tuuri T, Otonkoski T, Natunen J, Saarinen J, Laine J. N-glycolylneuraminic acid xenoantigen contamination of human embryonic and mesenchymal stem cells is substantially reversible. Stem Cells 2007, 25: 197-202.

Heliövaara M. Nivelrikon esiintyvyys ja kustannukset. Lääketieteellinen Aikakauskirja Duodecim 2008, 124: 1869-74.

Hench LL, Splinter RJ, Allen WC, Greenlee TK. Bonding mechanisms at the interface of ceramic prosthetic materials. . J Biomed Mater Res 1971, 5: 117.

Heng BC, Cao T, Lee EH. Directing stem cell differentiation into the chondrogenic lineage in vitro. Stem Cells 2004, 22: 1152-1167.

Hjelle K, Solheim E, Strand T, Muri R, Brittberg M. Articular cartilage defects in 1,000 knee arthroscopies. Arthroscopy 2002, 18: 730-734.

Holzer A, Pietschmann MF, Rosl C, Hentschel M, Betz O, Matsuura M, Jansson V, Muller PE. The interrelation of trabecular microstructural parameters of the greater tubercle measured for different species. J Orthop Res 2012, 30: 429-434.

Horwitz EM, Gordon PL, Koo WK, Marx JC, Neel MD, McNall RY, Muul L, Hofmann T. Isolated allogeneic bone marrow-derived mesenchymal cells engraft and stimulate growth in children with osteogenesis imperfecta: Implications for cell therapy of bone. Proc Natl Acad Sci U S A 2002, 99: 8932-8937.

Huang BJ, Hu JC, Athanasiou KA. Cell-based tissue engineering strategies used in the clinical repair of articular cartilage. Biomaterials 2016, 98: 1-22.

Hunter DJ, Schofield D, Callander E. The individual and socioeconomic impact of osteoarthritis. Nat Rev Rheumatol 2014, 10: 437-441.

Hunter W. Of the Structure and Diseases of Articulating "Cartilages". Philosophical Transactions (1682) 1743, 42: 514.

Hurtig M, Buschmann M, Fortier L, Hoemann C, Hunziker E, Jurvelin J, Mainil-Varlet P, McIlwraith C, Sah R, Whiteside R. Preclinical Studies for Cartilage Repair: Recommendations from the International Cartilage Repair Society. Cartilage 2011, 2: 137-152.

Hurtig MB, Fretz PB, Doige CE, Schnurr DL. Effects of lesion size and location on equine articular cartilage repair. Can J Vet Res 1988, 52: 137-146.

Hwang NS, Varghese S, Lee HJ, Zhang Z, Ye Z, Bae J, Cheng L, Elisseeff J. In vivo commitment and functional tissue regeneration using human embryonic stem cell-derived mesenchymal cells. Proc Natl Acad Sci U S A 2008, 105: 20641-20646.

International Cartilage Repair Society 2000. International Cartilage Repair Society (ICRS). ICRS Cartilage Injury Evaluation Package.

Jackson DW, Lalor PA, Aberman HM, Simon TM. Spontaneous repair of full-thickness defects of articular cartilage in a goat model. A preliminary study. J Bone Joint Surg Am 2001, 83: 53-64.

Johnson LL. Arthroscopic abrasion arthroplasty historical and pathologic perspective: present status. Arthroscopy 1986, 2: 54-69.

Kellgren JH, Lawrence JS. Radiological assessment of osteo-arthrosis. Annals of the rheumatic diseases JID - 0372355 1957. 16(4): 494-502.

Kellgren JH, Lawrence JS. Osteo-arthrosis and disk degeneration in an urban population. Annals of the rheumatic diseases 1958. 17(4): 388-97.

Kessler JI, Nikizad H, Shea KG, Jacobs JCJ, Bebchuk JD, Weiss JM. The demographics and epidemiology of osteochondritis dissecans of the knee in children and adolescents. The American journal of sports medicine 2014. 42(2): 320-6.

Kim HK, Moran ME, Salter RB. The potential for regeneration of articular cartilage in defects created by chondral shaving and subchondral abrasion. An experimental investigation in rabbits. J Bone Joint Surg Am 1991, 73: 1301-1315.

Kiviranta I, Tammi M, Jurvelin J, Arokoski J, Saamanen AM, Helminen HJ. Articular cartilage thickness and glycosaminoglycan distribution in the young canine knee joint after remobilization of the immobilized limb. J Orthop Res 1994, 12: 161-167.

Koerber F, Rolauffs B, Rogowski W. Early evaluation and value-based pricing of regenerative medicine technologies. Regen Med 2013, 8: 747-758.

Kold SE, Hickman J, Melsen F. An experimental study of the healing process of equine chondral and osteochondral defects. Equine Vet J 1986, 18: 18-24.

Kon E, Filardo G, Brittberg M, Busacca M, Condello V, Engebretsen L, Marlovits S, Niemeyer P, Platzer P, Posthumus M, Verdonk P, Verdonk R, Victor J, van dM, Widuchowski W, Zorzi C, Marcacci M. A multilayer biomaterial for osteochondral regeneration shows superiority vs microfractures for the treatment of osteochondral lesions in a multicentre randomized trial at 2 years. Knee Surg Sports Traumatol Arthrosc 2018, 26: 2704-2715.

Kon E, Filardo G, Perdisa F, Venieri G, Marcacci M. Clinical results of multilayered biomaterials for osteochondral regeneration. J Exp Orthop 2014, 1: 10-014-0010-0. Epub 2014 Aug 6.

Korhonen RK, Laasanen MS, Toyras J, Lappalainen R, Helminen HJ, Jurvelin JS. Fibril reinforced poroelastic model predicts specifically mechanical behavior of normal, proteoglycan depleted and collagen degraded articular cartilage. J Biomech 2003, 36: 1373-1379.

Kramer DB, Xu S, Kesselheim AS. Regulation of medical devices in the United States and European Union. N Engl J Med 2012, 366: 848-855.

Kreuz PC, Muller S, Freymann U, Erggelet C, Niemeyer P, Kaps C, Hirschmuller A. Repair of focal cartilage defects with scaffold-assisted autologous chondrocyte grafts: clinical and biomechanical results 48 months after transplantation. Am J Sports Med 2011, 39: 1697-1705.

Krych AJ, Pareek A, King AH, Johnson NR, Stuart MJ, Williams RJ. Return to sport after the surgical management of articular cartilage lesions in the knee: a meta-analysis. Knee Surg Sports Traumatol Arthrosc 2017, 25: 3186-3196.

Kulmala KA, Pulkkinen HJ, Rieppo L, Tiitu V, Kiviranta I, Brunott A, Brommer H, van Weeren R, Brama PA, Mikkola MT, Korhonen RK, Jurvelin JS, Toyras J. Contrast-Enhanced Micro-Computed Tomography in Evaluation of Spontaneous Repair of Equine Cartilage. Cartilage 2012, 3: 235-244.

Laupattarakasem W, Laopaiboon M, Laupattarakasem P, Sumananont C. Arthroscopic debridement for knee osteoarthritis. Cochrane Database Syst Rev 2008, (1):CD005118. doi: CD005118.

Lee EJ, Kasper FK, Mikos AG. Biomaterials for tissue engineering. Ann Biomed Eng 2014, 42: 323-337.

Lee JH, Ort T, Ma K, Picha K, Carton J, Marsters PA, Lohmander LS, Baribaud F, Song XY, Blake S. Resistin is elevated following traumatic joint injury and causes matrix degradation and release of inflammatory cytokines from articular cartilage in vitro. Osteoarthritis Cartilage 2009, 17: 613-620.

Lee JK, Responte DJ, Cissell DD, Hu JC, Nolta JA, Athanasiou KA. Clinical translation of stem cells: insight for cartilage therapies. Crit Rev Biotechnol 2014, 34: 89-100.

Lefebvre V. SOX9 is a potent activator of the chondrocyte-specific enhancer of the pro alpha1(II) collagen gene. Mol Cell Biol 1997, 17: 2336.

Levingstone TJ, Thompson E, Matsiko A, Schepens A, Gleeson JP, O'Brien FJ. Multi-layered collagen-based scaffolds for osteochondral defect repair in rabbits. Acta Biomater 2016, 32: 149-160.

Lewandrowski KU, Gresser JD, Wise DL, Trantol DJ. Bioresorbable bone graft substitutes of different osteoconductivities: a histologic evaluation of osteointegration of poly(propylene glycol-co-fumaric acid)-based cement implants in rats. Biomaterials 2000, 21: 757-764.

Lexer E. Substitution of whole or half joints from freshly amputated extremities by free plastic operations. Surg Gynecol Obstet 1908, 6: 601-7.

Lexer E. Joint transplantation and arthroplasty. Surg Gynecol Obstet 1925, 40: 782-809.

Li WJ, Chiang H, Kuo TF, Lee HS, Jiang CC, Tuan RS. Evaluation of articular cartilage repair using biodegradable nanofibrous scaffolds in a swine model: a pilot study. J Tissue Eng Regen Med 2009, 3: 1-10.

Libbin RM, Rivera ME. Regeneration of growth plate cartilage induced in the neonatal rat hindlimb by reamputation. J Orthop Res 1989, 7: 674-682.

Lindfors NC, Heikkila JT, Koski I, Mattila K, Aho AJ. Bioactive glass and autogenous bone as bone graft substitutes in benign bone tumors. J Biomed Mater Res B Appl Biomater 2009, 90: 131-136.

Lindfors NC, Hyvonen P, Nyyssonen M, Kirjavainen M, Kankare J, Gullichsen E, Salo J. Bioactive glass S53P4 as bone graft substitute in treatment of osteomyelitis. Bone 2010, 47: 212-218.

Liu YW, Tran MD, Skalski MR, Patel DB, White EA, Tomasian A, Gross JS, Vangsness CT, Matcuk GR Jr. MR imaging of cartilage repair surgery of the knee. Clin Imaging. 2019, 11: 129-139.

Livak KJ, Schmittgen TD. Analysis of relative gene expression data using real-time quantitative PCR and the 2(-Delta Delta C(T)) Method. Methods 2001, 25: 402-408.

Loeser RF, Goldring SR, Scanzello CR, Goldring MB. Osteoarthritis: a disease of the joint as an organ. Arthritis Rheum 2012. 64(6): 1697-7707.

Lopa S, Madry H. Bioinspired scaffolds for osteochondral regeneration. Tissue Eng Part A 2014, 20: 2052-2076.

Madry H, van Dijk CN, Mueller-Gerbl M. The basic science of the subchondral bone. Knee Surg Sports Traumatol Arthrosc 2010, 18: 419-433.

Magnuson PB. Joint debridement: a surgical treatment of degenerative arthritis. Surg Gynecol Obstet 1941, 73: 1-9.

Mainil-Varlet P, Aigner T, Brittberg M, Bullough P, Hollander A, Hunziker E, Kandel R, Nehrer S, Pritzker K, Roberts S, Stauffer E, International Cartilage RS. Histological assessment of cartilage repair: a report by the Histology Endpoint Committee of the International Cartilage Repair Society (ICRS). J Bone Joint Surg Am 2003, 85-A Suppl 2: 45-57.

Makris EA, Gomoll AH, Malizos KN, Hu JC, Athanasiou KA. Repair and tissue engineering techniques for articular cartilage. Nat Rev Rheumatol 2015, 11: 21-34.

Malda J, Benders KE, Klein TJ, de Grauw JC, Kik MJ, Hutmacher DW, Saris DB, van Weeren PR, Dhert WJ. Comparative study of depth-dependent characteristics of equine and human osteochondral tissue from the medial and lateral femoral condyles. Osteoarthritis Cartilage 2012, 20: 1147-1151.

Maroudas A, Bayliss MT, Uchitel-Kaushansky N, Schneiderman R, Gilav E. Aggrecan turnover in human articular cartilage: use of aspartic acid racemization as a marker of molecular age. Arch Biochem Biophys 1998, 350: 61-71.

Maroudas A, Bullough P. Permeability of articular cartilage. Nature 1968, 219: 1260-1.

Martinez I, Elvenes J, Olsen R, Bertheussen K, Johansen O. Redifferentiation of in vitro expanded adult articular chondrocytes by combining the hanging-drop cultivation method with hypoxic environment. Cell Transplant 2008, 17: 987-996.

Matsuo T, Kita K, Mae T, Yonetani Y, Miyamoto S, Yoshikawa H, Nakata K. Bone substitutes and implantation depths for subchondral bone repair in osteochondral defects of porcine knee joints. Knee Surg Sports Traumatol Arthrosc 2015, 23: 1401-1409.

Matsusue Y, Yamamuro T, Hama H. Arthroscopic multiple osteochondral transplantation to the chondral defect in the knee associated with anterior cruciate ligament disruption. Arthroscopy 1993, 9: 318-321.

McAdams TR, Mithoefer K, Scopp JM, Mandelbaum BR. Articular Cartilage Injury in Athletes. Cartilage 2010, 1: 165-179.

McIlwraith CW, Fortier LA, Frisbie DD, Nixon AJ. Equine Models of Articular Cartilage Repair. Cartilage 2011, 2: 317-326.

McIlwraith CW, Frisbie DD, Kawcak CE. The horse as a model of naturally occurring osteoarthritis. Bone Joint Res 2012, 1: 297-309.

McIlwraith CW, Frisbie DD, Kawcak CE, Fuller CJ, Hurtig M, Cruz A. The OARSI histopathology initiative - recommendations for histological assessments of osteoarthritis in the horse. Osteoarthritis Cartilage 2010, 18 Suppl 3: S93-105.

Methot S, Changoor A, Tran-Khanh N, Hoemann CD, Stanish WD, Restrepo A, Shive MS, Buschmann MD. Osteochondral Biopsy Analysis Demonstrates That BST-CarGel Treatment Improves Structural and Cellular Characteristics of Cartilage Repair Tissue Compared With Microfracture. Cartilage 2016, 7: 16-28.

Miller RH, Edwards WB, Deluzio KJ. Energy expended and knee joint load accumulated when walking, running, or standing for the same amount of time. Gait Posture 2015, 41: 326-328.

Minas T, Von Keudell A, Bryant T, Gomoll AH. The John Insall Award: A minimum 10-year outcome study of autologous chondrocyte implantation. Clin Orthop Relat Res 2014, 472: 41-51.

Mithoefer K, Hambly K, Della Villa S, Silvers H, Mandelbaum BR. Return to sports participation after articular cartilage repair in the knee: scientific evidence. Am J Sports Med 2009a, 37 Suppl 1: 76S.

Mithoefer K, McAdams T, Williams RJ, Kreuz PC, Mandelbaum BR. Clinical efficacy of the microfracture technique for articular cartilage repair in the knee: an evidence-based systematic analysis. Am J Sports Med 2009b, 37: 2053-2063.

Mollon B, Kandel R, Chahal J, Theodoropoulos J. The clinical status of cartilage tissue regeneration in humans. Osteoarthritis Cartilage 2013, 21: 1824-1833.

Mor A, Grijota M, Norgaard M, Munthe J, Lind M, Deruaz A, Pedersen AB. Trends in arthroscopy-documented cartilage injuries of the knee and repair procedures among 15-60-year-old patients. Scand J Med Sci Sports 2015, 25: 400.

Moran CJ, Ramesh A, Brama PA, O'Byrne JM, O'Brien FJ, Levingstone TJ. The benefits and limitations of animal models for translational research in cartilage repair. J Exp Orthop 2016, 3: x. Epub 2016 Jan 6.

Moskowitz RW, Altman RD, Hochberg MC, Buckwalter JA, Goldberg VM. Osteoarthritis. 4 ed. Lippincott Williams & Wilkins, 2007.

Mow VC, Holmes MH, Lai WM. Fluid transport and mechanical properties of articular cartilage: a review. J Biomech 1984. 17(5): 377-94.

Murphy M, Barry F. Cellular chondroplasty: a new technology for joint regeneration. J Knee Surg 2015, 28: 45-50.

Murphy MB, Moncivais K, Caplan AI. Mesenchymal stem cells: environmentally responsive therapeutics for regenerative medicine. Exp Mol Med 2013, 45: e54.

Muschler GF, Nakamoto C, Griffith LG. Engineering principles of clinical cell-based tissue engineering. J Bone Joint Surg Am 2004, 86-A: 1541-1558.

Nair LS, Laurencin CT. Biodegradable polymers as biomaterials. Progress in Polymer Science 2007. 32(8): 762-98.

Nakagawa Y, Mukai S, Yabumoto H, Tarumi E, Nakamura T. Serial Changes of the Cartilage in Recipient Sites and Their Mirror Sites on Second-Look Imaging After Mosaicplasty. Am J Sports Med 2016, 44: 1243-1248.

National Institute for Health and Care Excellence (NICE). Autologous chondrocyte implantation for treating symptomatic articular cartilage defects of the knee. Technology appraisal guidance [TA477]. 2017, 2017 Oct 27.

Niemeyer P, Salzmann G, Feucht M, Pestka J, Porichis S, Ogon P, Sudkamp N, Schmal H. First-generation versus second-generation autologous chondrocyte implantation for treatment of cartilage defects of the knee: a matched-pair analysis on long-term clinical outcome. Int Orthop 2014. 38(10): 2065-70.

Nieminen MT, Nissi MJ, Mattila L, Kiviranta I. Evaluation of chondral repair using quantitative MRI. J Magn Reson Imaging 2012, 36: 1287-99.

Nooeaid P, Salih V, Beier JP, Boccaccini AR. Osteochondral tissue engineering: scaffolds, stem cells and applications. J Cell Mol Med 2012, 16: 2247-2270.

Ogura T, Mosier BA, Bryant T, Minas T. A 20-Year Follow-up After First-Generation Autologous Chondrocyte Implantation. Am J Sports Med 2017, 45: 2751-2761.

Orth P, Cucchiarini M, Kohn D, Madry H. Alterations of the subchondral bone in osteochondral repair--translational data and clinical evidence. Eur Cell Mater 2013, 25: 6.

Oryan A, Alidadi S, Moshiri A, Maffulli N. Bone regenerative medicine: classic options, novel strategies, and future directions. J Orthop Surg Res 2014, 9: 18-799X-9-18.

Outerbridge RE. The etiology of chondromalacia patellae. J Bone Joint Surg Br 1961, 43-B: 752-757.

Pan J, Wang B, Li W, Zhou X, Scherr T, Yang Y, Price C, Wang L. Elevated cross-talk between subchondral bone and cartilage in osteoarthritic joints. Bone 2012, 51: 212-217.

Pan J, Zhou X, Li W, Novotny JE, Doty SB, Wang L. In situ measurement of transport between subchondral bone and articular cartilage. J Orthop Res 2009, 27: 1347-1352.

Pan Z, Duan P, Liu X, Wang H, Cao L, He Y, Dong J, Ding J. Effect of porosities of bilayered porous scaffolds on spontaneous osteochondral repair in cartilage tissue engineering. Regen Biomater 2015, 2: 9-19.

Pape HC, Evans A, Kobbe P. Autologous bone graft: properties and techniques. J Orthop Trauma 2010, 24 Suppl 1: 36.

Pearsall AW, Tucker JA, Hester RB, Heitman RJ. Chondrocyte viability in refrigerated osteochondral allografts used for transplantation within the knee. Am J Sports Med 2004, 32: 125-131.

Peterson L, Vasiliadis HS, Brittberg M, Lindahl A. Autologous chondrocyte implantation: a long-term follow-up. Am J Sports Med 2010, 38: 1117-1124.

Peyron JG, Balazs EA. Preliminary clinical assessment of Na-hyaluronate injection into human arthritic joints. Pathol Biol (Paris). 1974, 22: 731-6.

Pridie KH. A method of resurfacing osteoarthritic knee joints. J Bone Joint Surg (Br) 1959, 41: 618-9.

Pulkkinen HJ, Tiitu V, Valonen P, Jurvelin JS, Lammi MJ, Lammi MJ, Kiviranta I. Engineering of cartilage in recombinant human type II collagen gel in nude mouse model in vivo. Osteoarthritis Cartilage 2010, 18: 1077-1087.

Pulkkinen HJ, Tiitu V, Valonen P, Jurvelin JS, Rieppo L, Toyras J, Silvast TS, Lammi MJ, Kiviranta I. Repair of osteochondral defects with recombinant

human type II collagen gel and autologous chondrocytes in rabbit. Osteoarthritis Cartilage 2013a, 21: 481-490.

Pulkkinen HJ, Tiitu V, Valonen P, Jurvelin JS, Rieppo L, Toyras J, Silvast TS, Lammi MJ, Kiviranta I. Repair of osteochondral defects with recombinant human type II collagen gel and autologous chondrocytes in rabbit. Osteoarthritis Cartilage 2013b, 21: 481-490.

Radin EL, Orr RB, Kelman JL, Paul IL, Rose RM. Effect of prolonged walking on concrete on the knees of sheep. J Biomech 1982, 15: 487-492.

Rautiainen J, Lehto LJ, Tiitu V, Kiekara O, Pulkkinen H, Brunott A, van Weeren R, Brommer H, Brama PA, Ellermann J, Kiviranta I, Nieminen MT, Nissi MJ. Osteochondral repair: evaluation with sweep imaging with fourier transform in an equine model. Radiology 2013, 269: 113-121.

Raz G, Safir OA, Backstein DJ, Lee PT, Gross AE. Distal Femoral Fresh Osteochondral Allografts: Follow-up at a Mean of Twenty-two Years. J Bone Joint Surg Am 2014, 96: 1101-1107.

Regulation (EC) No 1394/2007 of the European Parliament and of the Council of 13 November 2007 on advanced therapy medicinal products and amending Directive 2001/83/EC and Regulation (EC) No 726/2004. Official Journal of the European Union (L 324):

Regulation (EU) 2017/745 of the European Parliament and of the Council of 5 April 2017 on medical devices, amending Directive 2001/83/EC, Regulation (EC) No 178/2002 and Regulation (EC) No 1223/2009 and repealing Council Directives 90/385/EEC and 93/42/EEC. Official Journal of the European Union (L 117):

Richie LB, Sytsma MJ. Matching osteochondritis dissecans lesions in identical twin brothers. Orthopedics 2013, 36: 1213.

Richter DL, Schenck RC, Wascher DC, Treme G. Knee Articular Cartilage Repair and Restoration Techniques: A Review of the Literature. Sports Health 2016, 8: 153-160.

Rieppo J, Hallikainen J, Jurvelin JS, Kiviranta I, Helminen HJ, Hyttinen MM. Practical considerations in the use of polarized light microscopy in the analysis of the collagen network in articular cartilage. Microsc Res Tech 2008, 71: 279-287.

Rose BJ, Kooyman DL. A Tale of Two Joints: The Role of Matrix Metalloproteases in Cartilage Biology. Dis Markers 2016, 2016: 4895050.

Runhaar J, Rozendaal RM, van Middelkoop M, Bijlsma HJW, Doherty M, Dziedzic KS, Lohmander LS, McAlindon T, Zhang W, Bierma Zeinstra S.

Subgroup analyses of the effectiveness of oral glucosamine for knee and hip osteoarthritis: a systematic review and individual patient data meta-analysis from the OA trial bank. Ann Rheum Dis. 2017, 76: 1862-1869.

Russell WM, Burch RL. TheÂœ principles of humane experimental technique. 1. publ ed. Methuen, London 1959.

Saris D, Price A, Widuchowski W, Bertrand-Marchand M, Caron J, Drogset JO, Emans P, Podskubka A, Tsuchida A, Kili S, Levine D, Brittberg M, SUMMIT sg. Matrix-Applied Characterized Autologous Cultured Chondrocytes Versus Microfracture: Two-Year Follow-up of a Prospective Randomized Trial. Am J Sports Med 2014, 42: 1384-1394.

Schiavone Panni A, Del Regno C, Mazzitelli G, D'Apolito R, Corona K, Vasso M. Good clinical results with autologous matrix-induced chondrogenesis

(Amic) technique in large knee chondral defects. Knee Surg Sports Traumatol Arthrosc 2018, 26: 1130-1136.

Schindelin J, Arganda-Carreras I, Frise E, Kaynig V, Longair M, Pietzsch T. Fiji: An Open-Source Platform for Biological-Image Analysis. Nature Methods 2012, 9: 676-682.

Sengupta P. The Laboratory Rat: Relating Its Age With Human's. Int J Prev Med 2013, 4: 624-630.

Seto CK, Statuta SM, Solari IL. Pediatric running injuries. Clin Sports Med 2010, 29: 499-511.

Sharma L, Song J, Dunlop D, Felson D, Lewis CE, Segal N, Torner J, Cooke TD, Hietpas J, Lynch J, Nevitt M. Varus and valgus alignment and incident and progressive knee osteoarthritis. Ann Rheum Dis 2010, 69: 1940-1945.

Shive MS, Stanish WD, McCormack R, Forriol F, Mohtadi N, Pelet S, Desnoyers J, Methot S, Vehik K, Restrepo A. BST-CarGel(R) Treatment Maintains Cartilage Repair Superiority over Microfracture at 5 Years in a Multicenter Randomized Controlled Trial. Cartilage 2015, 6: 62-72.

Skog M, Muhonen V, Nystedt J, Narcisi R, Kontturi LS, Urtti A, Korhonen M, van Osch GJ, Kiviranta I. Xeno-free chondrogenesis of bone marrow mesenchymal stromal cells: towards clinical-grade chondrocyte production. Cytotechnology 2015, 67: 905-919.

Somoza RA, Welter JF, Correa D, Caplan AI. Chondrogenic differentiation of mesenchymal stem cells: challenges and unfulfilled expectations. Tissue Eng Part B Rev 2014, 20: 596-608.

Stahl SS, Froum S. Histological evaluation of human intraosseous healing responses to the placement of tricalcium phosphate ceramic implants. I. Three to eight months. J Periodontol 1986, 57: 211-217.

Steadman JR, Rodkey WG, Singleton SB, Briggs KK. Microfracture technique forfull-thickness chondral defects: Technique and clinical results. Operative Techniques in Orthopaedics 1997. 7(4): 300-4.

Suda T, Takahashi N, Martin TJ. Modulation of osteoclast differentiation. Endocr Rev 1992, 13: 66-80.

Swindle MM. Swine in the laboratory. 2. ed. ed. CRC Press, Taylor & Francis, Boca Raton u.a.] 2007.

Takahashi K, Yamanaka S. Induction of pluripotent stem cells from mouse embryonic and adult fibroblast cultures by defined factors. Cell 2006, 126: 663-676.

Teitelbaum SL. Osteoclasts: what do they do and how do they do it? Am J Pathol 2007, 170: 427-435.

Tetta C, Busacca M, Moio A, Rinaldi R, Delcogliano M, Kon E, Filardo G, Marcacci M, Albisinni U. Knee osteochondral autologous transplantation: long-term MR findings and clinical correlations. Eur J Radiol 2010, 76: 117-123.

THL. Lonkan ja polven tekonivelet 2016. Tilastoraportti 2/2018.

Thomson JA, Itskovitz-Eldor J, Shapiro SS, Waknitz MA, Swiergiel JJ, Marshall VS, Jones JM. Embryonic stem cell lines derived from human blastocysts. Science 1998, 282: 1145-1147.

Ude CC, Sulaiman SB, Min-Hwei N, Hui-Cheng C, Ahmad J, Yahaya NM, Saim AB, Idrus RB. Cartilage regeneration by chondrogenic induced adult stem cells in osteoarthritic sheep model. PLoS One 2014, 9: e98770.

Uematsu K, Hattori K, Ishimoto Y, Yamauchi J, Habata T, Takakura Y, Ohgushi H, Fukuchi T, Sato M. Cartilage regeneration using mesenchymal stem cells and a three-dimensional poly-lactic-glycolic acid (PLGA) scaffold. Biomaterials 2005, 26: 4273-4279.

Uppstu P, Paakki C, Rosling A. In vitro hydrolysis and magnesium release of poly(d,l-lactide-co-glycolide)-based composites containing bioresorbable glasses and magnesium hydroxide. J Appl Polym Sci 2015, 132: 42646.

US Food and Drug Adminstration 2016. FDA approves first autologous cellularized scaffold for the repair of cartilage defects of the knee [FDA News Release].
https://www.fda.gov/newsevents/newsroom/pressannouncements/ucm533153.htm,

Vachon A, Bramlage LR, Gabel AA, Weisbrode S. Evaluation of the repair process of cartilage defects of the equine third carpal bone with and without subchondral bone perforation. Am J Vet Res 1986, 47: 2637-2645.

Van Norman GA. Drugs and Devices: Comparison of European and U.S. Approval Processes. JACC Basic Transl Sci 2016, 1: 399-412.

Vannini F, Spalding T, Andriolo L, Berruto M, Denti M, Espregueira-Mendes J, Menetrey J, Peretti GM, Seil R, Filardo G. Sport and early osteoarthritis: the role of sport in aetiology, progression and treatment of knee osteoarthritis. Knee Surg Sports Traumatol Arthrosc 2016, 24: 1786-1796.

Vanwanseele B, Eckstein F, Knecht H, Spaepen A, Stussi E. Longitudinal analysis of cartilage atrophy in the knees of patients with spinal cord injury. Arthritis Rheum 2003, 48: 3377-3381.

Vasara AI, Hyttinen MM, Lammi MJ, Lammi PE, Langsjo TK, Lindahl A, Peterson L, Kellomaki M, Konttinen YT, Helminen HJ, Kiviranta I. Subchondral bone reaction associated with chondral defect and attempted cartilage repair in goats. Calcif Tissue Int 2004, 74: 107-114.

Vasara AI, Hyttinen MM, Pulliainen O, Lammi MJ, Jurvelin JS, Peterson L, Lindahl A, Helminen HJ, Kiviranta I. Immature porcine knee cartilage lesions show good healing with or without autologous chondrocyte transplantation. Osteoarthritis Cartilage 2006, 14: 1066-1074.

Vasiliadis HS, Danielson B, Ljungberg M, McKeon B, Lindahl A, Peterson L. Autologous chondrocyte implantation in cartilage lesions of the knee: long-term evaluation with magnetic resonance imaging and delayed gadolinium-enhanced magnetic resonance imaging technique. Am J Sports Med 2010, 38: 943-949.

Verzijl N, DeGroot J, Bank RA, Bayliss MT, Bijlsma JW, Lafeber FP, Maroudas A, TeKoppele JM. Age-related accumulation of the advanced glycation endproduct pentosidine in human articular cartilage aggrecan: the use of pentosidine levels as a quantitative measure of protein turnover. Matrix Biol 2001, 20: 409-417.

Vinardell T, Sheehy EJ, Buckley CT, Kelly DJ. A comparison of the functionality and in vivo phenotypic stability of cartilaginous tissues engineered from different stem cell sources. Tissue Eng Part A 2012, 18: 1161-1170.

Viren T, Huang YP, Saarakkala S, Pulkkinen H, Tiitu V, Linjama A, Kiviranta I, Lammi MJ, Brunott A, Brommer H, Van Weeren R, Brama PA, Zheng YP, Jurvelin JS, Toyras J. Comparison of ultrasound and optical

coherence tomography techniques for evaluation of integrity of spontaneously repaired horse cartilage. J Med Eng Technol 2012, 36: 185-192.

Volz M, Schaumburger J, Frick H, Grifka J, Anders S. A randomized controlled trial demonstrating sustained benefit of Autologous Matrix-Induced Chondrogenesis over microfracture at five years. Int Orthop 2017, 41: 797-804.

von der Mark K, Gauss V, von der Mark H, Muller P. Relationship between cell shape and type of collagen synthesised as chondrocytes lose their cartilage phenotype in culture. Nature 1977, 267: 531-532.

Voor MJ, Yang S, Burden RL, Waddell SW. In vivo micro-CT scanning of a rabbit distal femur: repeatability and reproducibility. J Biomech 2008, 41: 186-193.

Vos T, Allen C, Arora M, Barber RM, Bhutta ZA, Brown J, Brown A, Carter A, Casey DC, Charlson FJ, Chen AZ, Coggeshall M, Cornaby L, Dandona L, Dandona R, Dicker DJ, Dilegge T, Erskine HE, Ferrari AJ, Fitzmaurice C, Fleming T, Forouzanfar MH, Fullman N, Gething PW, Goldberg EM, Graetz N, Haagsma JA, Hay RJ, Hay SI, Johnson CO, Kassebaum NJ, Kawashima T, Kemmer L, Khalil IA, Kinfu Y, Kyu HH, Leung R, Leung J, Liang J, Liang X, Lim SS, Lopez AD, Lozano R, Marczak L, Mensah GA, Mokdad AH, Naghavi M, Nguyen QL, Nguyen G, Nsoesie E, Olsen H, Pigott DM, Pinho C, Rankin Z, Reinig N, Salomon JA, Sandar L, Smith A, Stanaway J, Steiner C, Steiner TJ, Teeple S, Thomas BA, Troeger C, Wagner GR, Wagner JA, Wang H, Wang L, Wanga V, Whiteford HA, Zoeckler L, Abajobir AA, Abate KH, Abbafati C, Abbas KM, Abd-Allah F, Abraham B, Abubakar I, Abu-Raddad L, Abu-Rmeileh N, Ackerman IN, Adebiyi AO, Ademi Z, Adou AK, Afanvi KA, Agardh EE, Agarwal A, Kiadaliri AA, Ahmadieh H, Ajala ON, Akinyemi RO, Akseer N, Al-Aly Z, Alam K, Alam NKM, Aldhahri SF, Alegretti MA, Alemu ZA, Alexander LT, Alhabib S, ... Global, regional, and national incidence, prevalence, and years lived with disability for 310 diseases and injuries, 1990–2015: a systematic analysis for the Global Burden of Disease Study 2015. The Lancet 2016, 388: 1545-1602.

Wagner H. Surgical Treatment of Osteochondritis Dissecans, a Cause of Arthritis Deformans of the Knee. Rev Chir Orthop Reparatrice Appar Mot 1964, 50: 335-352.

Wang CT, Lin YT, Chiang BL, Lin YH, Hou SM. High molecular weight hyaluronic acid down-regulates the gene expression of osteoarthritis-associated cytokines and enzymes in fibroblast-like synoviocytes from patients with early osteoarthritis. Osteoarthritis Cartilage. 2006, 14 :1237–1247.

Wang T, Belkin NS, Burge AJ, Chang B, Pais M, Mahony G, Williams RJ. Patellofemoral Cartilage Lesions Treated With Particulated Juvenile Allograft Cartilage: A Prospective Study With Minimum 2-Year Clinical and Magnetic Resonance Imaging Outcomes. Arthroscopy 2018, 34: 1498-1505.

Woolf AD, Pfleger B. Burden of major musculoskeletal conditions. Bull World Health Organ 2003, 81: 646-656.

Yanke AB, Chubinskaya S. The state of cartilage regeneration: current and future technologies. Curr Rev Musculoskelet Med 2015, 8: 1-8.

Yoo JU, Barthel TS, Nishimura K, Solchaga L, Caplan AI, Goldberg VM, Johnstone B. The chondrogenic potential of human bone-marrow-derived mesenchymal progenitor cells. J Bone Joint Surg Am 1998, 80: 1745-1757.

Yu X, Tang X, Gohil SV, Laurencin CT. Biomaterials for Bone Regenerative Engineering. Adv Healthc Mater 2015, 4: 1268-1285.

Zayed M, Caniglia C, Misk N, Dhar MS. Donor-Matched Comparison of Chondrogenic Potential of Equine Bone Marrow- and Synovial Fluid-Derived Mesenchymal Stem Cells: Implications for Cartilage Tissue Regeneration. Front Vet Sci 2017, 3: 121.